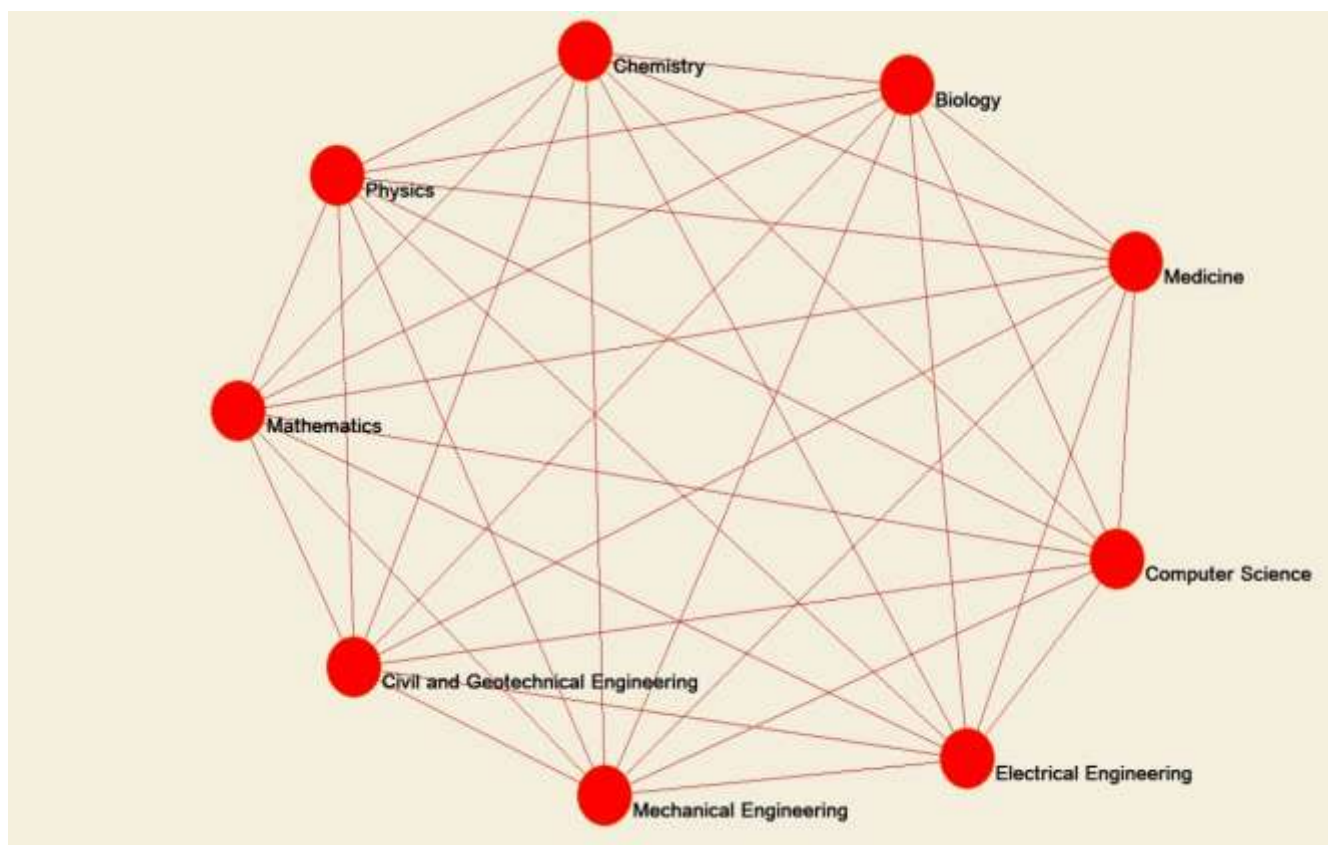


2. International Conference on New Research and Development in Technical and Natural Science,

ICNRDTNS



Novo mesto, Slovenia, 22.- 24. September 2021

The organizers of the 2. International Conference on New Research and Development in Technical and Natural Science, ICNRDTNS are expecting you, our dear participants and guests at another traditional gathering of all of those who are interested in the use of Mathematics, Physics, Chemistry, Biology, Medicine, Computer Science, Electrical Engineering, Mechanical Engineering, Civil and Geotechnical Engineering and all related high technologies in the fields of Engineering and Science.

During the whole week from 22. to 24. september 2021 in Novo mesto, Slovenia, the 2. convention ICNRDTNS offers you a number of interesting events. The programme of ICNRDTNS includes plenary sessions, core dialogues, debates, discovery demos, knowledge exchange sessions, knowledge factories, networking meet-ups, panel talks and poster presentations on specific topics and informal networking opportunities in which practitioners share their experiences, ideas, new information and perspectives.

On behalf of the International Program Committee we express our sincere gratitude to our sponsors.

Come to magical, ancient and sunny Radin, participate in ICNRDTNS 2021 and be part of the ICNRDTNS events from September 22 – 24, 2021.

Assist. Prof. Dr. Matej Babič, Ph.D.

International Program Committee General Chair

A handwritten signature in black ink, appearing to read 'Babič', is positioned below the text of the International Program Committee General Chair.

Organized by Complex System Company, s.p.

Editor: Asisit. Prof. Dr. Matej Babič, Ph.D.

Publisher: Complex System Company, s.p. Podgradje

Circulation: Electronic edition

Date: Podgradje, 2021

Kataložni zapis o publikaciji (CIP) pripravili v Narodni in univerzitetni knjižnici v Ljubljani
[COBISS.SI-ID 82300163](#)

ISBN 978-961-07-0827-8 (PDF)

icnrtns.com

International Organizing Committee

1. **Matej Babič, President**, Faculty of Information studies, Novo mesto (Slovenia)
2. **Branko Matovič**, Director of Centre of Excellence-CEXTREME MAT, Institute for nuclear sciences Vinca, Belgrade University, (Serbia)
3. **Michele Cali**, University of Catania, (Italy)
4. **Joel J. P. C. Rodrigues**, National Institute of Telecommunications (INATEL), Santa Rita do Sapucaí-MG, Brazil, Instituto de Telecomunicações, Portugal, Federal University of Piauí (UFPI), Teresina-PI, Brazil, Center of Excellence in Information Assurance (CoEIA), King Saud University, Riyadh, 11653, Saudi Arabia
5. **Cristiano Fragassa**, Alma Mater Studiorum University of Bologna, Bologna, (Italy)
6. **Ladislav Hluchý**, Director of the Institute of Informatics, Slovak Academy of Sciences, Head of the Department of Parallel and Distributed Computing
7. **Dragan Marinković**, TU Berlin, Germany and Professor at Faculty of Mechanical Engineering in Niš

International Scientific Committee

1. **Emilio Ramírez Juidías**, University of Seville, Spain
2. **Kumar Dookhitram**, University of Technology, Mauritius
3. **Abdulhamit Subasi**, University of Turku, Turku, Finland
4. **Mahmoud Moradi**, Coventry University, UK
5. **Bojan Đurin**, University North, Croatia
6. **Rita Ambu**, University of Cagliari, Italy
7. **Ana Pavlovic**, Alma Mater Studiorum University of Bologna, Italy
8. **Michał Jakubowicz**, Poznan University of Technology, Poland
9. **Borislav Savković**, University of Novi Sad, Serbia
10. **Olena Chernieva**, The Odessa State Academy of Civil Engineering, Odessa, Ukraine
11. **Grzegorz Lesiuk**, Wrocław University of Science and Technology, Poland
12. **Ivan Luković**, University of Novi Sad, Serbia,

Simulation of smart PPP model in MONM for in-15 stations

Matej Babič

Faculty of information studies, Novo mesto, Slovenia

Abstract

Introduction

In this study, we used a genetic programming (GP) simulation model to predict the bike rental of 15 GoNM stations according to weather conditions. The figure below shows the GP simulation model.

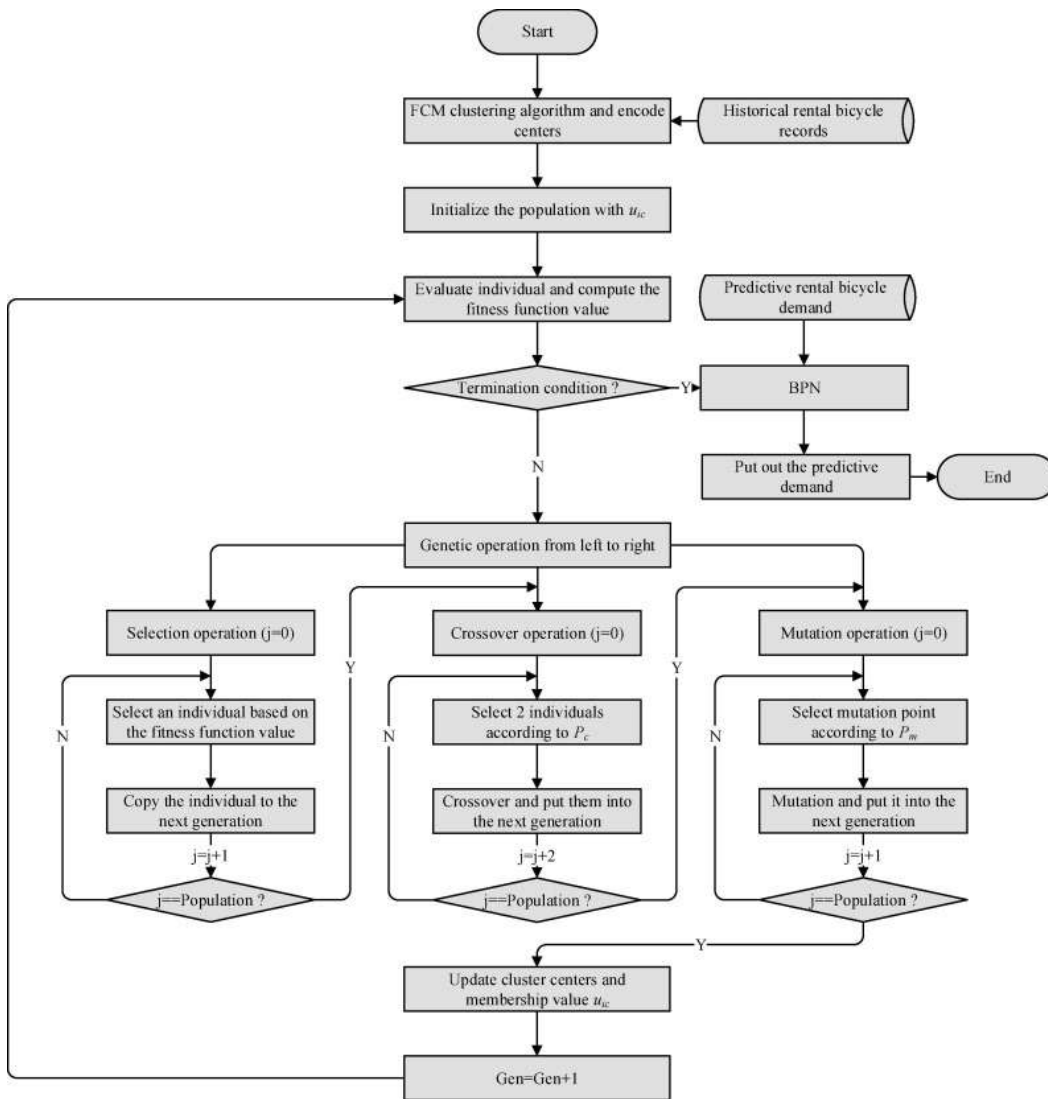


Figure 1: GP simulation model for GoNM bike rental

Experimental data and data analysis

The tables below show bike rental for 15 stations. In TABLE 2, column D represents the topological property Rate, column ND represents the network density, column BC represents the topological property Centrality of the center and column CC represents the topological property Clustering coefficient, column T represents the average temperature [C], column WV represents the average wind speed [m / s], column C represents average cloud [%], column RH represents average relative humidity [%], column AP represents average air pressure [hPa], column R represents average precipitation [mm], and last column SD represents average sun duration [h].

ADRIA - St	Avtobusna	BTC City N	Center - Se	Draska - Še	Glavni trg	Kandijski n	Ločna-Seid	Novi trg	OŠ Bršljin	OŠ Šmihej	Podbreznik	Ragovska	Šolski cent	Ulica Slavka Gruma
0	8	0	2	6	1	0	0	0	1	0	4	0	3	3
0	2	1	1	5	11	2	3	1	4	1	2	5	0	4
6	10	5	1	23	19	8	7	7	5	4	13	13	1	10
0	8	4	2	8	8	14	2	6	4	1	26	6	1	7
3	11	4	6	18	8	9	5	3	3	2	19	7	1	9
0	4	5	1	11	6	6	5	6	5	0	5	10	3	5
0	13	0	0	10	14	12	4	1	3	0	3	0	1	7
0	2	1	1	8	4	11	1	4	0	1	1	2	0	3
0	6	0	2	5	9	6	2	4	2	0	2	1	0	0
1	4	1	0	6	19	8	3	3	2	0	1	0	0	8
0	17	7	3	14	27	19	7	4	3	1	0	3	2	5
0	14	7	3	9	24	8	7	7	3	0	4	3	2	10
1	4	2	1	1	24	17	6	6	8	0	3	4	0	2
0	3	1	1	6	19	4	4	6	1	3	0	3	2	5
0	0	1	5	9	3	9	6	5	2	1	0	3	0	8
0	5	2	6	20	7	10	2	4	1	0	0	14	0	0
0	11	2	3	11	13	15	3	3	6	2	2	11	1	4
0	3	6	2	12	9	13	1	7	3	1	0	14	1	3
2	9	6	2	13	10	5	3	9	5	0	0	10	3	13
0	14	3	0	11	8	8	4	4	3	1	0	1	16	4
1	32	0	4	4	6	4	8	9	2	2	1	6	46	7
0	17	3	3	5	10	6	9	13	3		1	8	38	2
0	3	1	3	7	5	7	5	13	0	3	1	5	21	4
0	17	0	3	6	9	7	1	12	1	1	0	7	41	1
0	8	0	4	5	4	1	2	8	0	2	1	5	27	3
1	4	4	2	3	2	1	1	6	1	0	3	0	19	0
0	1	0	0	1	2	1	2	1	0	0	0	3	1	0
0	5	2	0	1	0	4	1	3	0	0	0	3	0	2
0	2	1	1	2	1	0	2	0	0	0	1	0	1	0
0	3	0	0	2	3	6	4	0	0	0	0	1	0	0

Table 1: Number of

rented bicycles for 15 stations

D	ND	BC	CC	T	WV	C	RH	AP	R	SD	Y
2,125	0,06641	0,09079	0,10417	14,27	1,56	64,86	73,57	984,57	4,49	4,57	0,0
2,625	0,08203	0,08794	0,00000	14,3	1,77	25,71	60,00	992,57	1,67	10,54	0,0
7,125	0,22266	0,29539	0,26667	14,76	2,49	73,86	72,00	988,0	3,03	4,66	6,0
5,25	0,16406	0,08159	0,25926	15,63	1,78	70,08	74,62	992,15	2,94	4,7	0,0
6,125	0,19141	0,27587	0,24219	14,96	1,44	66,63	73,84	995,68	3,83	5,29	3,0
4,125	0,12891	0,17344	0,12281	17,54	1,55	52,43	66,86	984,71	1,19	7,59	0,0
4,125	0,12891	0,17651	0,18367	18,11	1,73	34,14	73,00	985,29	5,04	8,47	0,0
3	0,09375	0,08487	0,25806	18,8	1,33	75,14	80,00	986,25	7,63	5,59	0,0
3,25	0,10156	0,15968	0,11364	20,74	1,29	42,29	66,29	992,29	2,13	10,2	0,0
4	0,125	0,19048	0,26875	21,73	1,39	43,29	75,86	988,43	2,09	8,79	1,0
6,25	0,19531	0,14519	0,15984	21,24	1,37	16,71	65,29	990,57	3,06	12,19	0,0
5,5	0,17188	0,12952	0,22043	17,6	1,63	48,63	72,63	991,88	4,68	10,05	0,0
4,125	0,12891	0,10127	0,27273	21,3	1,0	42,57	77,57	990,14	6,93	8,64	1,0
3,125	0,09766	0,0454	0,30000	25,03	1,2	21,71	73,43	990,29	1,33	11,41	0,0
3,5	0,10938	0,06148	0,28564	20,36	1,49	67,71	84,71	989,0	6,99	5,21	0,0
3,75	0,11719	0,08762	0,27500	23,16	1,03	29,86	79,14	990,14	2,64	8,89	0,0
5,125	0,16016	0,11725	0,24576	19,58	1,36	46,8	73,85	990,46	3,9	8,27	0,0
5,625	0,17578	0,15037	0,33108	21,91	1,59	49,43	70,43	987,43	0,13	8,33	0,0
5,875	0,18359	0,1379	0,28400	17,44	1,27	39,57	80,29	991,0	11,13	6,23	2,0
5,5	0,17188	0,12246	0,31000	18,83	1,36	29,57	76,00	994,57	0,0	8,57	0,0
6,125	0,19141	0,08933	0,27308	10,72	1,35	66,54	85,03	992,26	4,97	3,98	1,0
6,125	0,19141	0,12127	0,26546	15,71	1,3	79,0	83,57	983,83	6,53	4,79	0,0
5,875	0,18359	0,16186	0,24800	13,4	1,56	51,57	83,86	982,71	5,51	5,57	0,0
5,5	0,17188	0,15217	0,02355	12,79	1,56	53,71	83,43	989,43	9,79	5,66	0,0
3,875	0,12109	0,27852	0,22449	8,64	1,5	87,29	86,71	986,43	11,69	1,96	0,0
2,875	0,08984	0,13333	0,29310	11,39	1,71	41,57	81,71	995,0	0,07	5,13	1,0
1,375	0,04297	0,03841	0,15452	12,13	1,27	64,71	83,71	990,71	4,19	3,96	0,0
2	0,0625	0,05333	0,00000	10,0	1,09	56,57	80,14	1001,14	0,11	5,06	0,0
1,375	0,04297	0,01365	0,00000	5,57	1,05	90,57	91,29	1000,71	0,13	1,13	0,0
1,75	0,05469	0,0473	0,00000	5,72	1,03	82,83	93,17	999,67	7,78	1,48	0,0

Table 2: Number of borrowed bicycles for Adria station

D	ND	BC	CC	T	WV	C	RH	AP	R	SD	Y
2,125	0,06641	0,09079	0,10417	14,27	1,56	64,86	73,57	984,57	4,49	4,57	8,0
2,625	0,08203	0,08794	0,00000	14,3	1,77	25,71	60,00	992,57	1,67	10,54	2,0
7,125	0,22266	0,29539	0,26667	14,76	2,49	73,86	72,00	988,0	3,03	4,66	10,0
5,25	0,16406	0,08159	0,25926	15,63	1,78	70,08	74,62	992,15	2,94	4,7	8,0
6,125	0,19141	0,27587	0,24219	14,96	1,44	66,63	73,84	995,68	3,83	5,29	11,0
4,125	0,12891	0,17344	0,12281	17,54	1,55	52,43	66,86	984,71	1,19	7,59	4,0
4,125	0,12891	0,17651	0,18367	18,11	1,73	34,14	73,00	985,29	5,04	8,47	13,0
3	0,09375	0,08487	0,25806	18,8	1,33	75,14	80,00	986,25	7,63	5,59	2,0
3,25	0,10156	0,15968	0,11364	20,74	1,29	42,29	66,29	992,29	2,13	10,2	6,0
4	0,125	0,19048	0,26875	21,73	1,39	43,29	75,86	988,43	2,09	8,79	4,0
6,25	0,19531	0,14519	0,15984	21,24	1,37	16,71	65,29	990,57	3,06	12,19	17,0
5,5	0,17188	0,12952	0,22043	17,6	1,63	48,63	72,63	991,88	4,68	10,05	14,0
4,125	0,12891	0,10127	0,27273	21,3	1,0	42,57	77,57	990,14	6,93	8,64	4,0
3,125	0,09766	0,0454	0,30000	25,03	1,2	21,71	73,43	990,29	1,33	11,41	3,0
3,5	0,10938	0,06148	0,28564	20,36	1,49	67,71	84,71	989,0	6,99	5,21	0,0
3,75	0,11719	0,08762	0,27500	23,16	1,03	29,86	79,14	990,14	2,64	8,89	5,0
5,125	0,16016	0,11725	0,24576	19,58	1,36	46,8	73,85	990,46	3,9	8,27	11,0
5,625	0,17578	0,15037	0,33108	21,91	1,59	49,43	70,43	987,43	0,13	8,33	3,0
5,875	0,18359	0,1379	0,28400	17,44	1,27	39,57	80,29	991,0	11,13	6,23	9,0
5,5	0,17188	0,12246	0,31000	18,83	1,36	29,57	76,00	994,57	0,0	8,57	14,0
6,125	0,19141	0,08933	0,27308	10,72	1,35	66,54	85,03	992,26	4,97	3,98	32,0
6,125	0,19141	0,12127	0,26546	15,71	1,3	79,0	83,57	983,83	6,53	4,79	17,0
5,875	0,18359	0,16186	0,24800	13,4	1,56	51,57	83,86	982,71	5,51	5,57	3,0
5,5	0,17188	0,15217	0,02355	12,79	1,56	53,71	83,43	989,43	9,79	5,66	17,0
3,875	0,12109	0,27852	0,22449	8,64	1,5	87,29	86,71	986,43	11,69	1,96	8,0
2,875	0,08984	0,13333	0,29310	11,39	1,71	41,57	81,71	995,0	0,07	5,13	4,0
1,375	0,04297	0,03841	0,15452	12,13	1,27	64,71	83,71	990,71	4,19	3,96	1,0
2	0,0625	0,05333	0,00000	10,0	1,09	56,57	80,14	1001,14	0,11	5,06	5,0
1,375	0,04297	0,01365	0,00000	5,57	1,05	90,57	91,29	1000,71	0,13	1,13	2,0
1,75	0,05469	0,0473	0,00000	5,72	1,03	82,83	93,17	999,67	7,78	1,48	3,0

Table 3: Number of bicycles rented for the Bus station

D	ND	BC	CC	T	WV	C	RH	AP	R	SD	Y
2,125	0,06641	0,09079	0,10417	14,27	1,56	64,86	73,57	984,57	4,49	4,57	0,0
2,625	0,08203	0,08794	0,00000	14,3	1,77	25,71	60,00	992,57	1,67	10,54	1,0
7,125	0,22266	0,29539	0,26667	14,76	2,49	73,86	72,00	988,0	3,03	4,66	5,0
5,25	0,16406	0,08159	0,25926	15,63	1,78	70,08	74,62	992,15	2,94	4,7	4,0
6,125	0,19141	0,27587	0,24219	14,96	1,44	66,63	73,84	995,68	3,83	5,29	4,0
4,125	0,12891	0,17344	0,12281	17,54	1,55	52,43	66,86	984,71	1,19	7,59	5,0
4,125	0,12891	0,17651	0,18367	18,11	1,73	34,14	73,00	985,29	5,04	8,47	0,0
3	0,09375	0,08487	0,25806	18,8	1,33	75,14	80,00	986,25	7,63	5,59	1,0
3,25	0,10156	0,15968	0,11364	20,74	1,29	42,29	66,29	992,29	2,13	10,2	0,0
4	0,125	0,19048	0,26875	21,73	1,39	43,29	75,86	988,43	2,09	8,79	1,0
6,25	0,19531	0,14519	0,15984	21,24	1,37	16,71	65,29	990,57	3,06	12,19	7,0
5,5	0,17188	0,12952	0,22043	17,6	1,63	48,63	72,63	991,88	4,68	10,05	7,0
4,125	0,12891	0,10127	0,27273	21,3	1,0	42,57	77,57	990,14	6,93	8,64	2,0
3,125	0,09766	0,0454	0,30000	25,03	1,2	21,71	73,43	990,29	1,33	11,41	1,0
3,5	0,10938	0,06148	0,28564	20,36	1,49	67,71	84,71	989,0	6,99	5,21	1,0
3,75	0,11719	0,08762	0,27500	23,16	1,03	29,86	79,14	990,14	2,64	8,89	2,0
5,125	0,16016	0,11725	0,24576	19,58	1,36	46,8	73,85	990,46	3,9	8,27	2,0
5,625	0,17578	0,15037	0,33108	21,91	1,59	49,43	70,43	987,43	0,13	8,33	6,0
5,875	0,18359	0,1379	0,28400	17,44	1,27	39,57	80,29	991,0	11,13	6,23	6,0
5,5	0,17188	0,12246	0,31000	18,83	1,36	29,57	76,00	994,57	0,0	8,57	3,0
6,125	0,19141	0,08933	0,27308	10,72	1,35	66,54	85,03	992,26	4,97	3,98	0,0
6,125	0,19141	0,12127	0,26546	15,71	1,3	79,0	83,57	983,83	6,53	4,79	3,0
5,875	0,18359	0,16186	0,24800	13,4	1,56	51,57	83,86	982,71	5,51	5,57	1,0
5,5	0,17188	0,15217	0,02355	12,79	1,56	53,71	83,43	989,43	9,79	5,66	0,0
3,875	0,12109	0,27852	0,22449	8,64	1,5	87,29	86,71	986,43	11,69	1,96	0,0
2,875	0,08984	0,13333	0,29310	11,39	1,71	41,57	81,71	995,0	0,07	5,13	4,0
1,375	0,04297	0,03841	0,15452	12,13	1,27	64,71	83,71	990,71	4,19	3,96	0,0
2	0,0625	0,05333	0,00000	10,0	1,09	56,57	80,14	1001,14	0,11	5,06	2,0
1,375	0,04297	0,01365	0,00000	5,57	1,05	90,57	91,29	1000,71	0,13	1,13	1,0
1,75	0,05469	0,0473	0,00000	5,72	1,03	82,83	93,17	999,67	7,78	1,48	0,0

Table 4: Number of rented bicycles for BTC station

D	ND	BC	CC	T	WV	C	RH	AP	R	SD	Y
2,125	0,06641	0,09079	0,10417	14,27	1,56	64,86	73,57	984,57	4,49	4,57	2,0
2,625	0,08203	0,08794	0,00000	14,3	1,77	25,71	60,00	992,57	1,67	10,54	1,0
7,125	0,22266	0,29539	0,26667	14,76	2,49	73,86	72,00	988,0	3,03	4,66	1,0
5,25	0,16406	0,08159	0,25926	15,63	1,78	70,08	74,62	992,15	2,94	4,7	2,0
6,125	0,19141	0,27587	0,24219	14,96	1,44	66,63	73,84	995,68	3,83	5,29	6,0
4,125	0,12891	0,17344	0,12281	17,54	1,55	52,43	66,86	984,71	1,19	7,59	1,0
4,125	0,12891	0,17651	0,18367	18,11	1,73	34,14	73,00	985,29	5,04	8,47	0,0
3	0,09375	0,08487	0,25806	18,8	1,33	75,14	80,00	986,25	7,63	5,59	1,0
3,25	0,10156	0,15968	0,11364	20,74	1,29	42,29	66,29	992,29	2,13	10,2	2,0
4	0,125	0,19048	0,26875	21,73	1,39	43,29	75,86	988,43	2,09	8,79	0,0
6,25	0,19531	0,14519	0,15984	21,24	1,37	16,71	65,29	990,57	3,06	12,19	3,0
5,5	0,17188	0,12952	0,22043	17,6	1,63	48,63	72,63	991,88	4,68	10,05	3,0
4,125	0,12891	0,10127	0,27273	21,3	1,0	42,57	77,57	990,14	6,93	8,64	1,0
3,125	0,09766	0,0454	0,30000	25,03	1,2	21,71	73,43	990,29	1,33	11,41	1,0
3,5	0,10938	0,06148	0,28564	20,36	1,49	67,71	84,71	989,0	6,99	5,21	5,0
3,75	0,11719	0,08762	0,27500	23,16	1,03	29,86	79,14	990,14	2,64	8,89	6,0
5,125	0,16016	0,11725	0,24576	19,58	1,36	46,8	73,85	990,46	3,9	8,27	3,0
5,625	0,17578	0,15037	0,33108	21,91	1,59	49,43	70,43	987,43	0,13	8,33	2,0
5,875	0,18359	0,1379	0,28400	17,44	1,27	39,57	80,29	991,0	11,13	6,23	2,0
5,5	0,17188	0,12246	0,31000	18,83	1,36	29,57	76,00	994,57	0,0	8,57	0,0
6,125	0,19141	0,08933	0,27308	10,72	1,35	66,54	85,03	992,26	4,97	3,98	4,0
6,125	0,19141	0,12127	0,26546	15,71	1,3	79,0	83,57	983,83	6,53	4,79	3,0
5,875	0,18359	0,16186	0,24800	13,4	1,56	51,57	83,86	982,71	5,51	5,57	3,0
5,5	0,17188	0,15217	0,02355	12,79	1,56	53,71	83,43	989,43	9,79	5,66	3,0
3,875	0,12109	0,27852	0,22449	8,64	1,5	87,29	86,71	986,43	11,69	1,96	4,0
2,875	0,08984	0,13333	0,29310	11,39	1,71	41,57	81,71	995,0	0,07	5,13	2,0
1,375	0,04297	0,03841	0,15452	12,13	1,27	64,71	83,71	990,71	4,19	3,96	0,0
2	0,0625	0,05333	0,00000	10,0	1,09	56,57	80,14	1001,14	0,11	5,06	0,0
1,375	0,04297	0,01365	0,00000	5,57	1,05	90,57	91,29	1000,71	0,13	1,13	1,0
1,75	0,05469	0,0473	0,00000	5,72	1,03	82,83	93,17	999,67	7,78	1,48	0,0

Table 5: Number of rented bicycles for the Center - Seidlova cesta station

D	ND	BC	CC	T	WV	C	RH	AP	R	SD	Y
2,125	0,06641	0,09079	0,10417	14,27	1,56	64,86	73,57	984,57	4,49	4,57	6,0
2,625	0,08203	0,08794	0,00000	14,3	1,77	25,71	60,00	992,57	1,67	10,54	5,0
7,125	0,22266	0,29539	0,26667	14,76	2,49	73,86	72,00	988,0	3,03	4,66	23,0
5,25	0,16406	0,08159	0,25926	15,63	1,78	70,08	74,62	992,15	2,94	4,7	8,0
6,125	0,19141	0,27587	0,24219	14,96	1,44	66,63	73,84	995,68	3,83	5,29	18,0
4,125	0,12891	0,17344	0,12281	17,54	1,55	52,43	66,86	984,71	1,19	7,59	11,0
4,125	0,12891	0,17651	0,18367	18,11	1,73	34,14	73,00	985,29	5,04	8,47	10,0
3	0,09375	0,08487	0,25806	18,8	1,33	75,14	80,00	986,25	7,63	5,59	8,0
3,25	0,10156	0,15968	0,11364	20,74	1,29	42,29	66,29	992,29	2,13	10,2	5,0
4	0,125	0,19048	0,26875	21,73	1,39	43,29	75,86	988,43	2,09	8,79	6,0
6,25	0,19531	0,14519	0,15984	21,24	1,37	16,71	65,29	990,57	3,06	12,19	14,0
5,5	0,17188	0,12952	0,22043	17,6	1,63	48,63	72,63	991,88	4,68	10,05	9,0
4,125	0,12891	0,10127	0,27273	21,3	1,0	42,57	77,57	990,14	6,93	8,64	1,0
3,125	0,09766	0,0454	0,30000	25,03	1,2	21,71	73,43	990,29	1,33	11,41	6,0
3,5	0,10938	0,06148	0,28564	20,36	1,49	67,71	84,71	989,0	6,99	5,21	9,0
3,75	0,11719	0,08762	0,27500	23,16	1,03	29,86	79,14	990,14	2,64	8,89	20,0
5,125	0,16016	0,11725	0,24576	19,58	1,36	46,8	73,85	990,46	3,9	8,27	11,0
5,625	0,17578	0,15037	0,33108	21,91	1,59	49,43	70,43	987,43	0,13	8,33	12,0
5,875	0,18359	0,1379	0,28400	17,44	1,27	39,57	80,29	991,0	11,13	6,23	13,0
5,5	0,17188	0,12246	0,31000	18,83	1,36	29,57	76,00	994,57	0,0	8,57	11,0
6,125	0,19141	0,08933	0,27308	10,72	1,35	66,54	85,03	992,26	4,97	3,98	4,0
6,125	0,19141	0,12127	0,26546	15,71	1,3	79,0	83,57	983,83	6,53	4,79	5,0
5,875	0,18359	0,16186	0,24800	13,4	1,56	51,57	83,86	982,71	5,51	5,57	7,0
5,5	0,17188	0,15217	0,02355	12,79	1,56	53,71	83,43	989,43	9,79	5,66	6,0
3,875	0,12109	0,27852	0,22449	8,64	1,5	87,29	86,71	986,43	11,69	1,96	5,0
2,875	0,08984	0,13333	0,29310	11,39	1,71	41,57	81,71	995,0	0,07	5,13	3,0
1,375	0,04297	0,03841	0,15452	12,13	1,27	64,71	83,71	990,71	4,19	3,96	1,0
2	0,0625	0,05333	0,00000	10,0	1,09	56,57	80,14	1001,14	0,11	5,06	1,0
1,375	0,04297	0,01365	0,00000	5,57	1,05	90,57	91,29	1000,71	0,13	1,13	2,0
1,75	0,05469	0,0473	0,00000	5,72	1,03	82,83	93,17	999,67	7,78	1,48	2,0

Table 6: Number of borrowed bicycles for Drska - Šegova ulica station

D	ND	BC	CC	T	WV	C	RH	AP	R	SD	Y
2,125	0,06641	0,09079	0,10417	14,27	1,56	64,86	73,57	984,57	4,49	4,57	1,0
2,625	0,08203	0,08794	0,00000	14,3	1,77	25,71	60,00	992,57	1,67	10,54	11,0
7,125	0,22266	0,29539	0,26667	14,76	2,49	73,86	72,00	988,0	3,03	4,66	19,0
5,25	0,16406	0,08159	0,25926	15,63	1,78	70,08	74,62	992,15	2,94	4,7	8,0
6,125	0,19141	0,27587	0,24219	14,96	1,44	66,63	73,84	995,68	3,83	5,29	8,0
4,125	0,12891	0,17344	0,12281	17,54	1,55	52,43	66,86	984,71	1,19	7,59	6,0
4,125	0,12891	0,17651	0,18367	18,11	1,73	34,14	73,00	985,29	5,04	8,47	14,0
3	0,09375	0,08487	0,25806	18,8	1,33	75,14	80,00	986,25	7,63	5,59	4,0
3,25	0,10156	0,15968	0,11364	20,74	1,29	42,29	66,29	992,29	2,13	10,2	9,0
4	0,125	0,19048	0,26875	21,73	1,39	43,29	75,86	988,43	2,09	8,79	19,0
6,25	0,19531	0,14519	0,15984	21,24	1,37	16,71	65,29	990,57	3,06	12,19	27,0
5,5	0,17188	0,12952	0,22043	17,6	1,63	48,63	72,63	991,88	4,68	10,05	24,0
4,125	0,12891	0,10127	0,27273	21,3	1,0	42,57	77,57	990,14	6,93	8,64	24,0
3,125	0,09766	0,0454	0,30000	25,03	1,2	21,71	73,43	990,29	1,33	11,41	19,0
3,5	0,10938	0,06148	0,28564	20,36	1,49	67,71	84,71	989,0	6,99	5,21	3,0
3,75	0,11719	0,08762	0,27500	23,16	1,03	29,86	79,14	990,14	2,64	8,89	7,0
5,125	0,16016	0,11725	0,24576	19,58	1,36	46,8	73,85	990,46	3,9	8,27	13,0
5,625	0,17578	0,15037	0,33108	21,91	1,59	49,43	70,43	987,43	0,13	8,33	9,0
5,875	0,18359	0,1379	0,28400	17,44	1,27	39,57	80,29	991,0	11,13	6,23	10,0
5,5	0,17188	0,12246	0,31000	18,83	1,36	29,57	76,00	994,57	0,0	8,57	8,0
6,125	0,19141	0,08933	0,27308	10,72	1,35	66,54	85,03	992,26	4,97	3,98	6,0
6,125	0,19141	0,12127	0,26546	15,71	1,3	79,0	83,57	983,83	6,53	4,79	10,0
5,875	0,18359	0,16186	0,24800	13,4	1,56	51,57	83,86	982,71	5,51	5,57	5,0
5,5	0,17188	0,15217	0,02355	12,79	1,56	53,71	83,43	989,43	9,79	5,66	9,0
3,875	0,12109	0,27852	0,22449	8,64	1,5	87,29	86,71	986,43	11,69	1,96	4,0
2,875	0,08984	0,13333	0,29310	11,39	1,71	41,57	81,71	995,0	0,07	5,13	2,0
1,375	0,04297	0,03841	0,15452	12,13	1,27	64,71	83,71	990,71	4,19	3,96	2,0
2	0,0625	0,05333	0,00000	10,0	1,09	56,57	80,14	1001,14	0,11	5,06	0,0
1,375	0,04297	0,01365	0,00000	5,57	1,05	90,57	91,29	1000,71	0,13	1,13	1,0
1,75	0,05469	0,0473	0,00000	5,72	1,03	82,83	93,17	999,67	7,78	1,48	3,0

Table 7: Number of rented bicycles for the Main Square station

D	ND	BC	CC	T	WV	C	RH	AP	R	SD	Y
2,125	0,06641	0,09079	0,10417	14,27	1,56	64,86	73,57	984,57	4,49	4,57	0,0
2,625	0,08203	0,08794	0,00000	14,3	1,77	25,71	60,00	992,57	1,67	10,54	2,0
7,125	0,22266	0,29539	0,26667	14,76	2,49	73,86	72,00	988,0	3,03	4,66	8,0
5,25	0,16406	0,08159	0,25926	15,63	1,78	70,08	74,62	992,15	2,94	4,7	14,0
6,125	0,19141	0,27587	0,24219	14,96	1,44	66,63	73,84	995,68	3,83	5,29	9,0
4,125	0,12891	0,17344	0,12281	17,54	1,55	52,43	66,86	984,71	1,19	7,59	6,0
4,125	0,12891	0,17651	0,18367	18,11	1,73	34,14	73,00	985,29	5,04	8,47	12,0
3	0,09375	0,08487	0,25806	18,8	1,33	75,14	80,00	986,25	7,63	5,59	11,0
3,25	0,10156	0,15968	0,11364	20,74	1,29	42,29	66,29	992,29	2,13	10,2	6,0
4	0,125	0,19048	0,26875	21,73	1,39	43,29	75,86	988,43	2,09	8,79	8,0
6,25	0,19531	0,14519	0,15984	21,24	1,37	16,71	65,29	990,57	3,06	12,19	19,0
5,5	0,17188	0,12952	0,22043	17,6	1,63	48,63	72,63	991,88	4,68	10,05	8,0
4,125	0,12891	0,10127	0,27273	21,3	1,0	42,57	77,57	990,14	6,93	8,64	17,0
3,125	0,09766	0,0454	0,30000	25,03	1,2	21,71	73,43	990,29	1,33	11,41	4,0
3,5	0,10938	0,06148	0,28564	20,36	1,49	67,71	84,71	989,0	6,99	5,21	9,0
3,75	0,11719	0,08762	0,27500	23,16	1,03	29,86	79,14	990,14	2,64	8,89	10,0
5,125	0,16016	0,11725	0,24576	19,58	1,36	46,8	73,85	990,46	3,9	8,27	15,0
5,625	0,17578	0,15037	0,33108	21,91	1,59	49,43	70,43	987,43	0,13	8,33	13,0
5,875	0,18359	0,1379	0,28400	17,44	1,27	39,57	80,29	991,0	11,13	6,23	5,0
5,5	0,17188	0,12246	0,31000	18,83	1,36	29,57	76,00	994,57	0,0	8,57	8,0
6,125	0,19141	0,08933	0,27308	10,72	1,35	66,54	85,03	992,26	4,97	3,98	4,0
6,125	0,19141	0,12127	0,26546	15,71	1,3	79,0	83,57	983,83	6,53	4,79	6,0
5,875	0,18359	0,16186	0,24800	13,4	1,56	51,57	83,86	982,71	5,51	5,57	7,0
5,5	0,17188	0,15217	0,02355	12,79	1,56	53,71	83,43	989,43	9,79	5,66	7,0
3,875	0,12109	0,27852	0,22449	8,64	1,5	87,29	86,71	986,43	11,69	1,96	1,0
2,875	0,08984	0,13333	0,29310	11,39	1,71	41,57	81,71	995,0	0,07	5,13	1,0
1,375	0,04297	0,03841	0,15452	12,13	1,27	64,71	83,71	990,71	4,19	3,96	1,0
2	0,0625	0,05333	0,00000	10,0	1,09	56,57	80,14	1001,14	0,11	5,06	4,0
1,375	0,04297	0,01365	0,00000	5,57	1,05	90,57	91,29	1000,71	0,13	1,13	0,0
1,75	0,05469	0,0473	0,00000	5,72	1,03	82,83	93,17	999,67	7,78	1,48	6,0

Table 8: Number of bicycles borrowed for Kandijski most station

D	ND	BC	CC	T	WV	C	RH	AP	R	SD	Y
2,125	0,06641	0,09079	0,10417	14,27	1,56	64,86	73,57	984,57	4,49	4,57	0,0
2,625	0,08203	0,08794	0,00000	14,3	1,77	25,71	60,00	992,57	1,67	10,54	3,0
7,125	0,22266	0,29539	0,26667	14,76	2,49	73,86	72,00	988,0	3,03	4,66	7,0
5,25	0,16406	0,08159	0,25926	15,63	1,78	70,08	74,62	992,15	2,94	4,7	2,0
6,125	0,19141	0,27587	0,24219	14,96	1,44	66,63	73,84	995,68	3,83	5,29	5,0
4,125	0,12891	0,17344	0,12281	17,54	1,55	52,43	66,86	984,71	1,19	7,59	5,0
4,125	0,12891	0,17651	0,18367	18,11	1,73	34,14	73,00	985,29	5,04	8,47	4,0
3	0,09375	0,08487	0,25806	18,8	1,33	75,14	80,00	986,25	7,63	5,59	1,0
3,25	0,10156	0,15968	0,11364	20,74	1,29	42,29	66,29	992,29	2,13	10,2	2,0
4	0,125	0,19048	0,26875	21,73	1,39	43,29	75,86	988,43	2,09	8,79	3,0
6,25	0,19531	0,14519	0,15984	21,24	1,37	16,71	65,29	990,57	3,06	12,19	7,0
5,5	0,17188	0,12952	0,22043	17,6	1,63	48,63	72,63	991,88	4,68	10,05	7,0
4,125	0,12891	0,10127	0,27273	21,3	1,0	42,57	77,57	990,14	6,93	8,64	6,0
3,125	0,09766	0,0454	0,30000	25,03	1,2	21,71	73,43	990,29	1,33	11,41	4,0
3,5	0,10938	0,06148	0,28564	20,36	1,49	67,71	84,71	989,0	6,99	5,21	6,0
3,75	0,11719	0,08762	0,27500	23,16	1,03	29,86	79,14	990,14	2,64	8,89	2,0
5,125	0,16016	0,11725	0,24576	19,58	1,36	46,8	73,85	990,46	3,9	8,27	3,0
5,625	0,17578	0,15037	0,33108	21,91	1,59	49,43	70,43	987,43	0,13	8,33	1,0
5,875	0,18359	0,1379	0,28400	17,44	1,27	39,57	80,29	991,0	11,13	6,23	3,0
5,5	0,17188	0,12246	0,31000	18,83	1,36	29,57	76,00	994,57	0,0	8,57	4,0
6,125	0,19141	0,08933	0,27308	10,72	1,35	66,54	85,03	992,26	4,97	3,98	8,0
6,125	0,19141	0,12127	0,26546	15,71	1,3	79,0	83,57	983,83	6,53	4,79	9,0
5,875	0,18359	0,16186	0,24800	13,4	1,56	51,57	83,86	982,71	5,51	5,57	5,0
5,5	0,17188	0,15217	0,02355	12,79	1,56	53,71	83,43	989,43	9,79	5,66	1,0
3,875	0,12109	0,27852	0,22449	8,64	1,5	87,29	86,71	986,43	11,69	1,96	2,0
2,875	0,08984	0,13333	0,29310	11,39	1,71	41,57	81,71	995,0	0,07	5,13	1,0
1,375	0,04297	0,03841	0,15452	12,13	1,27	64,71	83,71	990,71	4,19	3,96	2,0
2	0,0625	0,05333	0,00000	10,0	1,09	56,57	80,14	1001,14	0,11	5,06	1,0
1,375	0,04297	0,01365	0,00000	5,57	1,05	90,57	91,29	1000,71	0,13	1,13	2,0
1,75	0,05469	0,0473	0,00000	5,72	1,03	82,83	93,17	999,67	7,78	1,48	4,0

Table 9: Number of borrowed bicycles for Ločna-Seidlova cesta station

D	ND	BC	CC	T	WV	C	RH	AP	R	SD	Y
2,125	0,06641	0,09079	0,10417	14,27	1,56	64,86	73,57	984,57	4,49	4,57	0,0
2,625	0,08203	0,08794	0,00000	14,3	1,77	25,71	60,00	992,57	1,67	10,54	1,0
7,125	0,22266	0,29539	0,26667	14,76	2,49	73,86	72,00	988,0	3,03	4,66	7,0
5,25	0,16406	0,06159	0,25926	15,63	1,78	70,08	74,62	992,15	2,94	4,7	6,0
6,125	0,19141	0,27587	0,24219	14,96	1,44	66,63	73,84	995,68	3,83	5,29	3,0
4,125	0,12891	0,17344	0,12281	17,54	1,55	52,43	66,86	984,71	1,19	7,59	6,0
4,125	0,12891	0,17651	0,18367	18,11	1,73	34,14	73,00	985,29	5,04	8,47	1,0
3	0,09375	0,08487	0,25806	18,8	1,33	75,14	80,00	986,25	7,63	5,59	4,0
3,25	0,10156	0,15968	0,11364	20,74	1,29	42,29	66,29	992,29	2,13	10,2	4,0
4	0,125	0,19048	0,26875	21,73	1,39	43,29	75,86	988,43	2,09	8,79	3,0
6,25	0,19531	0,14519	0,15984	21,24	1,37	16,71	65,29	990,57	3,06	12,19	4,0
5,5	0,17188	0,12952	0,22043	17,6	1,63	48,63	72,63	991,88	4,68	10,05	7,0
4,125	0,12891	0,10127	0,27273	21,3	1,0	42,57	77,57	990,14	6,93	8,64	6,0
3,125	0,09766	0,0454	0,30000	25,03	1,2	21,71	73,43	990,29	1,33	11,41	6,0
3,5	0,10938	0,06148	0,28564	20,36	1,49	67,71	84,71	989,0	6,99	5,21	5,0
3,75	0,11719	0,08762	0,27500	23,16	1,03	29,86	79,14	990,14	2,64	8,89	4,0
5,125	0,16016	0,11725	0,24576	19,58	1,36	46,8	73,85	990,46	3,9	8,27	3,0
5,625	0,17578	0,15037	0,33108	21,91	1,59	49,43	70,43	987,43	0,13	8,33	7,0
5,875	0,18359	0,1379	0,28400	17,44	1,27	39,57	80,29	991,0	11,13	6,23	9,0
5,5	0,17188	0,12246	0,31000	18,83	1,36	29,57	76,00	994,57	0,0	8,57	4,0
6,125	0,19141	0,08933	0,27308	10,72	1,35	66,54	85,03	992,26	4,97	3,98	9,0
6,125	0,19141	0,12127	0,26546	15,71	1,3	79,0	83,57	983,83	6,53	4,79	13,0
5,875	0,18359	0,16186	0,24800	13,4	1,56	51,57	83,86	982,71	5,51	5,57	13,0
5,5	0,17188	0,15217	0,02355	12,79	1,56	53,71	83,43	989,43	9,79	5,66	12,0
3,875	0,12109	0,27852	0,22449	8,64	1,5	87,29	86,71	986,43	11,69	1,96	8,0
2,875	0,08984	0,13333	0,29310	11,39	1,71	41,57	81,71	995,0	0,07	5,13	6,0
1,375	0,04297	0,03841	0,15452	12,13	1,27	64,71	83,71	990,71	4,19	3,96	1,0
2	0,0625	0,05333	0,00000	10,0	1,09	56,57	80,14	1001,14	0,11	5,06	3,0
1,375	0,04297	0,01365	0,00000	5,57	1,05	90,57	91,29	1000,71	0,13	1,13	0,0
1,75	0,05469	0,0473	0,00000	5,72	1,03	82,83	93,17	999,67	7,78	1,48	0,0

Table 10: Number of borrowed bicycles for the Novi trg station

D	ND	BC	CC	T	WV	C	RH	AP	R	SD	Y
2,125	0,06641	0,09079	0,10417	14,27	1,56	64,86	73,57	984,57	4,49	4,57	1,0
2,625	0,08203	0,08794	0,00000	14,3	1,77	25,71	60,00	992,57	1,67	10,54	4,0
7,125	0,22266	0,29539	0,26667	14,76	2,49	73,86	72,00	988,0	3,03	4,66	5,0
5,25	0,16406	0,08159	0,25926	15,63	1,78	70,08	74,62	992,15	2,94	4,7	4,0
6,125	0,19141	0,27587	0,24219	14,96	1,44	66,63	73,84	995,68	3,83	5,29	3,0
4,125	0,12891	0,17344	0,12281	17,54	1,55	52,43	66,86	984,71	1,19	7,59	5,0
4,125	0,12891	0,17651	0,18367	18,11	1,73	34,14	73,00	985,29	5,04	8,47	3,0
3	0,09375	0,08487	0,25806	18,8	1,33	75,14	80,00	986,25	7,63	5,59	0,0
3,25	0,10156	0,15968	0,11364	20,74	1,29	42,29	66,29	992,29	2,13	10,2	2,0
4	0,125	0,19048	0,26875	21,73	1,39	43,29	75,86	988,43	2,09	8,79	2,0
6,25	0,19531	0,14519	0,15984	21,24	1,37	16,71	65,29	990,57	3,06	12,19	3,0
5,5	0,17188	0,12952	0,22043	17,6	1,63	48,63	72,63	991,88	4,68	10,05	3,0
4,125	0,12891	0,10127	0,27273	21,3	1,0	42,57	77,57	990,14	6,93	8,64	8,0
3,125	0,09766	0,0454	0,30000	25,03	1,2	21,71	73,43	990,29	1,33	11,41	1,0
3,5	0,10938	0,06148	0,28564	20,36	1,49	67,71	84,71	989,0	6,99	5,21	2,0
3,75	0,11719	0,08762	0,27500	23,16	1,03	29,86	79,14	990,14	2,64	8,89	1,0
5,125	0,16016	0,11725	0,24576	19,58	1,36	46,8	73,85	990,46	3,9	8,27	6,0
5,625	0,17578	0,15037	0,33108	21,91	1,59	49,43	70,43	987,43	0,13	8,33	3,0
5,875	0,18359	0,1379	0,28400	17,44	1,27	39,57	80,29	991,0	11,13	6,23	5,0
5,5	0,17188	0,12246	0,31000	18,83	1,36	29,57	76,00	994,57	0,0	8,57	3,0
6,125	0,19141	0,08933	0,27308	10,72	1,35	66,54	85,03	992,26	4,97	3,98	2,0
6,125	0,19141	0,12127	0,26546	15,71	1,3	79,0	83,57	983,83	6,53	4,79	3,0
5,875	0,18359	0,16186	0,24800	13,4	1,56	51,57	83,86	982,71	5,51	5,57	0,0
5,5	0,17188	0,15217	0,02355	12,79	1,56	53,71	83,43	989,43	9,79	5,66	1,0
3,875	0,12109	0,27852	0,22449	8,64	1,5	87,29	86,71	986,43	11,69	1,96	0,0
2,875	0,08984	0,13333	0,29310	11,39	1,71	41,57	81,71	995,0	0,07	5,13	1,0
1,375	0,04297	0,03841	0,15452	12,13	1,27	64,71	83,71	990,71	4,19	3,96	0,0
2	0,0625	0,05333	0,00000	10,0	1,09	56,57	80,14	1001,14	0,11	5,06	0,0
1,375	0,04297	0,01365	0,00000	5,57	1,05	90,57	91,29	1000,71	0,13	1,13	0,0
1,75	0,05469	0,0473	0,00000	5,72	1,03	82,83	93,17	999,67	7,78	1,48	0,0

Table 11: Number of borrowed bicycles for the Bršljin Primary School station

D	ND	BC	CC	T	WV	C	RH	AP	R	SD	Y
2,125	0,06641	0,09079	0,10417	14,27	1,56	64,86	73,57	984,57	4,49	4,57	0,0
2,625	0,08203	0,08794	0,00000	14,3	1,77	25,71	60,00	992,57	1,67	10,54	1,0
7,125	0,22266	0,29539	0,26667	14,76	2,49	73,86	72,00	988,0	3,03	4,66	4,0
5,25	0,16406	0,08159	0,25926	15,63	1,78	70,08	74,62	992,15	2,94	4,7	1,0
6,125	0,19141	0,27587	0,24219	14,96	1,44	66,63	73,84	995,68	3,83	5,29	2,0
4,125	0,12891	0,17344	0,12281	17,54	1,55	52,43	66,86	984,71	1,19	7,59	0,0
4,125	0,12891	0,17651	0,18367	18,11	1,73	34,14	73,00	985,29	5,04	8,47	0,0
3	0,09375	0,08487	0,25806	18,8	1,33	75,14	80,00	986,25	7,63	5,59	1,0
3,25	0,10156	0,15968	0,11364	20,74	1,29	42,29	66,29	992,29	2,13	10,2	0,0
4	0,125	0,19048	0,26875	21,73	1,39	43,29	75,86	988,43	2,09	8,79	0,0
6,25	0,19531	0,14519	0,15984	21,24	1,37	16,71	65,29	990,57	3,06	12,19	1,0
5,5	0,17188	0,12952	0,22043	17,6	1,63	48,63	72,63	991,88	4,68	10,05	0,0
4,125	0,12891	0,10127	0,27273	21,3	1,0	42,57	77,57	990,14	6,93	8,64	0,0
3,125	0,09766	0,0454	0,30000	25,03	1,2	21,71	73,43	990,29	1,33	11,41	3,0
3,5	0,10938	0,06148	0,28564	20,36	1,49	67,71	84,71	989,0	6,99	5,21	1,0
3,75	0,11719	0,08762	0,27500	23,16	1,03	29,86	79,14	990,14	2,64	8,89	0,0
5,125	0,16016	0,11725	0,24576	19,58	1,36	46,8	73,85	990,46	3,9	8,27	2,0
5,625	0,17578	0,15037	0,33108	21,91	1,59	49,43	70,43	987,43	0,13	8,33	1,0
5,875	0,18359	0,1379	0,28400	17,44	1,27	39,57	80,29	991,0	11,13	6,23	0,0
5,5	0,17188	0,12246	0,31000	18,83	1,36	29,57	76,00	994,57	0,0	8,57	1,0
6,125	0,19141	0,08933	0,27308	10,72	1,35	66,54	85,03	992,26	4,97	3,98	2,0
6,125	0,19141	0,12127	0,26546	15,71	1,3	79,0	83,57	983,83	6,53	4,79	3,0
5,875	0,18359	0,16186	0,24800	13,4	1,56	51,57	83,86	982,71	5,51	5,57	3,0
5,5	0,17188	0,15217	0,02355	12,79	1,56	53,71	83,43	989,43	9,79	5,66	1,0
3,875	0,12109	0,27852	0,22449	8,64	1,5	87,29	86,71	986,43	11,69	1,96	2,0
2,875	0,08984	0,13333	0,29310	11,39	1,71	41,57	81,71	995,0	0,07	5,13	0,0
1,375	0,04297	0,03841	0,15452	12,13	1,27	64,71	83,71	990,71	4,19	3,96	0,0
2	0,0625	0,05333	0,00000	10,0	1,09	56,57	80,14	1001,14	0,11	5,06	0,0
1,375	0,04297	0,01365	0,00000	5,57	1,05	90,57	91,29	1000,71	0,13	1,13	0,0
1,75	0,05469	0,0473	0,00000	5,72	1,03	82,83	93,17	999,67	7,78	1,48	0,0

Table 12: Number of borrowed bicycles for the Šmihel - Šmihel primary school station

D	ND	BC	CC	T	WV	C	RH	AP	R	SD	Y
2,125	0,06641	0,09079	0,10417	14,27	1,56	64,86	73,57	984,57	4,49	4,57	4,0
2,625	0,08203	0,08794	0,00000	14,3	1,77	25,71	60,00	992,57	1,67	10,54	2,0
7,125	0,22266	0,29539	0,26667	14,76	2,49	73,86	72,00	988,0	3,03	4,66	13,0
5,25	0,16406	0,08159	0,25926	15,63	1,78	70,08	74,62	992,15	2,94	4,7	26,0
6,125	0,19141	0,27587	0,24219	14,96	1,44	66,63	73,84	995,68	3,83	5,29	19,0
4,125	0,12891	0,17344	0,12281	17,54	1,55	52,43	66,86	984,71	1,19	7,59	5,0
4,125	0,12891	0,17651	0,18367	18,11	1,73	34,14	73,00	985,29	5,04	8,47	3,0
3	0,09375	0,08487	0,25806	18,8	1,33	75,14	80,00	986,25	7,63	5,59	1,0
3,25	0,10156	0,15968	0,11364	20,74	1,29	42,29	66,29	992,29	2,13	10,2	2,0
4	0,125	0,19048	0,26875	21,73	1,39	43,29	75,86	988,43	2,09	8,79	1,0
6,25	0,19531	0,14519	0,15984	21,24	1,37	16,71	65,29	990,57	3,06	12,19	0,0
5,5	0,17188	0,12952	0,22043	17,6	1,63	48,63	72,63	991,88	4,68	10,05	4,0
4,125	0,12891	0,10127	0,27273	21,3	1,0	42,57	77,57	990,14	6,93	8,64	3,0
3,125	0,09766	0,0454	0,30000	25,03	1,2	21,71	73,43	990,29	1,33	11,41	0,0
3,5	0,10938	0,06148	0,28564	20,36	1,49	67,71	84,71	989,0	6,99	5,21	0,0
3,75	0,11719	0,08762	0,27500	23,16	1,03	29,86	79,14	990,14	2,64	8,89	0,0
5,125	0,16016	0,11725	0,24576	19,58	1,36	46,8	73,85	990,46	3,9	8,27	2,0
5,625	0,17578	0,15037	0,33108	21,91	1,59	49,43	70,43	987,43	0,13	8,33	0,0
5,875	0,18359	0,1379	0,28400	17,44	1,27	39,57	80,29	991,0	11,13	6,23	0,0
5,5	0,17188	0,12246	0,31000	18,83	1,36	29,57	76,00	994,57	0,0	8,57	0,0
6,125	0,19141	0,08933	0,27308	10,72	1,35	66,54	85,03	992,26	4,97	3,98	1,0
6,125	0,19141	0,12127	0,26546	15,71	1,3	79,0	83,57	983,83	6,53	4,79	1,0
5,875	0,18359	0,16186	0,24800	13,4	1,56	51,57	83,86	982,71	5,51	5,57	1,0
5,5	0,17188	0,15217	0,02355	12,79	1,56	53,71	83,43	989,43	9,79	5,66	0,0
3,875	0,12109	0,27852	0,22449	8,64	1,5	87,29	86,71	986,43	11,69	1,96	1,0
2,875	0,08984	0,13333	0,29310	11,39	1,71	41,57	81,71	995,0	0,07	5,13	3,0
1,375	0,04297	0,03841	0,15452	12,13	1,27	64,71	83,71	990,71	4,19	3,96	0,0
2	0,0625	0,05333	0,00000	10,0	1,09	56,57	80,14	1001,14	0,11	5,06	0,0
1,375	0,04297	0,01365	0,00000	5,57	1,05	90,57	91,29	1000,71	0,13	1,13	1,0
1,75	0,05469	0,0473	0,00000	5,72	1,03	82,83	93,17	999,67	7,78	1,48	0,0

Table 13: Number of borrowed bicycles for Podbreznik station

D	ND	BC	CC	T	WV	C	RH	AP	R	SD	Y
2,125	0,06641	0,09079	0,10417	14,27	1,56	64,86	73,57	984,57	4,49	4,57	0,0
2,625	0,08203	0,08794	0,00000	14,3	1,77	25,71	60,00	992,57	1,67	10,54	5,0
7,125	0,22266	0,29539	0,26667	14,76	2,49	73,86	72,00	988,0	3,03	4,66	13,0
5,25	0,16406	0,08159	0,25926	15,63	1,78	70,08	74,62	992,15	2,94	4,7	6,0
6,125	0,19141	0,27587	0,24219	14,96	1,44	66,63	73,84	995,68	3,83	5,29	7,0
4,125	0,12891	0,17344	0,12281	17,54	1,55	52,43	66,86	984,71	1,19	7,59	10,0
4,125	0,12891	0,17651	0,18367	18,11	1,73	34,14	73,00	985,29	5,04	8,47	0,0
3	0,09375	0,08487	0,25806	18,8	1,33	75,14	80,00	986,25	7,63	5,59	2,0
3,25	0,10156	0,15968	0,11364	20,74	1,29	42,29	66,29	992,29	2,13	10,2	1,0
4	0,125	0,19048	0,26875	21,73	1,39	43,29	75,86	988,43	2,09	8,79	0,0
6,25	0,19531	0,14519	0,15984	21,24	1,37	16,71	65,29	990,57	3,06	12,19	3,0
5,5	0,17188	0,12952	0,22043	17,6	1,63	48,63	72,63	991,88	4,68	10,05	3,0
4,125	0,12891	0,10127	0,27273	21,3	1,0	42,57	77,57	990,14	6,93	8,64	4,0
3,125	0,09766	0,0454	0,30000	25,03	1,2	21,71	73,43	990,29	1,33	11,41	3,0
3,5	0,10938	0,06148	0,28564	20,36	1,49	67,71	84,71	989,0	6,99	5,21	3,0
3,75	0,11719	0,08762	0,27500	23,16	1,03	29,86	79,14	990,14	2,64	8,89	14,0
5,125	0,16016	0,11725	0,24576	19,58	1,36	46,8	73,85	990,46	3,9	8,27	11,0
5,625	0,17578	0,15037	0,33108	21,91	1,59	49,43	70,43	987,43	0,13	8,33	14,0
5,875	0,18359	0,1379	0,28400	17,44	1,27	39,57	80,29	991,0	11,13	6,23	10,0
5,5	0,17188	0,12246	0,31000	18,83	1,36	29,57	76,00	994,57	0,0	8,57	1,0
6,125	0,19141	0,08933	0,27308	10,72	1,35	66,54	85,03	992,26	4,97	3,98	6,0
6,125	0,19141	0,12127	0,26546	15,71	1,3	79,0	83,57	983,83	6,53	4,79	8,0
5,875	0,18359	0,16186	0,24800	13,4	1,56	51,57	83,86	982,71	5,51	5,57	5,0
5,5	0,17188	0,15217	0,02355	12,79	1,56	53,71	83,43	989,43	9,79	5,66	7,0
3,875	0,12109	0,27852	0,22449	8,64	1,5	87,29	86,71	986,43	11,69	1,96	5,0
2,875	0,08984	0,13333	0,29310	11,39	1,71	41,57	81,71	995,0	0,07	5,13	0,0
1,375	0,04297	0,03841	0,15452	12,13	1,27	64,71	83,71	990,71	4,19	3,96	3,0
2	0,0625	0,05333	0,00000	10,0	1,09	56,57	80,14	1001,14	0,11	5,06	3,0
1,375	0,04297	0,01365	0,00000	5,57	1,05	90,57	91,29	1000,71	0,13	1,13	0,0
1,75	0,05469	0,0473	0,00000	5,72	1,03	82,83	93,17	999,67	7,78	1,48	1,0

Table 14: Number of rented bicycles for Ragovska ulica station

D	ND	BC	CC	T	WV	C	RH	AP	R	SD	Y
2,125	0,06641	0,09079	0,10417	14,27	1,56	64,86	73,57	984,57	4,49	4,57	3,0
2,625	0,08203	0,08794	0,00000	14,3	1,77	25,71	60,00	992,57	1,67	10,54	0,0
7,125	0,22266	0,29539	0,26667	14,76	2,49	73,86	72,00	988,0	3,03	4,66	1,0
5,25	0,16406	0,08159	0,25926	15,63	1,78	70,08	74,62	992,15	2,94	4,7	1,0
6,125	0,19141	0,27587	0,24219	14,96	1,44	66,63	73,84	995,68	3,83	5,29	1,0
4,125	0,12891	0,17344	0,12281	17,54	1,55	52,43	66,86	984,71	1,19	7,59	3,0
4,125	0,12891	0,17651	0,18367	18,11	1,73	34,14	73,00	985,29	5,04	8,47	1,0
3	0,09375	0,08487	0,25806	18,8	1,33	75,14	80,00	986,25	7,63	5,59	0,0
3,25	0,10156	0,15968	0,11364	20,74	1,29	42,29	66,29	992,29	2,13	10,2	0,0
4	0,125	0,19048	0,26875	21,73	1,39	43,29	75,86	988,43	2,09	8,79	0,0
6,25	0,19531	0,14519	0,15984	21,24	1,37	16,71	65,29	990,57	3,06	12,19	2,0
5,5	0,17188	0,12952	0,22043	17,6	1,63	48,63	72,63	991,88	4,68	10,05	2,0
4,125	0,12891	0,10127	0,27273	21,3	1,0	42,57	77,57	990,14	6,93	8,64	0,0
3,125	0,09766	0,0454	0,30000	25,03	1,2	21,71	73,43	990,29	1,33	11,41	2,0
3,5	0,10938	0,06148	0,28564	20,36	1,49	67,71	84,71	989,0	6,99	5,21	0,0
3,75	0,11719	0,08762	0,27500	23,16	1,03	29,86	79,14	990,14	2,64	8,89	0,0
5,125	0,16016	0,11725	0,24576	19,58	1,36	46,8	73,85	990,46	3,9	8,27	1,0
5,625	0,17578	0,15037	0,33108	21,91	1,59	49,43	70,43	987,43	0,13	8,33	1,0
5,875	0,18359	0,1379	0,28400	17,44	1,27	39,57	80,29	991,0	11,13	6,23	3,0
5,5	0,17188	0,12246	0,31000	18,83	1,36	29,57	76,00	994,57	0,0	8,57	16,0
6,125	0,19141	0,08933	0,27308	10,72	1,35	66,54	85,03	992,26	4,97	3,98	46,0
6,125	0,19141	0,12127	0,26546	15,71	1,3	79,0	83,57	983,83	6,53	4,79	38,0
5,875	0,18359	0,16186	0,24800	13,4	1,56	51,57	83,86	982,71	5,51	5,57	21,0
5,5	0,17188	0,15217	0,02355	12,79	1,56	53,71	83,43	989,43	9,79	5,66	41,0
3,875	0,12109	0,27852	0,22449	8,64	1,5	87,29	86,71	986,43	11,69	1,96	27,0
2,875	0,08984	0,13333	0,29310	11,39	1,71	41,57	81,71	995,0	0,07	5,13	19,0
1,375	0,04297	0,03841	0,15452	12,13	1,27	64,71	83,71	990,71	4,19	3,96	1,0
2	0,0625	0,05333	0,00000	10,0	1,09	56,57	80,14	1001,14	0,11	5,06	0,0
1,375	0,04297	0,01365	0,00000	5,57	1,05	90,57	91,29	1000,71	0,13	1,13	1,0
1,75	0,05469	0,0473	0,00000	5,72	1,03	82,83	93,17	999,67	7,78	1,48	0,0

Table 15: Number of borrowed bicycles for Ragovska ulica station

D	ND	BC	CC	T	WV	C	RH	AP	R	SD	Y
2,125	0,06641	0,09079	0,10417	14,27	1,56	64,86	73,57	984,57	4,49	4,57	3,0
2,625	0,08203	0,08794	0,00000	14,3	1,77	25,71	60,00	992,57	1,67	10,54	4,0
7,125	0,22266	0,29539	0,26667	14,76	2,49	73,86	72,00	988,0	3,03	4,66	10,0
5,25	0,16406	0,08159	0,25926	15,63	1,78	70,08	74,62	992,15	2,94	4,7	7,0
6,125	0,19141	0,27587	0,24219	14,96	1,44	66,63	73,84	995,68	3,83	5,29	9,0
4,125	0,12891	0,17344	0,12281	17,54	1,55	52,43	66,86	984,71	1,19	7,59	5,0
4,125	0,12891	0,17651	0,18367	18,11	1,73	34,14	73,00	985,29	5,04	8,47	7,0
3	0,09375	0,08487	0,25806	18,8	1,33	75,14	80,00	986,25	7,63	5,59	3,0
3,25	0,10156	0,15968	0,11364	20,74	1,29	42,29	66,29	992,29	2,13	10,2	0,0
4	0,125	0,19048	0,26875	21,73	1,39	43,29	75,86	988,43	2,09	8,79	8,0
6,25	0,19531	0,14519	0,15984	21,24	1,37	16,71	65,29	990,57	3,06	12,19	5,0
5,5	0,17188	0,12952	0,22043	17,6	1,63	48,63	72,63	991,88	4,68	10,05	10,0
4,125	0,12891	0,10127	0,27273	21,3	1,0	42,57	77,57	990,14	6,93	8,64	2,0
3,125	0,09766	0,0454	0,30000	25,03	1,2	21,71	73,43	990,29	1,33	11,41	5,0
3,5	0,10938	0,06148	0,28564	20,36	1,49	67,71	84,71	989,0	6,99	5,21	8,0
3,75	0,11719	0,08762	0,27500	23,16	1,03	29,86	79,14	990,14	2,64	8,89	0,0
5,125	0,16016	0,11725	0,24576	19,58	1,36	46,8	73,85	990,46	3,9	8,27	4,0
5,625	0,17578	0,15037	0,33108	21,91	1,59	49,43	70,43	987,43	0,13	8,33	3,0
5,875	0,18359	0,1379	0,28400	17,44	1,27	39,57	80,29	991,0	11,13	6,23	13,0
5,5	0,17188	0,12246	0,31000	18,83	1,36	29,57	76,00	994,57	0,0	8,57	4,0
6,125	0,19141	0,08933	0,27308	10,72	1,35	66,54	85,03	992,26	4,97	3,98	7,0
6,125	0,19141	0,12127	0,26546	15,71	1,3	79,0	83,57	983,83	6,53	4,79	2,0
5,875	0,18359	0,16186	0,24800	13,4	1,56	51,57	83,86	982,71	5,51	5,57	4,0
5,5	0,17188	0,15217	0,02355	12,79	1,56	53,71	83,43	989,43	9,79	5,66	1,0
3,875	0,12109	0,27852	0,22449	8,64	1,5	87,29	86,71	986,43	11,69	1,96	3,0
2,875	0,08984	0,13333	0,29310	11,39	1,71	41,57	81,71	995,0	0,07	5,13	0,0
1,375	0,04297	0,03841	0,15452	12,13	1,27	64,71	83,71	990,71	4,19	3,96	0,0
2	0,0625	0,05333	0,00000	10,0	1,09	56,57	80,14	1001,14	0,11	5,06	2,0
1,375	0,04297	0,01365	0,00000	5,57	1,05	90,57	91,29	1000,71	0,13	1,13	0,0
1,75	0,05469	0,0473	0,00000	5,72	1,03	82,83	93,17	999,67	7,78	1,48	0,0

Table 16: Number of rented bicycles for Slavka Gruma Street station

Bicycle rental simulation models for 15 stations

$$Y = \frac{1 \cdot BC \left(-\frac{4 \cdot 01016}{BC} + RH + \frac{1 \cdot (CC - (CC + R) RH)}{D} - TT + RH (CC + TT) + \frac{1 \cdot (-BC ND + TT)}{ND WV} \right)}{SD \left(\frac{4 \cdot 01016}{BC} + SD - ND SD - TT \right) \left(\frac{4 \cdot 01016}{BC} + SD - TT - \frac{1 \cdot R \left(-C + \frac{1 \cdot R}{BC} + SD \right) \left(-1 + \frac{4 \cdot 01016}{BC} + SD - TT \right)}{SD \left(D + RH + \frac{1 \cdot BC C}{BC + \frac{4 \cdot 01016}{TT} - ND TT} \right)} \right)}$$

Model 1: Simulation model for bicycle rental for Adria station

$$Y = 2D + ND + \frac{1 \cdot WV}{WV - RW} + \frac{1 \cdot WV}{-CCR + WV} - \frac{1 \cdot WV}{-D + \frac{1 \cdot (BC + CC + 2D + 2ND) (-ND - DR + WV)}{CWV} - \frac{1 \cdot WV}{-ND - DR + WV}}$$

$$1 \cdot \left(2D - ND + WV + \frac{1 \cdot WV}{-ND - BC R + WV} + \frac{1 \cdot WV}{-ND - CC R + WV} - \frac{1 \cdot (D - ND - BC R + WV + \frac{1 \cdot WV}{-ND - CC R + WV})}{D \left(D + ND - \frac{1 \cdot D (D + 2ND) R}{C} + \frac{1 \cdot (D + \frac{1 \cdot WV}{WV - RW})}{-ND - C R + WV} \right)} \right)$$

$$D \left(D + ND - \frac{1 \cdot D (D + 2ND) R}{C} + \frac{1 \cdot WV}{-ND - C R + R WV} \right)$$

Model 2: Simulation model for bicycle rental for the Bus Station

$$Y = 0.221253 ND \left(D + ND + \frac{1 \cdot \left(2C + 7ND - 2RH + 7SD - \frac{5.11087}{ND + \frac{1 \cdot (C + 2ND - RH + 2SD)}{SD}} \right)}{C} \right)$$

$$\left(5.59047 + SD + ND \left(C + 5ND - RH + 4SD + \frac{1 \cdot (C - \frac{5.11087}{CC - ND} + 3ND - RH + 4SD)}{C + ND + SD} - \frac{5.11087}{ND + \frac{1 \cdot (C + 2ND + DND - RH + 2SD)}{SD}} \right) \right) +$$

$$1 \cdot \left(C - \frac{5.11087}{CC - ND} + ND - RH + 3SD - \frac{5.11087 D}{2ND + \frac{1 \cdot (C - \frac{5.11087}{CC - ND} + 2ND - RH + 3SD)}{C + ND + SD}} \right) +$$

$$1 \cdot \left(-C - ND + \frac{5.11087}{CC - RH} + RH - 4SD - \frac{5.11087}{ND + \frac{1 \cdot (C + ND - RH + 2SD)}{C} + \frac{1 \cdot (C + 4ND - RH + 4SD)}{C}} - \frac{5.11087}{2ND + \frac{1 \cdot (C + 5ND - RH + 4SD)}{C}} \right)$$

Model 3: Simulation model for bicycle rental for BTC station

$$Y = \frac{1}{C} \cdot 1. \left(C - 2 CC + C ND + 1. BC \left(C - CC + \frac{1. (C - CC + ND)}{C} + ND (C - (C - ND) ND) \right) + \right. \\ \left. \frac{1. (C - ND)}{BC (-BC C (CC (C - ND) - ND) + RH)} + \frac{1. (C - ND)}{BC (-BC C (C - CC D + ND) + RH)} \right) + \\ BC ND \left(C - CC + \frac{1. (-BC CC (C - CC D + ND) + RH)}{CC (-BC C (C - CC D + ND) + RH)} + \frac{1. (-BC CC (C - CC D + ND) + RH)}{CC (RH - BC (CC (C - ND) - ND) RH)} - \right. \\ \left. BC \left(C - CC + \frac{1. (C - CC + ND)}{C} + ND \left(C - CC + (C - ND) ND + \frac{1. (C - CC + ND)}{C} \right) \right) \right) WV \Bigg)$$

Model 4: Simulation model for bicycle rental for the station for the Center - Seidlova cesta station

$$Y = BC D SD \left(WV + \frac{8.65746 CC ND}{-\frac{1.}{WV} + WV} + \frac{8.65746 CC^2 ND}{D \left(WV + \frac{8.65746 CC ND WV}{-CC + BC CC - \frac{8.65746 CC ND}{RH}} \right)} - \frac{1.}{8.65746 + \frac{1. CC WV}{-BC + BC CC + \frac{74.9516 CC^2}{RH}} + \frac{1. (8.65746 + WV)}{RH}} - \right. \\ \left. \frac{1.}{8.65746 + WV + \frac{1. (8.65746 CC + WV)}{RH}} - \frac{1. WV}{BC \left(8.65746 + \frac{1. (8.65746 + CC RH)}{RH} + \frac{1. CC WV}{-BC + BC CC - \frac{8.65746 CC ND}{RH}} \right)} \right)$$

Model 5: Simulation

model for bicycle rental for the station for the station Drska - Šegova ulica

$$Y = 0.24005 D SD + \left(0.24005 SD^2 \left(-BC + \frac{1. R (0. + BC - SD)}{BC} + 1.35725 SD \right) \right) / \\ \left(-AP - 0.0857579 \left(-0.057624 + 0.660502 R - 0.0857579 SD + \frac{1. SD}{-BC - 0.0857579 R SD^2} \right) \left(-1.514 - BC + \right. \right. \\ \left. \left. \frac{4.1658 R \left(-\frac{1. R}{SD} + 0.24005 BC \left(-BC - 0.24005 R SD^3 + \frac{1. R \left(\frac{1. R}{BC} - SD^2 \right)}{BC} \right) \right)}{BC SD} \right) \right)$$

Model 6: Simulation model for bicycle rental for the station for the Main Square station

$$\mathbf{Y} = \left(\begin{array}{c} 1. \left(R RH + \frac{1. AP}{\left(-D + \frac{1. BC}{R}\right) WV} - WV \right) \\ TT + \frac{\quad}{AP R} \end{array} \right) \left(\begin{array}{c} CC + ND + \frac{1}{AP} 1. \left(9.07701 + 2 R + TT + \right. \\ \left. CC \left(BC - R - RH - \frac{1. RH}{R - WV} \right) + CC \left(-R + \frac{1. D (2.75667 - BC - 2 RH - TT^2)}{AP R} - \frac{1. RH}{BC + R - WV} \right) + \right. \\ \left. WV - ND \left(-BC + D - ND - RH + R RH + \frac{1. RH}{-D + R} - TT^2 - \frac{1. (6.77065 R + SD) (AP + C TT)}{-RH + R RH + \frac{1. AP}{WV \left(-D + \frac{1. BC}{R (R+WV)}\right)}} \right) \right) \right)$$

Model 7: Simulation model for bicycle rental for Kandijski most station

$$\mathbf{Y} = \mathbf{D} - \frac{1. \left(-1. + D + ND - \frac{1. (D - ND - \frac{1. (D+R)}{0. + R})}{7.17952 - D + ND} \right)}{7.17952 - ND} - \left(\begin{array}{c} 1. \left(\begin{array}{c} D - ND - \frac{1. R}{7.17952 - D + ND} \\ \frac{1. (D + ND - \frac{1. (-1. + D - ND)}{7.17952 - R})}{7.17952 - R} \end{array} \right) + \left(\begin{array}{c} 1. \left(\begin{array}{c} \frac{1. (-1. + D - ND)}{7.17952 - ND} - \frac{1. R}{7.17952 - D + ND} - \frac{1. (-1. + D - ND)}{7.17952 - R} \\ \frac{1. R}{7.17952 - ND} \end{array} \right) + \left(\begin{array}{c} 1. \left(\begin{array}{c} \frac{1. (-1. + D - ND)}{7.17952 - R} \\ \frac{1. (-1. + D - ND)}{7.17952 - R} \end{array} \right) \end{array} \right) \right) \\ 7.17952 - WV
 \end{array} \right)$$

Model 8: Simulation model for bicycle rental for the Ločna-Seidlova cesta station

$$Y = 1. D + \frac{1. (CC + ND) \left(\frac{1. D}{R} + \frac{1. ND R}{-(CC+ND) R + \frac{1. SD}{DR}} \right)}{-D (CC + ND) + \frac{1. SD}{DR}} +$$

$$\frac{1. ND R}{\frac{1. SD}{DR} + 1.64588 \left(\frac{1.}{CND} + \frac{1. CC}{C \left(\frac{1. SD}{DR} - 1. ND \left(\frac{1.}{CND} + \frac{1. SD}{CND R} \right) \right)} \right)} + \frac{1. ND \left(\frac{1. ND}{-ND^2 R + \frac{1. SD}{DR}} + \frac{1. CC}{1. ND \left(\frac{1. D}{R} + \frac{1. ND}{-ND^2 R + \frac{1. SD}{DR}} \right)} \right)}{1. D + \frac{\frac{1. SD}{DR} - D \left(\frac{1.}{CND} + \frac{1. CC}{C \left(-1. ND^2 (CC+ND) + \frac{1. SD}{DR} \right)} \right)}{1. ND R}} + \frac{1. SD}{DR} - D \left(\frac{1.}{CND} + \frac{1. CC}{C \left(-1. ND^2 (CC+ND) + \frac{1. SD}{DR} \right)} \right)$$

Model 9: Simulation

model for bicycle rental for the Novi trg station

$$Y = \frac{1. R}{RH} + ND (-4.30398 + TT + 5 WV) +$$

$$1. \left(-WV - \frac{1. (-R+WV)}{R} + \frac{1. (CC+R)}{\frac{1. R}{RH} + ND (-6.45597 + TT + 3 WV) + \frac{1. (BC TT^2 + \frac{1. (CC+R) RH}{-R+WV})}{TT WV} + \frac{1. (-R + \frac{1. (CC+R) WV}{-R+WV})}{RH}} \right) +$$

$$\left(1. \left(\frac{1. RH (-CC + R + WV)}{-R + WV} + TT (-2.15199 + BC + WV) \right) \right) / \left(TT + 2.15199 (-2.15199 + TT + 2 WV + 0.464686 (-R + WV)) \right)$$

$$\left(RH \left(-2.15199 + TT + \frac{1. \left(-CC + R + \frac{1. R}{\frac{1. R}{ND} + \frac{1. \left(\frac{1. (CC+R) RH}{-R+WV} + BC TT^2 \right)}{TT WV}} - WV \right)}{\frac{1. R}{RH} + ND (-6.45597 + TT + 3 WV) + \frac{1. (BC TT^2 + \frac{1. (CC+R) RH}{-R+WV})}{TT WV} + \frac{1. (-R + \frac{1. (CC+R) WV}{-R+WV})}{RH}} \right) \right)$$

Model 10: Simulation model for bicycle rental for the Bršljin Primary School station

$$y = 0.136029 ND$$

$$\left(\frac{1 \cdot D}{D - \frac{1 \cdot (D-SD)(ND-SD)}{D}} + 0.136029 D \left(-CC + 0.136029 \left(C + \frac{0.136029 ND \left(D + \frac{1 \cdot D}{D-SD} \right)}{SD} \right) \right) (2D - SD) - SD + \right. \\ \left. 0.136029 D \left(-BC + D + \frac{1 \cdot D}{-CC + D - SD} + 2SD \right) + \frac{7.35136}{SD + \frac{1 \cdot (BC+D+SD)}{D-SD}} + \right. \\ \left. \frac{1 \cdot D}{0.136029 ND \left(\frac{1 \cdot D}{D-SD} + SD \right) + \frac{1 \cdot ND (CC+SD)}{D+0.136029 (CC+2D-SD) (7.35136+0.136029 D (BC+2SD))} \right) \right)$$

Model 11: Simulation model for bicycle rental for the station for the Šmihel - Šmihel primary school station

$$Y = -BC - WV + WV \left(WV^2 - \frac{1 \cdot \left(2 \cdot - \frac{1 \cdot \left(-\frac{2 \cdot CC}{ND (CC+WV)} + \frac{1 \cdot WV^2 \left(-\frac{1 \cdot (CC-ND+WV)}{ND (-ND+WV)} + WV (CC+WV) (BC+CC+WV) \left(WV (CC+WV) - \frac{1 \cdot (CC-ND+WV)}{WV} \right) \right)}{ND (-WV+WV^2)} \right)}{ND + \frac{1 \cdot (WV^2 (CC+WV) - \frac{1 \cdot (BC-ND+WV)}{ND (-ND+WV)})}{ND \left(-ND + \frac{1 \cdot (BC+CC-ND+WV)}{WV} \right)}} \right) \right) \\ WV + \frac{1 \cdot \left(-\frac{1 \cdot (CC-ND+WV)}{ND (-ND+WV)} + WV (CC+WV) \right) \left(WV (CC+WV) - \frac{1 \cdot (CC-ND+WV)}{WV} \right)}{ND (-ND+WV^2)}$$

Model 12: Simulation model for bicycle rental for Podbreznik station

$$\begin{aligned}
\mathbf{Y} = & D + 2 BC \left(-SD + \frac{1 \cdot (BC + D) WV}{1.17504 + BC} - \frac{1 \cdot (2 BC + WV)}{D - \frac{1 \cdot WV}{BC+R}} \right) + \\
& BC \left(-2 BC - D - WV - \frac{1 \cdot \left(-BC - WV + 1 \cdot (BC + D) WV - \frac{2 \cdot WV}{-BC+D-R-WV} \right)}{-R + \frac{1 \cdot WV}{BC+R}} + \right. \\
& \left. \frac{1 \cdot \left(\frac{1 \cdot (BC+D) (-1.17504-BC+D-WV) WV}{BC+WV} - \frac{1 \cdot \left(WV + \frac{1 \cdot WV^2}{BC(1.17504+BC)} \right)}{WV} \right)}{BC + SD} + \right. \\
& \left. D \left(1.17504 + BC \left(D - SD - \frac{1 \cdot \left(BC + D + WV - \frac{1 \cdot (BC+WV)}{WV} \right)}{BC + R} \right) \right) \right)
\end{aligned}$$

Model 13: Simulation model for bicycle rental for Ragovska ulica station

$$\mathbf{Y} = \frac{1 \cdot D}{CC \cdot ND \cdot SD \cdot TT} + BC \left(\frac{1 \cdot D}{CC \cdot ND^2 \cdot R \cdot TT^2} - WV + \frac{1 \cdot \left(-BC + \frac{1 \cdot BC \cdot ND \cdot R \cdot RH}{WV} + 1 \cdot ND^2 \cdot R \cdot TT \cdot WV \right)}{CC \cdot SD} + \right.$$

$$\left. \frac{1 \cdot D \left(\frac{1 \cdot BC \cdot ND \cdot R \cdot RH}{WV} - \frac{1 \cdot CC \left(-BC + R \cdot WV + \frac{1 \cdot WV}{TT} \right)}{BC} + \frac{1 \cdot WV}{-WV + \frac{1 \cdot \left(-BC + \frac{1 \cdot BC \cdot ND \cdot R \cdot RH}{WV} + \frac{1 \cdot WV}{TT} \right)}{SD}} \right)}{SD} - \right.$$

$$\left. \frac{1 \cdot D \left(\frac{1 \cdot BC \cdot ND \cdot R \cdot RH}{WV} - \frac{1 \cdot CC \left(-BC + \frac{1 \cdot BC \cdot ND \cdot R \cdot RH}{WV} + \frac{1 \cdot \left(BC + \frac{1 \cdot WV}{TT} \right)}{TT} \right)}{BC} + \frac{1 \cdot (1 + BC)}{-R + \frac{1 \cdot \left(-BC + ND \cdot R \cdot RH \cdot WV + \frac{1 \cdot WV}{TT} \right)}{SD}} \right)}{SD} \right)$$

Model 14: Simulation model for renting bicycles for the Ragoška ulica station

$$\begin{aligned}
Y = & WV + BC \left(D + \frac{1 \cdot SD}{D (-4.2978 CC + D + \frac{1 \cdot SD}{D (-4.2978 + CC + WV)} + \frac{0.0541387 SD}{-4.2978 + CC + CC (D + TT) + WV})} - \right. \\
& \frac{1}{D (CC + D - SD + WV)} 0.232677 \left(D + ND - D (D + TT) + \frac{1 \cdot SD}{(-4.2978 + CC + CC (CC + 2 D - TT)) WV} - \right. \\
& \left. \left. WV + WV \left(-4.2978 + CC + D + \frac{1 \cdot SD}{(-4.2978 + CC (D + TT)) WV} + WV \right) \right) \right) + \\
& \frac{1}{RH} 1 \cdot \left(TT + \frac{1 \cdot (D + SD)}{D (-4.2978 + CC + D + \frac{1 \cdot SD}{WV (-4.2978 + CC + WV)})} \right) \left(D + RH + \right. \\
& \left. \left. \frac{1 \cdot SD}{(-4.2978 CC + D + \frac{1 \cdot SD}{D (-4.2978 + CC + WV)} + \frac{0.0541387 SD}{-4.2978 + CC + CC (D + TT) + WV})} \left(WV + \frac{1 \cdot (D + SD)}{D (-4.2978 + CC + D + \frac{1 \cdot SD}{WV (-4.2978 + CC + WV)})} \right) \right) \right)
\end{aligned}$$

Model 15: Simulation model for bicycle rental for the Slavka Gruma Street station

Conclusion

In this research, I made a simulation model for renting bicycles for in-15 stations in the GoNM system.

Acknowledgement

The investment is co-financed by the Republic of Slovenia and the European Union from the European Regional Development Fund.

References

Shuttle Ground Operations Simulator (SGOS) Summary Description Manual. National Aeronautics and Space Administration KSC Document # KSC-LPS-SGOS-1000, Revision 3 CHG-A, 1995.

Heavy metals in plasters concentration (ICP -OES, SEM analysis) from Lublin (SE Poland) and Lviv (NW Ukraine) cities centers as an environment indicator

Miłosz Huber^{1*}, Lesia Lata¹, Olga Iakovleva², Victoriya Pantyley³

¹Geology, Soil Sciences and Geoinformacy Department, Earth Science and Spatial Management Faculty, Maria Curie –Skłodowska University in Lublin, Poland. Tel: +48692283572

²Department of Applied Linguistics, Faculty of Humanity, Maria Curie Skłodowska –University. 5 Maria Curie – Skłodowska Sq, Poland. L.L

³Department of Socio-Economic Geography, Department of Earth Sciences and Spatial Management, Maria Curie-Skłodowska University, 20-718 Lublin, 2cd Kraśnicka rd., Poland O.I.

*corresponding author: e-mail: mhuber@umcs.lublin.pl

Abstract

Selected plasters from the tenements from the historical centers of Lublin and Lviv cities, use to perform comparative exercises of the centers and pollutions characteristics of these cities. We do fieldwork along with documentation and sampling, microanalysis (SEM-EDS), and chemical analysis (ICP-OES). The concentrations of such elements as Fe, Cr, Cu, Mn, Ni, Pb, Zn, Cd, Ti. By looking at the overall results to the degree of those metals whose content was differentiated from the type of element. The plaster surface as a form of pollution testing allows us to determine the cumulative values in a multi-year space, which is a big advantage in the environmental study of city centers. This applies especially to elements such as cadmium, lead, titanium, arsenic, nickel, and iron. In Lublin plasters, the concentration of chromium, copper, manganese, and zinc is much higher, while in Lviv are more additions of arsenic, cadmium, lead, and nickel. That indicates more pollutions of the center of Lviv, which is coal-type of house heating and manufacturing places. Lublin is the most agricultural region.

Keywords – Environmental analysis, Lublin, Lviv, plasters, heavy metal contents, ICP-OES, SEM analysis

1. Introduction

Plaster analysis is analyzed in various places around the world [1-4]. They are designed to determine how to make them in various historical buildings. In this context, numerous analyzes are performed showing the origin of materials, the use of pigments, and their state of preservation. This type of analysis also allows us to determine the secondary processes occurring on their surface associated with their corrosion and the appearance of precipitates, stains, fungi, and mold. Isotope analyzes of the precipitates allow the determination of the origin of their components in the context of environmental pollution testing. The analyzes of precipitates showed in many cases the presence of admixtures indicating the isotope contamination of solutions of these plasters together with elements derived from a specific type of impurities [5,6]. Examination of their surface also allows for the qualitative and quantitative determination of admixtures related to the exposure of plasters in the urban atmosphere. Various solids have been found on their surface, the accumulation of which results from the adsorption of dust suspended in the city air and admixtures resulting from the specificity of the environment (e.g. corrosion of metal elements which along with rainwater are moved along the facade of houses). Therefore, examinations of plaster surfaces allow determining the ingredients from which they were made, to examine secondary processes occurring on their surface as a result of corrosion and accumulation of impurities [7-19]. To this end, systematic analyzes of plasters were carried out in the centers of the cities of Lublin and Lviv in order to be able to demonstrate their state of preservation, determine their secondary processes and examine secondary admixtures.

2. Methods

Samples taken within the old town (Table 1) were subjected to corrosion observations [20,21]. To this end, field tests were carried out, consisting of observing architectural details that allowed us to distinguish several types of corrosion and efflorescence related to human activity. In the selection of samples, attempts were made to collect counterparts with different conservation status and secondary processes. Plaster samples were taken from the facades of houses, which indicated advanced secondary processes and were not renovated for a long time. Due to the pilot nature of the work, the number of attempts was limited to around 20 from each city. The collected wall samples were observed using a Leica DM2500P optical microscope in reflected light. Subsequently, tests were performed in the micro area using a scanning electron microscope Hitachi SU6600 with an EDS attachment, 15kV beam energy, and 180s exposure of measuring in points in low vacuum conditions [20, 22-28]. The analyzed samples were also examined for the

presence of metals associated with emissions using ICP-MS and ASA methods [21,22]. These analyses were performed at the Geology, Soil Science and Geoinformacy Department at the Maria Curie – Skłodowska University in Lublin (Poland).

Sample*	Localization	Sample*	Localization
Lu01	Wall of Tysiąclecia Rd.	Lu17	3 Maja 22 St.
Lu02	Kowalska St.	Lu18	Litewski Sq./ 3 Maja St.
Lu03	Grodzka podwórze St.	Lu19	Złota 9 St.
Lu04	Plac po Farze St.	Lu20	Zamkowy Sq.
Lu05	Złota 6 St.	Lv01	Rynek 2 Sq.
Lu06	Brama Krakowska St.	Lv02	Iwana Franki 3 St.
Lu07	Lubartowska 39 St.	Lv03	Magazynowa 5 St.
Lu08	Lubartowska 24 St.	Lv04	Politechniczna 1 St.
Lu09	Ruska St.	Lv05	Szewczenki 8 St.
Lu10	Krakowskie Przedmieście 43 St.	Lv06	Pidzamcze 10 St.
Lu11	Plac Wolności 5 St.	Lv07	Odeska 14 St.
Lu12	Żmigród St.	Lv08	Oleny Stepanovny 7 St.
Lu13	Kardynała Wyszyńskiego 3 St.	Lv09	Metropolity Andreja 10 St.
Lu14	Lubartowska St./Świętoduska St.	Lv10	Bazarna 2 St.
Lu15	St. Staszica/ Potockich St.	Lv11	Prospekt Svobody 11 St.
Lu16	Niecała 10 St.	Lv12	Furmanska 4 St.

Table 1: List and localization of samples *Lu-Lublin, Lv-Lviv

3. Results

Lublin is a voivodship city since the middle ages. The first houses in this place were built in the early Middle Ages [29-34]. During the Renaissance, the city flourishes, which is visible in numerous monuments, including secular tenements. In later centuries, especially during the partitions, Lublin becomes a provincial city, and in the 20th century, it regains the rank of a provincial city again and undergoes a number of changes [33,34]. This significantly affects the use of stone in its architectural details. During the PRL, various production plants were located in Lublin, which for the most part did not withstand political changes. In Lublin, there are numerous examples of the use of various stone in architectural details and these rocks react in different ways to destructive factors associated with human activities [29-34].

Lviv already in the fourteenth became a powerful center of economic and political life in Galicia, and in the fifteenth century - the center of the principality of Rus. In the 16th century, the city received the right to "store" eastern goods, which allowed it to become one of the largest shopping centers in the region of Central and Eastern Europe [35-38]. The city was actively developing as a craft center; the number of craft guilds at that time reached about twenty. It was inhabited by representatives of many nationalities. Until the beginning of the 16th century, there were many stone buildings in Lviv, primarily sacral centers, and the lower floors of buildings at the market square and adjacent streets [39]. In 1527, the city was almost completely destroyed by a great fire, so in Lviv, it can rarely see buildings in the Gothic style, there are at most certain elements of Gothic in the architecture of the oldest buildings. After a fire in the 16th-17th centuries, the center of Lviv was rebuilt in the Baroque and Renaissance style, the most famous buildings were designed by architects from northern Italy. It is from this period that most of the buildings of the historic city center of Lviv with an area of 120 ha come from, which were included in the UNESCO World Heritage List in 1998. The decision to include this part of the city on the UNESCO list was caused by two factors: an outstanding example of combining architectural traditions and the tradition of art Eastern Europe with the traditions of Italy and Germany as well as the urban architectural landscape, as an example of the interrelationships of the city's communities with various cultural and religious traditions [40]. In 1772 Lviv, as part of Austria, became the capital of the crown country. From this period until 1917, several dozen magnificent buildings of administrative, economic and cultural significance were built in the city center, mainly in classicist and eclectic styles, and from the 20th century in the modernist style (in particular the building of the Galician Sejm, theaters, banks, courts, universities). At that time, most of the

city's industrial buildings were also created. In 1919–1939, Lviv became a provincial center in the composition of interwar Poland, but its economic and political significance slightly weakened compared to the pre-partition period. In the Soviet period and after Ukraine gained independence, only a few new buildings were built in the city center, mostly located in vacant areas or in places of former buildings, damaged for various reasons.

Field observations made it possible to determine that at present in Lublin, especially in the center, there is quite a heavy traffic and many houses are still heated with stoves. Many house walls are heavily cracked, shabby, dusty with numerous stains and efflorescence [29-34,41]. This promotes fungus and even the settlement of lichen and higher plants [42]. Research carried out inside the old town clearly shows that many of the historic houses have neglected facades to varying degrees. The walls of these tenement houses are also damaged, which improperly discharge rainwater straight to the street without the use of drain pipes connecting rainwater flow to the sewers. Such cases in Lublin are commonplace even in contemporary homes, contributing to the corrosion of buildings, not to mention the danger of pedestrians on the sidewalks. In addition, sprinkling salt on sidewalks in winter promotes the absorption of brines and their efflorescence in those parts of the walls that adhere directly to the sidewalk (Figure 1A-C).



Fig. 1: Examples of buildings in Lublin and Lviv cities. Lublin: Lubartowska St.(A), corner of Kowalska and Grodzka Streets (B), Krakowska Gate (C). Lviv: old historic building in Rynek square (D), building of interwar period (E), buildings of soviet period (F).

In many places, visible molds extend through all stories of the houses. In the worst cases, along with the loosening of the walls and the accumulation of dust, higher plants appear, which effectively destroy the walls with the root system. In the periphery of Lubartowska, Krakowskie Przedmieście streets, and 1000-year Rd there are clearly visible signs of increased pollution associated with road traffic. The houses are very dusty, the walls are gray and dirty. The condition of these walls is evident in the image of a binocular magnifier which shows the occurrence of infiltrates and secondary efflorescence, dirt, and lichen activity.

Field studies carried out in Lviv have shown that there is also a lot of urban traffic there, especially within important thoroughfares and around the Railway Station [36, 42,43]. Many buildings in the center of Lviv are restored, but today tenements are also found, whose condition indicates an urgent need for renovation also in the very center of the city. In Lviv, there are numerous examples of tenement houses from very many periods of the city's existence, representing various architectural styles. There are historical buildings from many centuries ago, many examples of which can be found even in the market square, there are houses during the Austro-Hungarian rule as well as from the inter-war and Soviet times (Figure 1D-F).

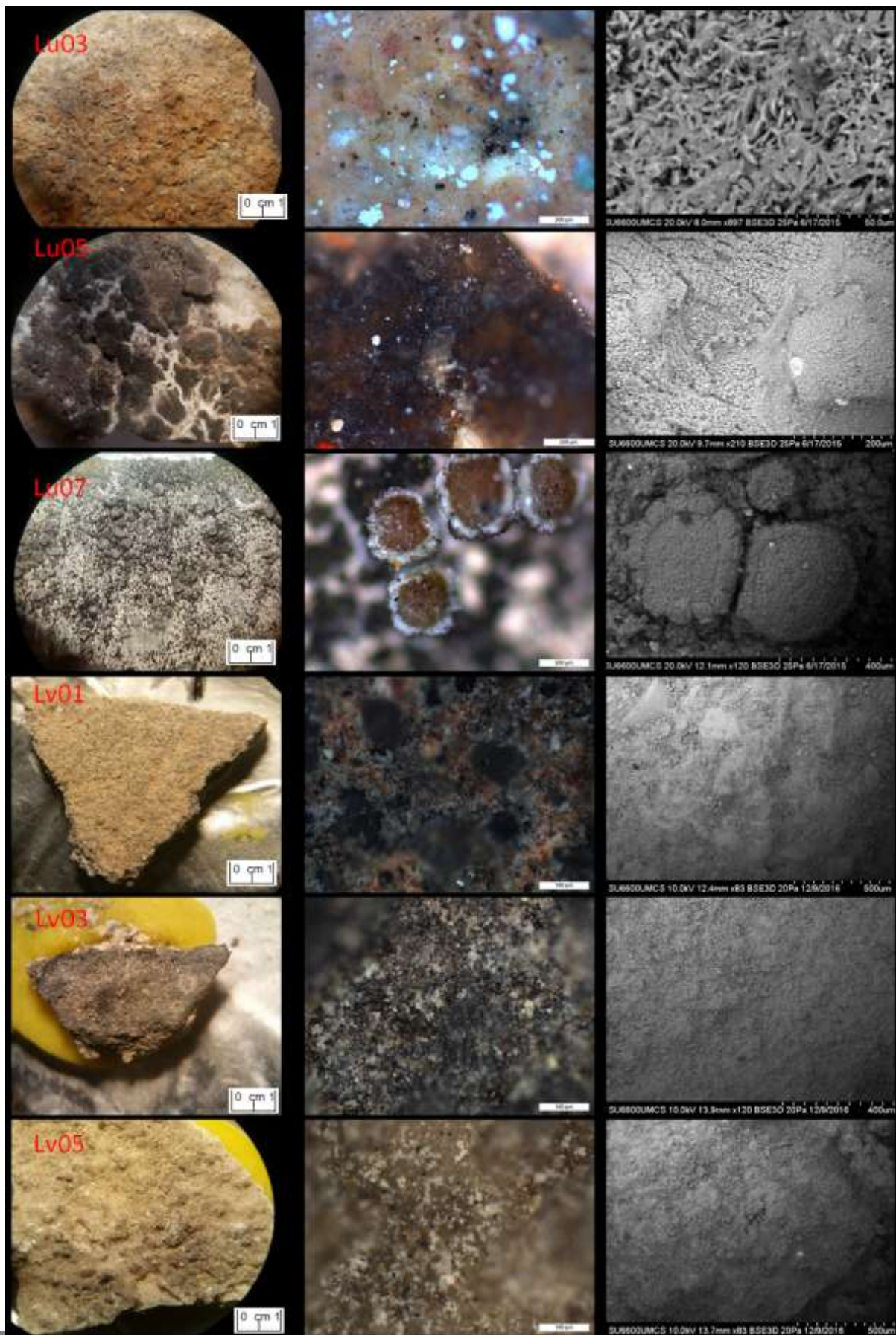


Fig. 2:

Microphotographs of selected parts of the buildings' plasters from Lublin city (sample Lu03, Lu05, Lu07) and Lviv city (samples Lv01, Lv03, Lv05) with visible fragments of paint, soot, mushrooms and precipitates made by the optical microscope (in left), polarizing microscope (center) and electron microscope (in right).

Many houses have facades whose condition indicates that they have not been renovated a long time ago, and they are often damp and molded. Reflected polarizing microscope analysis shows many traces of human activity on the plaster surface. These are various paints and their crumbs, small impurities adsorbed on the plaster surface as well as molds and lichen. The latter is quite common especially on the surfaces of low walls, fences, which usually do not have their own drainage system (Figure 2). Studies in the micro area particularly well show the presence of precipitates on the surface of plasters and the activity of living organisms.

Plaster samples were collected mainly in the very center of Lublin. Field studies and macroscopic observations have shown that at the moment in the city, especially in the center, there is quite a heavy traffic and many houses are still heated with stoves. In Lviv, around 66% of homes are heated with central heating, 27% with stoves, and 7% have individual heating (Galinfo). Characteristically, furnace heating dominates in the city center. Many houses exhibit different technical conditions, sometimes differing in appearance and advanced corrosion processes from accepted standards. The walls of these houses are heavily cracked, shabby, dusty with numerous stains and efflorescence. This promotes fungus and even the settlement of lichen and higher plants. Houses within the Market Square and Prospekt Svobody are relatively well-maintained, which was favored by the Euro 2012 championships in Lviv. The train station building has also been renovated relatively recently. The remaining places are in a different condition, many houses have facades from the pre-war period. In some homes, various stains, moisture, and solid pollutants are readable.

According to the data of the Department of Ecology and Landscape Planning of the City of Lviv, the total value of pollutants from stationary and non-stationary sources of pollution in the city was over 61 kg per capita, with 96% of all pollution coming from non-stationary sources of pollution (road, rail, and air transport). For comparison, in 2000 this rate was 92% [44]. Thermal power generation poses the biggest problem among stationary sources of pollution. According to the data of I. Strilec and M. Petrovska [37], the streets of the city center of Lviv are the most polluted, as well as its northern and southern parts, which is favored by the most intense car transport traffic in these parts of the city. According to the data of the Lviv Regional Hydrometeorological Center, the following heavy metal concentrations in the air were recorded in Lviv in 2014: Cd - 0.000, Fe - 0.519, Mn - 0.016, Cu - 0.016, Ni - 0.019, Pb - 0.022, Cr - 0.027 and Zn - 0.021 [$\mu\text{g}/\text{cm}^3$]. Compared to previous years, there was a tendency to increase the concentration of such metals as Mn, Ni, Pb and Cr in the air. The content of heavy metals in soils is tested by the State Ecological Inspection in the Lviv Oblast and in the Lviv Regional Laboratory Center of the State Sanitary Service of Ukraine, mainly in waste concentration areas. In 2014, LKP "Zbyranka" waste treatment territory was heavy metal content, with the exception of copper. The concentration of this element was 1.7 times the norm and was 5.2 [$\mu\text{g}/\text{kg}$]. The content of other heavy metals fluctuated within the norm: Zn - 11.1, Pb - 14.7, Cr - 0.045, Ni - 1.1, Co - 0.24 and Mn - 17.6 [$\mu\text{g}/\text{kg}$]. In 2015, increased content of petroleum products was found in soils at the Zbyranka garbage disposal point [33-34,45-57].

Samples	Fe	Cr	Cu	Mn	Ni	Pb	Zn	Cd	Ti	As	Summa
Lu01	4802	14,40	4,84	201,0	5,89	<	29,2	<	747	0,95	5805,28
Lu02	3834	14,20	12,20	76,6	6,71	<	34,3	<	738	<	4716,01
Lu03	1442	10,40	2,68	179,0	3,97	<	39,8	<	954	0,85	2632,70
Lu04	6869	14,30	2,39	531,0	4,60	<	28,2	<	704	1,05	8154,54
Lu05	2995	6,91	485,00	114,0	4,21	<	56,0	<	634	0,85	4295,97
Lu06	3398	14,70	66,90	126,0	8,01	<	571,0	<	507	0,64	4692,25
Lu07	4083	57,30	15,10	212,0	8,69	<	185,0	<	711	0,85	5272,94
Lu09	1349	15,30	<	37,2	4,22	<	31,2	<	908	<	2344,92
Lu11	3163	10,10	76,10	289,0	4,54	<	158,0	<	1011	0,78	4712,52

Lu12	2712	4,26	5,15	65,9	2,75	<	74,5	<	832	0,94	3697,50
Lu13	5178	11,10	10,10	142,0	6,22	<	77,1	<	945	<	6369,52
Lu14	2768	5,57	7,29	106,0	5,37	<	40,4	<	1025	<	3957,63
Lu15	2270	10,80	6,56	165,0	5,01	<	548,0	<	545	<	3550,37
Lu16	2996	7,99	<	52,7	6,92	<	196,0	<	931	0,64	4191,25
Lu17	3208	3,74	7,78	71,9	6,05	<	396,0	<	693	0,95	4387,42
Lu18	3525	33,00	<	115,0	18,60	<	136,0	<	705	<	4532,60

Table 2: Content of heavy metals in samples from Lublin city [ppm].

Studies in the micro area of plaster samples taken in the old town of Lublin have shown their large diversity. Various plaster textures, pigments, beauty agents (e.g. sand grains) are visible. Analyzes in the micro area have shown that these samples contain substances such as titanium compounds, barite, quartz grains, and feldspar (Figure 2). Many of these samples show traces of secondary processes on their surface, and these are efflorescence. The samples tested using the ICP-OES technique showed a relatively large variation in metal content (Table 2, Figure 3,4). Examined plaster samples in Lublin show a great variety. In the case of copper content, most of it was in the sample Lu05, and Lu06 and Lu11 (Figure 04).

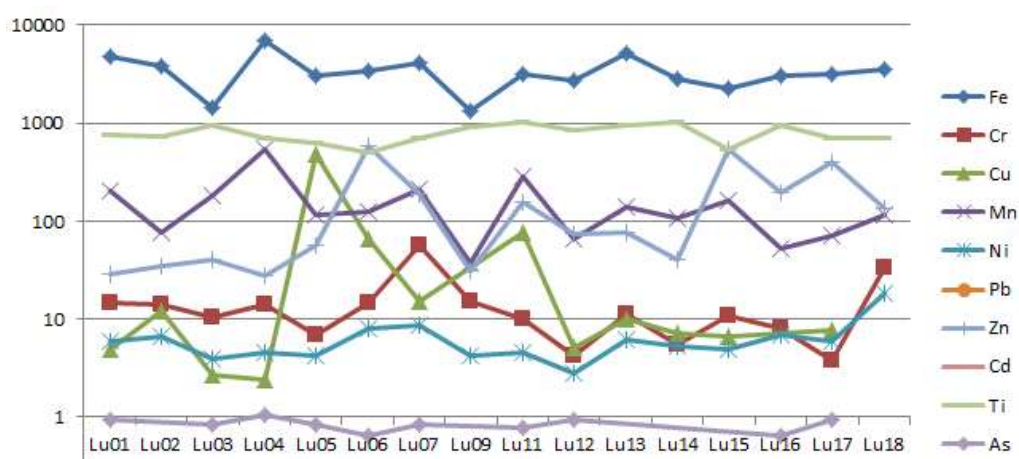


Fig. 3: Content of heavy metals in samples from buildings' plasters in Lublin city.

The lowest content of this element was found in samples Lu09 and Lu18, where the amount of Cu was below the detection limit. In the case of Manganese, Lu11 and Lu Lu07 contained most of this metal. The least copper had sample Lu09. The highest nickel content was found in the Lu18 sample, roughly twice as high as in the other samples. The last nickel was in sample Lu12. In the case of iron, the highest content of this metal was found in the sample Lu04 and the lowest in the samples Lu03 and Lu09. The share of Chromium varied from less than 4ppm for the Lu17 sample to over 75ppm for the Lu07 sample. Zinc proportions were also variable, being less than 30ppm for Lu04 and Lu01 samples and over 570ppm for Lu06 sample. Most titanium was found in samples Lu14 and Lu11 (1011 and 1025ppm, respectively), while the lowest values were found in samples Lu06 and Lu15 (507 and 545ppm, respectively). Arsenic values reached 1ppm only in sample No. Lu04, in the others they were much lower. Lead and cadmium content was not found in any of the tested samples.

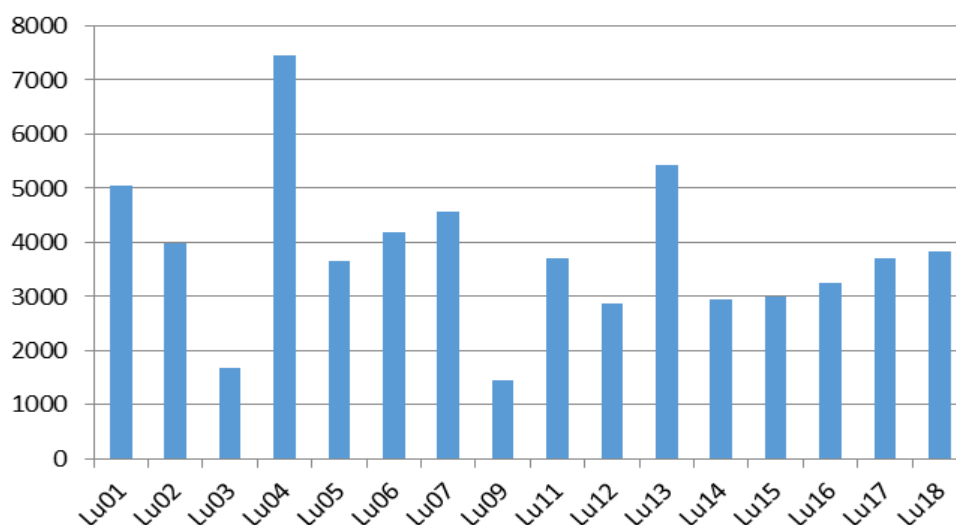


Fig. 4: Summarized content of heavy metals in samples from buildings' plasters in Lublin city.

Sample	Fe	Cr	Cu	Mn	Ni	Pb	Zn	Cd	Ti	As	Summa
LV01	3084	0,70	1,10	91,6	0,03	6,50	91,4	<	765,0	0,76	4061,09
LV02	3616	8,19	2,20	01,0	0,03	15,90	757,0	<	1011,0	1,45	5522,77
LV03	2901	6,97	4,50	75,1	0,03	11,70	214,0	7,7	934,0	0,85	4165,84
LV04	2929	0,90	9,27	73,2	0,03	7,46	80,9	5,2	687,0	1,01	3804,01
Lv05	2833	6,23	5,22	53,8	0,03	3,08	37,5	4,5	905,0	2,51	3850,84
LV06	3427	3,20	7,10	65,0	3,20	15,70	750,0	8,1	887,0	2,84	5499,15
Lv07	3041	9,31	0,70	04,0	0,90	<	36,5	<	10,4	1,42	3254,23
LV08	2550	2,50	1,70	07,0	9,90	48,00	34,8	1,1	765,3	0,98	3561,28
LV09	13587	3,50	0,50	80,0	7,70	212,00	170,0	<	992,1	1,24	15304,04
LV10	4074	4,12	8,96	66,7	4,30	9,33	28,4	<	581,3	1,03	4798,14
LV11	2886	1,54	6,52	46,8	3,60	<	21,0	<	634,5	0,72	3620,68
LV12	3028	8,50	7,98	62,5	0,10	46,70	17,7	<	981,7	1,36	4204,54

Table 3: Content of heavy metals in samples from buildings' plasters in Lviv city.

Results of the content of metals in Lublin showed that in the case of their total content, most of this type of impurities are found in the sample Lu04 and Lu13 and the lowest content of these impurities was found in two samples: Lu09 and Lu03 (Figure 5, Table 3). Samples with the highest metal content were taken from around Fara Square and from 3 Cardinal Wyszyński Street. Samples with the lowest amounts of metals come from Ruska and Grodzka Streets (yard), respectively. In turn, the tested pollution of Lviv is illustrated in Table 3, and the graphs in Figures 5 and 6. These results showed that Lv09 sample has the most iron, on average over 5 times more than in other samples where the values range from 2-3th. ppm. The Lv08 sample has the least iron (Figure 6, Table 3). In the case of chromium, the highest content was found in the Lv09 sample, being more than five times higher than in the other samples LV04, LV06 and Lv08, where these values were still high. The lowest chromium content was found in the Lv091 sample at 1.5ppm. In the case of copper, its quantity also fluctuates in the samples tested. Lv09 sample and Lv06, Lv03, and Lv02 samples have

the most copper. In turn, the lowest values of this metal were found in the Lv05 sample. The manganese content in the samples tested also undergoes some variation. Most of this element was found in the sample Lv06 and Lv09, Lv08, and Lv07 respectively.

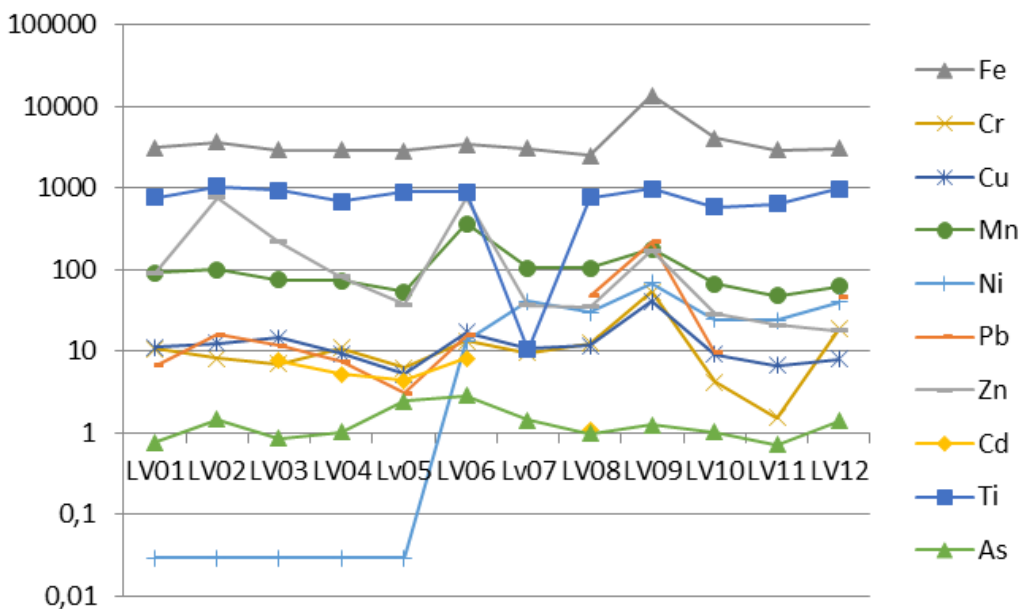


Fig. 5: Changeability of heavy metal pollution in samples from Lviv city.

Relatively the lowest manganese content was found in the Lv11 sample. The highest nickel content was tested in Lv09 and Lv 07 samples, while the lowest nickel content was found in the first five plaster samples. The most lead was found in the sample Lv09 as well as Lv08 and Lv12. In the samples like Lv07 and Lv11 this element was not found. The highest amount of zinc was found in the samples Lv06 and Lv02, the least of the wheels of this element was found in the samples Lv 12, Lv11 and Lv10. Cadmium was tested in a few samples mainly in Lv06 (highest quantity) and Lv03, Lv04, Lv05, and Lv08. In the remaining samples, cadmium was not shown. The highest amount of titanium was measured in the sample Lv02 and in the samples Lv09, Lv12, and Lv03, the lowest content of titanium was found in the sample Lv07, more than 100 times lower than the highest content of this metal. In the case of arsenic, the highest content is in the samples Lv06 and Lv 06 and the lowest in the samples Lv01 and Lv11. Considering the total amount of impurities, most of these metals were found in the Lv09 sample. And in the sample Lv 02 and Lv06 respectively (Figure 6). Relatively the lowest content of these impurities was found in the samples Lv07 and Lv08.

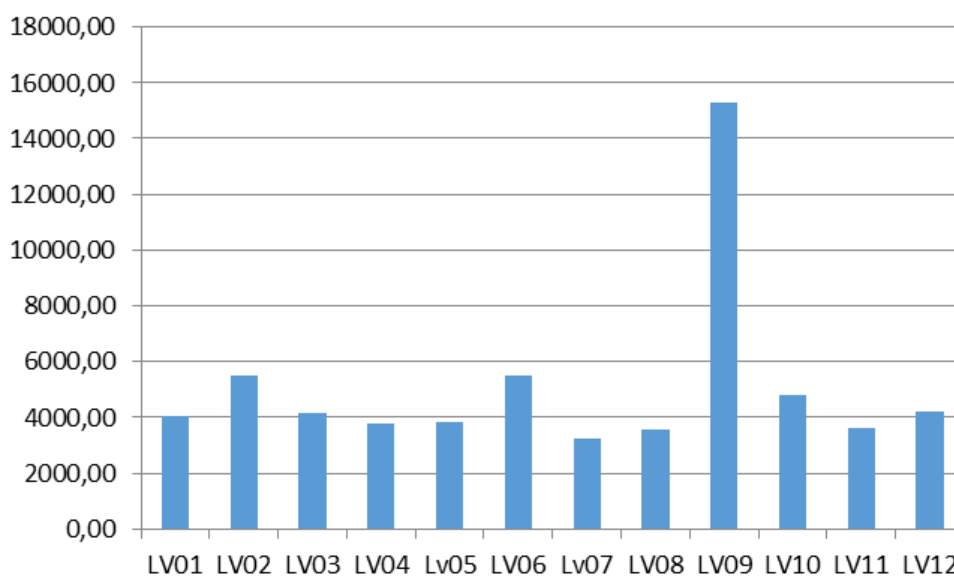


Figure 6. Average number of pollution in samples from Lviv city.

Samples containing the highest metal content come from Metropoly Andrieja, Pidzaczce, and Iwana Franko St. These streets are very busy places in the city. In addition, Pidzaczce Street is an industrial zone of the city, located near the railway station. Ivan Franko St., according to various sources, is the city's most polluted street (in the case of gas pollution). It is also one of the most congested streets in the city, especially the section near Zelena St., Fr. Roman and Lewicki St. In the case of Metropolitan Andrieja Street, the most likely source of pollution is road transport, as well as the immediate vicinity (within a 50 m radius) of a confectionery factory. Samples located in the area of Odeska and Olena Stepanivna Streets show relatively the lowest pollution, they are located slightly away from the closest city center and are located within the residential zone.

4. Discussion

Field and microscopic studies showed a relatively large diversity of samples. While macroscopic analyzes showed a different state of houses and these trends are visible in both Lublin and Lviv, studies in the micro area and chemical analyzes using ICP-OES showed relatively large fluctuations in heavy metals among the plasters tested [45-57,58,59]. Examined samples of plaster in both cities showed the presence of various types of admixtures associated with the process of their beautification, such as the use of grains of sand or muscovite for decorative purposes. Studies of their surface also showed numerous infiltrates and secondary processes resulting from the condition of the building facades. Pollution related to the appearance of lichen, algae, or moss was also visible. Studies in the micro area and chemical analyzes of plaster samples also showed the presence of numerous solid impurities on their surface. These pollutants are generally more abundant in more polluted areas (e.g. on busy streets). Similar tendencies are shown by chemical analyzes of selected metals in samples that can be correlated with secondary processes (e.g. streaks) as well as with the settlement of certain pollutants that may be related to the state of the environment in the city [45]. To this end, the contents of metals collected in plasters were compared with known data on air and soil pollution. The content of metals in samples of plaster from Lublin seems to be more uniform (Table 4). For this purpose, the average content of impurities and their amplitude (determining the difference between their maximum and minimum content) were measured. While the individual metal contents collected in the main street samples are high, the total metal content is characteristic for samples located in the city center, where traffic is not disturbed as much as air suspensions caused by heating houses using a furnace method (burning waste, etc.). Samples from Ruska Street, where bus traffic is now significantly reduced, are also due to the fact that this wall was recently renovated (washed). Comparison of Lublin and Lviv samples shows that much higher pollution amplitudes are characteristic of Lviv for most of the metals tested (iron, nickel, and zinc, lead, cadmium, arsenic), while for Lublin larger amplitudes are characteristic for copper, manganese, and titanium. For chromium, these differences are very similar.

Amplitude	Fe	Cr	Cu	Mn	Ni	Pb	Zn	Cd	Ti	As
amplitude Lu	5520	53,04	485,00	493,8	15,85		539,8		518,0	1,05
average Lu	3412	14,62	43,88	155,27	6,36		162,54		786,0	0,53
amplitudeLv	10701	51,96	35,28	318,2	67,67	212	736	8,2	1006	1006
average Lv	3996	12,97	12,97	110,56	19,99	31,36	31,36	2,2	762,9	1,34

Table 4: Comparative amplitude and average content of heavy metals in samples from buildings' plasters in Lublin and Lviv cities

Research on average metal pollution in these samples shows that compared to each other Lviv shows higher pollution in the case of iron, nickel, and lead, cadmium, titanium, and arsenic [45-57]. Lublin in the case of chromium, copper, manganese, and zinc. It follows that generally, Lviv is a city more polluted than Lublin primarily in such metals as arsenic, cadmium, lead, nickel, and iron. The conclusions of this comparison are unequivocal, indicating the urgent need to take care of the natural environment in both cities, but with a greater emphasis on Lviv.

The plasters tested include a comparative example and reference point of reference for other methods of analyzing results due to city comparison and dependence. The properties of the plaster allowing for long exposure time and the microporosity of transferring to the retention of fine us on the surface and advertising along with the results of precision search The plaster surface tests include the accumulated content of heavy metals (as shown above) indicating the state of use of the cities in question. An important advantage of plasters is the fact that they are not changed as often as soils in urban greens (fertilization), they are also active in winter when the degree of air pollution is high (no vegetation of plants). The downside is the difficulty of determining the accumulation of pollutants in a year-to-year period, but this can be determined by other research methods. The accumulated state of pollution affects vegetation (e.g. trees) and other organisms, including the human who lives in cities, breathes city air, and has direct contact with pollution. Therefore, the research method postulated by the authors has great potential.

5. Conclusions

Both Lviv and Lublin are cities with centuries-old history, in which there are many very interesting architectural styles. Tenements in both cities in the very center are generally well preserved, although in Lviv more of them are in worse condition. Studies of plasters have shown that those elements come from Lviv have a much higher total content of the studied metals than plasters from Lublin. This applies especially to elements such as cadmium, lead, titanium, arsenic, nickel, and iron. In Lublin plasters, the concentration of chromium, copper, manganese, and zinc is much higher. The plaster surface as a form of pollution testing allows determining the cumulative values in a multi-year space, which is a big advantage in the environmental study of city centers.

Ethics approval and consent to participate: not applicable.

Consent for publication: not applicable.

Availability of data and materials: not applicable.

Competing interests: the authors declare no competing interests.

Funding: not applicable.

Acknowledgments: The authors would like to thank Ukrainian colleagues, specially prof. R. Lozynskyy from Department of Geography of Ukraine, Department of Geography in Lviv National University

Authors' contributions: conceptualization: H.M., methodology: H.M., L.L., software H.M., P.V., validation I.O., P.V., investigation H.M., I.O., L.L., resources I.O., P.V., data curation L.L., H.M., writing H.M. All authors have read and agreed to the published version of the manuscript.

References

- [1]. Abadie M., Limam K., Allard F. (2001) Indoor particle pollution: effect of wall textures on particle deposition, *Building and Environment*, 36, 821-827.
- [2]. Ahmed F., Ishiga H. (2006) Trace metal concentrations in street dusts of Dhaka city, Bangladesh, *Atmos. Environ*, 40, 3835-3844.
- [3]. Anenberg S.C., Horowitz L.W., Tong D.Q., West J.J. (2010) An Estimate of the Global Burden of Anthropogenic Ozone and Fine Particulate Matter on Premature Human Mortality using Atmospheric Modeling, *Environmental Health Perspectives*, 118,9,1189-1195.
- [4]. Belkorissat R., Kadoun A. ed daim, Dupeyrat M., Khelifa B., Mathieu C. (2004) Direct Measurement of Electron Beam Scattering in the Low Vacuum SEM, *Microchim. Acta*, DOI: 10.1007/s00604-004-0182-x
- [5]. Bell M.L., Davis D.L. (2001) Reassessment of the Lethal London Fog of 1952: Novel Indicators of Acute and Chronic Consequences of Acute Exposure to Air Pollution, *Environmental Health Perspectives*, 109, 3, 389-394.
- [6]. Bell ML, Ebisu K, Peng RD, Samet JM, Dominici F. (2009) Hospital Admissions and Chemical Composition of Fine Particle Air Pollution, *American Journal of Respiratory and Critical Care Medicine*, 179, 1115-1120.
- [7]. Birulova J. O. (2008) Architecture of Lviv: times and styles XIII-XXI centuries, State University Lviv Polytechnic, Institute of Architecture, Lviv.
- [8]. Chen J., Dong L., Deng B. (1989) A study on heavy metal partitioning in sediments from Poyang Lake in China, *Hydrobiologia*, 176- 177, 159-170.
- [9]. Chen W., Qu Y., Xu Z., He F., Chen Z., Huang S. (2017) Heavy metal (Cu, Cd, Pb, Cr) washing from river sediment using biosurfactant rhamnolipid, *Environ. Sci. Pollut. Res.*, 24, 16344-16350.
- [10]. Cohen A.J., Anderson H.R., Ostra B., Dev Pandey K., Krzyzanowski M., Kunzli N., Guschmidt K., Pope A., Romieu I., Samet J.M., Smith K. (2005) The Global Burden of Disease due to Outdoor Air Pollution, *Journal of Toxicology and Environmental Health, Part A.*, 68,1-7.
- [11]. Davis D.L., Bell M., Fletcher T. (2002) A Look Back at the London Smog of 1952 and the Half Century Since, *Environmental Health Perspectives*, 110, 12, A734.
- [12]. Demoulin T., Girardet F., Flatt T.J. (2014) Reprofilng of altered building sandstones : on-site measurement of the environmental conditions and their evolution in the stone, 32èmes Rencontres de l'AUGC, Polytech Orlans, 4, 6.
- [13]. Dereń J., Haber J., Pampuch R. (1971) Chemistry of solid solution, *AGH Publ., Kraków* vol. 1, 2, 368.
- [14]. Dopovidi http://www.menr.gov.ua/docs/activity-dopovidi/regionalni/rehionalni-dopovidi-u-2014-rotsi/Lvivska_2014.pdf Accessed 23 April 2015
- [15]. European Commission, (2000) Ambient air pollution by As, Cd and Ni compounds. Position paper. Final version, European Commission DG Environment.
- [16]. Faryna M., Sztwiertnia K., Sikorski K. (2006) Simultaneous WDXS and EBSD Investigations of Dense PLZT Ceramics, *Journal of the European Ceramic Society*, 2967-2971.
- [17]. Galinfo <http://galinfo.com.ua/> Accessed 20 November 2018
- [18]. Gawarecki H. (1974) On former Lublin. Sketches of the city's pas., Ed. Lubelskie, Lublin.
- [19]. Gawarecki H., Gawdzik C. (1964) Lublin landscape and architecture, Arkady, Warsaw.
- [20]. Grondys K., Kott I., Sukiennik K. (2017) The functioning of Polish cities in the era of sustainable development from the transport point of view, *Scientific Notebooks of the Częstochowa University of Technology Management*, 25, 1, 237-245. (in Polish).
- [21]. Helfand W.H., Lazarus J., Theerman P. (2001) Donora, Pennsylvania: an Environmental Disaster of the 20th Century, *American Journal of Public Health*, 91, 4:553. 2003.
- [22]. Huang J., Huang R., Jiao J., Chen K. (2007) Speciation and mobility of heavy metals in mud in coastal reclamation areas in Shenzhen, China, *Environ. Geol.*, 53, 221-228.
- [23]. Huber M., Blicharska E., Muraczyńska B., Oszust K., Kocjan R. (2013) Application of electron and optical microscopy in biomedical research, *Innovative Materials Forum*, 165-166.
- [24]. Huber M., Hałas S., (2015) Geochemical study of precipitates in the architectural Surfaces from Bern, Switzerland, *Annales UMCS, AAA, LXX*, 113-120

- [25]. Huber M., Lata L. (2016) Environmental and pollution characteristics of the Lublin Roughcast, *Geo-Science Education Journal*, 2, 44-45.
- [26]. Huber M., Menshakova M.Y., Chmiel S., Zhigunova G.V., Dębicki R., Iakovleva O.A. (2018) Heavy metal composition in the Plantago major L. from center of the Murmansk City, Kola Peninsula, Russia, *European Journal of Biological Research*, 8, 4, 214-223
- [27]. Huber M., Mroczek P. (2012) Stone in the architecture of Lublin over the centuries, *Bulletin of the Polish Geological Institute*, 448, 441-450.
- [28]. Jędrak J., Konduracka E., Bandyta J.A, Dąbrowiecki P. (2014) Impact of air pollution on health, Municipality of the Krakow city, 144.
- [29]. Kashulina G.M. (2018) Monitoring of soil contamination by heavy metals in the impact zone of copper-nickel smelter on the Kola Peninsula, *Eurasian Soil Science*, 51, 4, 467-478.
- [30]. Kittel Ch. (1999) *Introduction to the Physics of solid solution*, PWN Publ, 356.
- [31]. Knight R.D., Klassen R.A., Hunt P. (2002) Mineralogy of fine-grained sediment by energy-dispersive spectrometry (EDS) image analysis – a methodology, *Environmental Geology*. DOI: 10.1007/s00254-002-0538-7
- [32]. Kunze K., Buzzi S., Löffler J., Burg J.P. (2008) Benefits of Low Vacuum SEM for EBSD Applications. EMC 2008 14th European, DOI: 10.1007/978-3-540-85156-1_288
- [33]. Li X.D., Lee S., Wong S., Shi W., Thornton I. (2004) The study of metal contamination in urban soils of Hongkong using a GIS-based approach, *Environmental Pollution*, 129, 113–124.
- [34]. Li X.D., Poon C., Liu P.S. (2001) Heavy metal contamination of urban soils and street dusts in Hong Kong, *Applied Geochemistry*, 16, 1361–1368.
- [35]. Lou X., Bing H., Luo Z., Wang Y., Jin L. (2019) Impacts of atmospheric particulate matter pollution on environmental biogeochemistry of trace metals in soil-plan system: A review, *Environmental Pollution* 255, 113-138.
- [36]. Luna C., Lloreda C., Almagro Bello J., Botella J., Orts M.J., Gozalb A. (2004) Design and Application of a Set of Vitreous Standards for EDS-SEM Microanalysis of Melting Shop Slags, *Microchim. Acta*. DOI: 10.1007/s00604-003-0140-z
- [37]. Luo X.S., Yu S., Zhu Y.G., Li XD. (2012) Trace metal contamination in urban soils of China. *Sci. Total Environ.* 421, 17-30.
- [38]. L'viv – the Ensemble of the Historic Centre <http://whc.unesco.org/en/list/865/> Accessed 23 October 2020
- [39]. Menclt T. (1974) *History of the Lublin Region*. PWN, Warsaw.
- [40]. Newbury D.E., Ritchie N.W.M. (2015) Performing elemental microanalysis with high accuracy and high precision by scanning electron microscopy/silicon drift detector energy-dispersive X-ray spectrometry (SEM/SDD-EDS). *J Mater Sci*. DOI: 10.1007/s10853-014-8685-2
- [41]. Patel K.S., Dahariya N.S., Chakradhari S., Sahu P.K., Rajhans K.P., Ramteke S., Lata L., Huber M. (2015) Sewage Pollution in Central India, *American Journal of Analytical Chemistry*, 6, 787-796.
- [42]. Perry P.M., Pavlik J.W., Sheets R.W., Biagioni R.N. (2005) Lead, cadmium, and zinc concentrations in plaster and mortar from structures in Jasper and Newton Counties, Missouri (Tri-State Mining District), *Sci Total Environ.*; 336, 1-3, 275-281.
- [43]. Rossini Oliva S., Fernandez Espinoza A.J. (2007) Monitoring of heavy metal in topsoils, atmospheric particles and plant leaves to identify possible contamination sources, *Microchemical Journal*, 86:131-139.
- [44]. Roy D., Singh G., Gosai N. (2015) Identification of possible sources of atmospheric PM10 using particle size, SEM-EDS and XRD analysis, Jharia Coalfield Dhanbad, India, *Environ Monit Assess*. DOI: 10.1007/s10661-015-4853-3
- [45]. Rozwałka A. (1997) *Lublin Old Town Hill in the process of forming a medieval city*, Ed. UMCS, -Lublin
- [46]. Rozwałka A., Niedźwiadek R., Stasiak M. (2006) Early medieval Lublin: a study of spatial development, *Foundation for Polish Science*. Ed. Trio, Warsaw.
- [47]. Sharma R., Patel K.S., Lata L., Huber M. (2016) Characterization of Urban Soil with SEM-EDX, *American Journal of Analytical Chemistry*, 7.
- [48]. Sharma R., Ramteke S., Patel K.S., Kumar S., Sarangi B., Agrawal S.G., Lata L., Huber M. (2015) Contamination of Lead and Mercury in Coal Basin of India, *Journal of Environmental Protection*, 6, 1430-1441.
- [49]. Shuangwen J.I. (2003) An Analysis for Forming Reason of the Plaster Rock in Shasi Segment of Zhanche sag, Fault-block Oil & Gas Field, 6, 45-58.
- [50]. Slukovskaya M.V., Vasenev V.I., Ivashchenko K.V., Morev D.V., Drogobuzhskaya S.V., Ivanova L.A., Kremenetskaya I.P. (2019) Technosols on mining wastes in the subarctic: Efficiency of remediation under Cu-Ni atmospheric pollution, *International Soil and Water Cinservation Research*, 7, 297-307.

- [51]. Sówka I.M., Bezyk Y., Pachurka Ł. (2015) Analysis and assessment of air quality in the cities area of Wrocław (Poland) and Lviv (Ukraine), *Scientific Review – Engineering and Environmental Sciences*, 68, 178-192.
- [52]. Srithawirat T., Latif M.T. (2015) Concentration of selected heavy metals in the surface dust of residential buildings in Phitsanulok, Thailand, *Environmental Earth Sciences*; 74, 3, 2701-2706.
- [53]. Strilec' I., Petrovska M. (2015) Lviv city atmospheric air quality assessment, *Constructive Geography and Geoecology, Scientific Notes*, 2:179-186.
- [54]. Tessier A., Campbell P., Bisson M. (1979) Sequential extraction procedure for the speciation of particulate trace metals, *Anal. Chem.*, 51, 7, 844-851.
- [55]. Thiel B.L. (2004) Image Formation in Low Vacuum SEM, *Microchim. Acta*, DOI: 10.1007/s00604-003-0161-7
- [56]. U Ivovi 66 zhytlovoi ploshchi
http://galinfo.com.ua/news/u_lvovi_66_zhytlovoi_ploshchi_obigrivaietsya_za_dopomogyu_tsentralizovanogo_opalenny_a_27__pichnogo_ta_7__indyvidualnogo_12819.html Accessed 15 May 2018
- [57]. Unesco <http://whc.unesco.org> Accessed 23 October 2020
- [58]. Verma N., Sharma V., Kumar R., Sharma R.T., Joshi M.C., Umopathy G.R., Ohja S., Chopra S. (2019) On the spectroscopic examination of printed documents by using a field emission scanning electron microscope with energy-dispersive X-ray spectroscopy (FE-SEM-EDS) and chemometric methods: application in forensic science, *Analytical and Bioanalytical Chemistry*. DOI: 10.1007/s00216-019-01824-z
- [59]. Weckwerth G. (2001) Verification of traffic emitted aerosol components in the ambient air of Cologne (Germany), *Atmospheric Environment* 35, 5525-5536.

Milosz Huber. Dr eng. Geologist, supervisor of the Laboratory of Optical and Electron Microscopy, specialist in the field of mineralogy, petrography, geochemistry. He is engaged in geological, fractal and stable isotope analysis research, multiple participant in polar expeditions to NE Scandinavia

Lesia Lata. Chemist, engaged in environmental research with the use of specialized ICP and ASA equipment.

Olga Iakovleva. Specialist in the field of humanities, he also studies the impact of the environment on living conditions.

Victoriya Pantyley. specialist in the field of social geography. She is involved in research on the influence of environmental factors on the community inhabiting them.

Process of robot laser hardening with different angels

Matej Babič

Faculty of information studies, Novo mesto, Slovenia

Abstract

Laser hardening is a metal surface treatment process complementary to conventional flame and induction hardening processes. A high-power laser beam is used to heat a metal surface rapidly and selectively to produce hardened case depths of up to 1,5mm with hardness value of up to 65 HRc. The high hardness of the martensitic micro-structure provides improved properties such as wear resistance and increase strength.

Introduction

Different tool steels are widely used in industrial applications based on good performance, a wide range of mechanical properties, machinability, wear resistance, and cheapness. By laser remelting the surface of the materials, we can significantly improve their wear properties. Robot laser surface remelting is one of the most promising techniques for surface modification of the microstructure of a material to improve wear and corrosion resistance. Laser hardening is a metal surface treatment process complementary to conventional flame and induction hardening processes. A high-power laser beam is used to rapidly and selectively heat a metal surface to produce hardened case depths of up to 1.5 mm with a hardness value of up to 65 HRc. The high hardness of the martensitic microstructure provides improved properties such as wear resistance and strengthAdvantages of laser hardening

- Laser is source of energy with outstanding characteristics (contactless method, controlled input of energy, high capacity, constant process, precise positioning)
- Lower costs for additional machining
- No use of cooling agents or chemicals
- High flexibility
- The process can be automated and integrated in the production process
- Local hardening
- Minimal deformation
- High accuracy
- No 3D CAD data necessary
- Hardness up to 65 HRc
- Laser width 5 – 28 mm
- Hardness depth to 1,5 mm



Fig. 1: Robot laser cell for hardening

Experimental work

We are interested in how we can achieve a hardness of hardening material, as if changing the laser beam on the substrate material. We have two options like we see on Fig 2.

First, we change $\varphi \in \{15^\circ, 30^\circ, 45^\circ, 60^\circ, 75^\circ, 90^\circ\}$ and hardening like we can see on Fig 2 (red arrow).

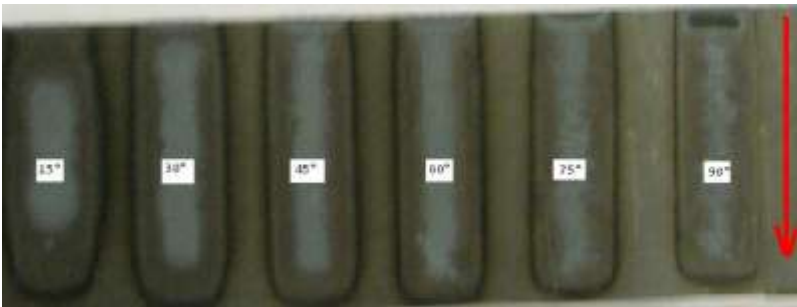


Fig 2: Robot laser hardening on different angels

We change $\varphi \in \{15^\circ, 30^\circ, 45^\circ, 60^\circ, 75^\circ, 90^\circ\}$ and hardening like we can see on Fig 3 (red arrow).

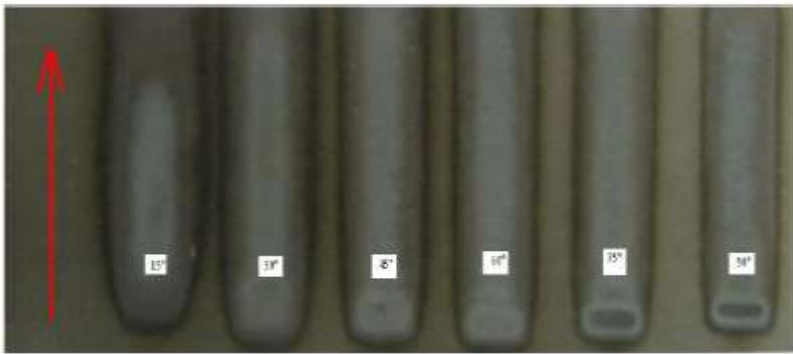


Fig 3: Robot laser hardening on different angels

Second, we change $\varphi \in \{15^\circ, 30^\circ, 45^\circ, 60^\circ, 75^\circ, 90^\circ\}$ and hardening like we can see on Fig 4 (red arrow). But we hardening like we can see on Fig 3 on right.

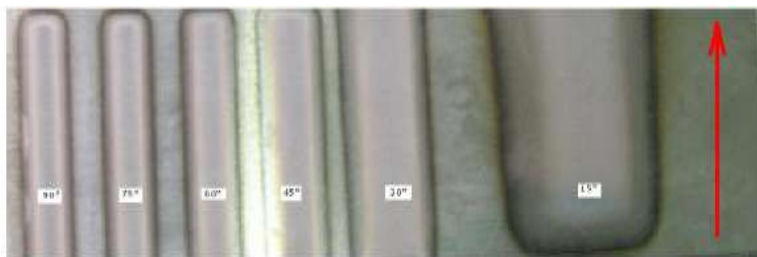


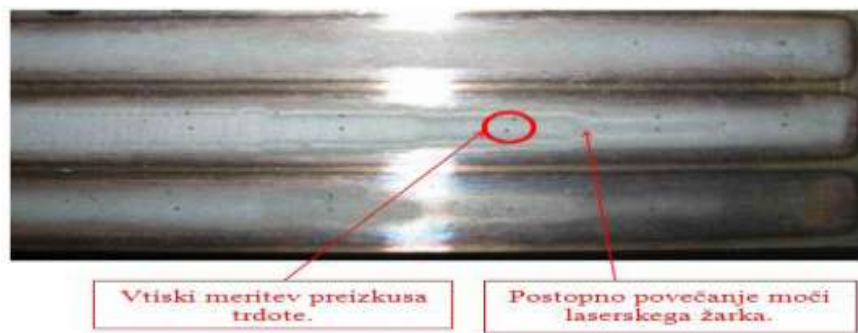
Fig 4: Robot laser hardening on different angels

We can calculated width of hadening on bellow formul (1)

$$\sin\varphi = d/x ,$$

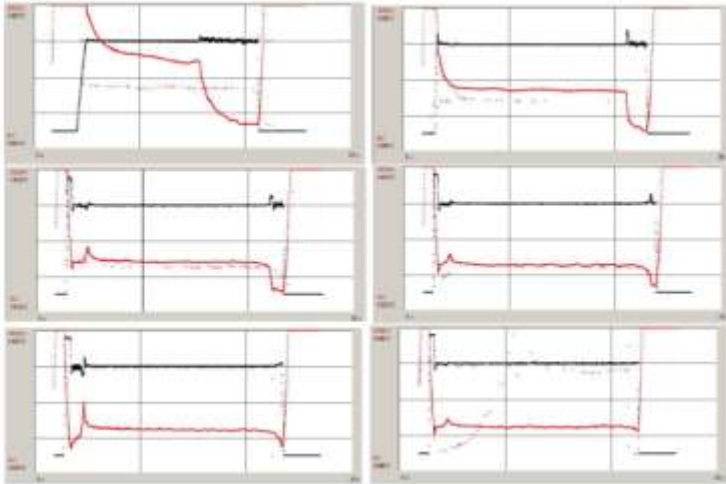
$$d \in \{5, 8, 13, 16, 23, 28\}, \varphi \in (0^\circ, 180^\circ) . \quad (1)$$

Different width of hardening we can see on Fig 5.

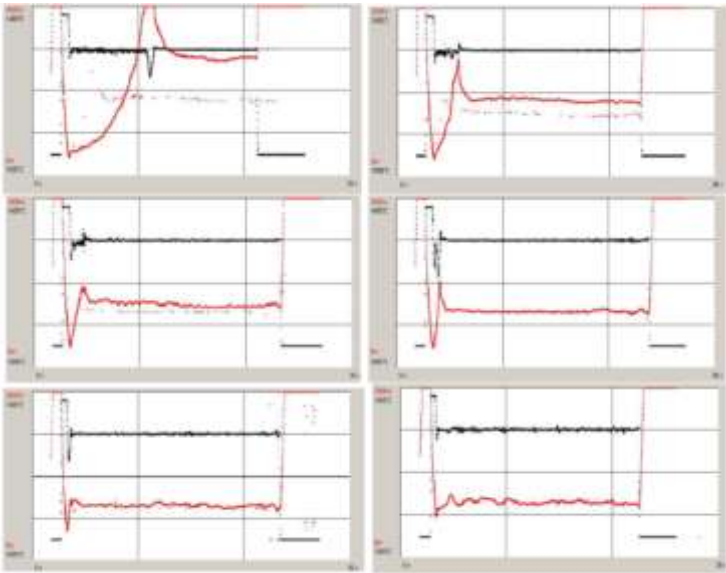


Slika 5: hardness measurements

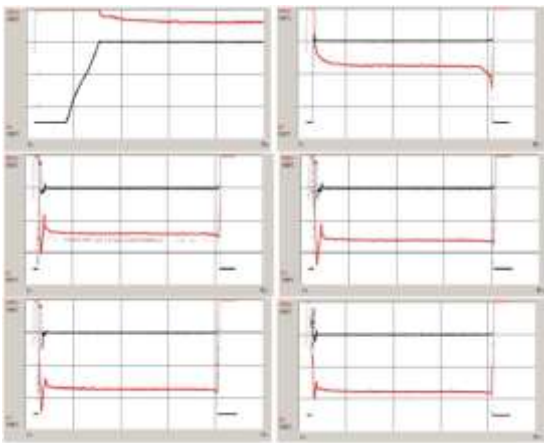
Results



Graph 1: Graph of power for Fig 2



Graph 2: Graph of power for Fig 3



Graph 3: Graph of power for Fig 4

$\varphi(^{\circ})$	Trdnost (HRc)	povprečna trdota (HRc)	trdota materiala (HRc)
15	62, 63, 63, 62, 56	61,5	9
30	59, 59, 59, 63, 62	60,4	9
45	61, 61, 61, 60, 61	60,8	9
60	61, 62, 61, 50, 56	58	9
75	61, 62, 61, 50, 61	59	9
90	61, 61, 61, 48, 62	58,6	9

Table 1: hardness for Fig 2

$\varphi(^{\circ})$	Trdnost (HRc)	povprečna trdota (HRc)	trdota materiala (HRc)
15	51, 59, 52, 57, 56	55	9
30	54, 57, 58, 56, 56	56,2	9
45	51, 56, 56, 49, 54	53,2	9
60	52, 55, 54, 54, 56	54,2	9
75	50, 55, 56, 23, 43	45,4	9
90	53, 53, 51, 44, 11	42,4	9

Table 2: hardness for Fig 3

$\varphi(^{\circ})$	Trdnost (Hrc)	povprečna trdota (HRC)	trdota materiala (HRC)
15	49, 48, 49, 61, 60	53,4	13
30	56, 57, 57, 63, 63	59,2	13
45	54, 56, 55, 64, 61	58	13
60	56, 57, 58, 63, 63	59,4	13
75	57, 57, 59, 63, 63	59,8	13
90	57, 60, 58, 58, 60	58,6	13

Table 3: hardness for Fig 4

Conclusion

Robot laser hardening is very useful in the car (eg machine parts for transmission shafts, axles, running surface, torsion springs, gears), military and aerospace industries.

Naturally, the robot laser hardening several advantages over conventional induction hardening.

However, even in the robot laser hardening have we many problems as described in this paper.

Thus, in the future that we still have enough unsolved problems in the robot laser hardening.

References

- [1] J. Grum, P. Žerovnik, R. Šturm: Measurement and Analysis of Residual Stresses after Laser Hardening and Laser Surface Melt Hardening on Flat Specimens; *Proceedings of the Conference "Quenching '96"*, Ohio, Cleveland, 1996.
- [2] B. Ryu in S. Lowen, Fractal Trac Model for Internet Simulation, Proceedings of the Fifth IEEE Symposium on Computers and Communications (ISCC 2000).

OPTIMIZATION OF ENGINEERING SOLUTIONS USING RELATIONS MONEY - TIME

Milan Vukčević¹, Mileta Janjić²

¹ Faculty of Mechanical Engineering, University of Montenegro,
Podgorica, 81000, Montenegro
milanvu@ucg.ac.me

² Faculty of Mechanical Engineering, University of Montenegro,
Podgorica, 81000, Montenegro
mileta@ucg.ac.me

Abstract

The successful economic project must meet certain technical characteristics and must be economically justified. This means, that during the creation of a project there are two key issues: whether the project is in all its stages technically correct and whether it is cost-effective. The answer to the second question provides engineering economics, and it deals with the economic viability of the project. The paper specifically deals with the importance of the time value of money, interest, and profit. It explains the basic principles used in comparing alternative engineering design solutions. Methods used in the evaluation of the economic feasibility of alternatives are discussed, as well as the manner of their application to specific examples. The consistent application of alternatives is emphasized and the most common application errors are pointed out.

Keywords – Worth Method, Internal Rate, Return Method, Money-Time

6. Introduction

Success in the global market implies that companies must make effective and rapid business decisions, and constantly invest in new projects. Engineers are the ones who are looking for solutions to specific problems, but it is necessary to examine the economic value of each solution of the specific problem together with the technical aspects. The engineering economy is the basis for the assessment of investment projects and feasibility studies. This is the monetary side of the decision that engineers make or propose.

In global conditions, the companies are in a continual race with the competition. Because of that, the firms have to enroll in economically cost-effective projects where there is a positive relation between long-range benefits and long-range costs. To bring correct decisions application methods of money-time relationships for economic analysis of engineering projects are needed [1-4].

7. APPLICATIONS OF MONEY-TIME RELATIONSHIPS

Because patterns of capital investment, revenue (or saving) cash flows, and disbursement cash flows can be quite different in various projects, there is no single method for performing engineering economic analyses that is ideal for all cases. Consequently, several methods are commonly used: Present Worth (PW), Annual Worth (AW), Future Worth (FW), and Internal Rate of Return (IRR). The first three methods convert cash flows resulting from a proposed solution into their equivalent worth at some point in time by using an interest rate known as the Minimum Attractive Rate of Return (MARR). The IRR method produces annual rates of profit, or returns, resulting from an investment, and are then compared against the MARR [4-8].

The Present Worth Method

To find the PW as a function of $i\%$ (per interest period) of a series of cash inflows and outflows, it is necessary to discount future amounts to the present by using the interest rate over the appropriate study period (years, for example) in the following manner:

$$PW(i\%) = \sum_{k=0}^N F_k (1 + i)^{-k} \quad (1)$$

Where i = effective interest rate, or MARR, per compounding period

k = index for each compounding period ($0 \leq k \leq N$)

F_k = future cash flow at the end of period k

N = number of compounding periods in the planning horizon (i.e., study period)

The relationship given in Equation 1 is based on the assumption of a constant interest rate throughout the life of a particular project. If the interest rate is assumed to change, the PW must be computed in two or more steps.

The Future Worth Method

The future worth method is based on the equivalent worth of all cash inflows and outflows at the end of the planning horizon (study period) at an interest rate that is generally the MARR. Also, the FW of a project is equivalent to its PW; that is, $FW = PW(F/P, i\%, N)$. If $FW \geq 0$ for the project, it would be economically justified. Equation 2 summarizes the general calculations necessary to determine a project's future worth:

$$FW(i\%) = \sum_{k=0}^N F_k (1 + i)^{N-k} \quad (2)$$

The Annual Worth Method

The Annual Worth (AW) of a project is an equal annual series of money amounts, for a stated study period, that is equivalent to the cash inflows and outflows at an interest rate that is generally the MARR. Hence, the AW of a project is annual equivalent revenues or savings (R) minus annual equivalent expenses (E), less its annual equivalent Capital Recovery (CR) amount. The annual equivalent value of R , E , and CR is computed for the study period, N , which is usually in years. In equation form the AW, which is a function of $i\%$, is

$$AW(i\%) = R - E - CR(i\%) \quad (3)$$

Also, we need to notice that the AW of a project is equivalent to its PW and FW. That is, $AW = PW(A/P, i\%, N)$, and $AW = FW(A/F, i\%, N)$. Hence, it can be easily computed for a project from these equivalent values.

As long as the AW is greater than or equal to zero, the project is economically attractive. An AW of zero means that an annual return exactly equal to the MARR.

There are several convenient formulas by which the CR amount (cost) may be calculated. Thus

$$CR(i\%) = I(A/P, i\%, N) - S(A/F, i\%, N) \quad (4)$$

Where I = initial investment or the project

S = salvage (market) value at the end of the study period

N = project study period

Another way to calculate the CR amount is to add an annual fund amount (or deposit) to the interest on the original investment. Thus

$$CR(i\%) = (I - S)(A/F, i\%, N) + I(i\%) \quad (5)$$

Yet another way to calculate the CR amount is to add the equivalent annual cost of the uniform loss in value of the investment to the interest on the salvage value.

$$CR(i\%) = (I - S)(A/P, i\%, N) + S(i\%) \quad (6)$$

The Internal Rate of Return Method

IRR method is the most widely used rate of return method for performing engineering analyses, it sometimes calls by several other names, such as the investor's method, discounted cash flow method, and profitability index.

By using a PW formulation, the IRR is the $i\%$ at which

$$\sum_{k=0}^N R_k \left(\frac{P}{F}, i\%, k \right) = \sum_{k=0}^N E_k \left(\frac{P}{F}, i\%, k \right) \quad (7)$$

Where R_k = net revenues or savings for the k-th year
 E_k = net expenditures including any investment costs for the k-th year
 N = project life (or study period)

Once i' has been calculated, it is compared with the MARR to assess whether the alternative in question is acceptable. If $i' \geq \text{MARR}$, the alternative is acceptable; otherwise, it is not.

A popular variation of Equation 7 for computing IRR for an alternative is to determine the i' at which its net PW is zero.

$$PW = \sum_{k=0}^N R_k \left(\frac{P}{F}, i' \%, k \right) - \sum_{k=0}^N E_k \left(\frac{P}{F}, i' \%, k \right) = 0 \quad (8)$$

The value of i' can also be determined as the interest rate at which $FW = 0$ or $AW = 0$. For example, by settings net FW equal to zero, Equation 9 would result:

$$FW = \sum_{k=0}^N R_k \left(\frac{F}{P}, i' \%, N - k \right) - \sum_{k=0}^N E_k \left(\frac{F}{P}, i' \%, N - k \right) = 0 \quad (9)$$

8. APPLICATIONS OF MONEY-TIME RELATIONSHIPS

Alternatives in economic engineering analysis are compared when they give similar results, serve the same purpose, or achieve the same function. When comparing it is important to reduce alternatives to an equivalent basis, depending on: (1) interest rates, (2) the amount of included money, (3) the timing of cash income and/or expense, and (4) how the interest, or profit, for invested capital is paid and the initial capital returned.

A comparison of alternative design solutions is based solely on economic indicators, and also analysis and comparison of possible alternatives are primarily done, and then the best alternative is selected. It is necessary to meet the primary purpose of alternative investments, that is, to create at least the minimum rate of return (MARR). The problem of how to choose the best alternative is most easily solved using rule: the alternative that requires minimal investment is chosen, and thereby generates satisfactory results unless additional capital investment in the project does not create additional benefits or greater results.

By relying on this rule, as a base is taken an acceptable alternative which requires a minimum investment. Investment in additional capital, beyond the requirements of a basic alternative, most often gives results which are reflected in an increase in capacity, an increase in quality, increasing revenue, reduction of operating costs, or an increase of lifetime. For this reason, before we decide to invest additional capital, it must be shown that each of these benefits of investment can be better than any other alternative form of investment. This means, according to this rule, we should invest more capital at a rate of return equal to or higher than the minimum profit rate (MARR) [9,10,11].

Therefore, the economic analysis of possible alternatives for a specific project needs to be done on a comparative basis. Each of the alternatives must meet the basic functions required by the project, and yet between them, there are differences in various parameters. The economic impact of these differences should be included in the cash flow or in the analysis itself.

8.1. Example of the software selection in a construction firm

The construction firm that specializes in the design and construction of commercial and residential buildings purchase of software for the design and business activities is carried out. After completion of the tender in circulation are three alternatives. Each of the alternatives requires the support of the same service, but there are differences between the investment and the profit gained from the use of new software. The observation period is ten years and the life span of all three alternatives is ten years. It is assumed that the market value after the period for all three alternatives will be zero. The minimum profit rate is 10%, and based on the data given in Table 1 a choice of alternative should be made.

	Alternative		
	A	B	C
Investment	-312 000 €	-736 000 €	-528 000 €
Annual cost savings	55 000 €	134 000 €	107 000 €
PW	25 951 €	87 372 €	129 469 €
FW	67 310 €	226 619 €	335 807 €
AW	4 223 €	14 219 €	21 070 €

Table 1: Choice of alternative for software selection

For each alternative, it is possible to find present worth PW (Equation 1), the future worth of FW (Equation 2), and the annual worth AW (Equation 3). The calculated values are given in Table 1. The ratio of $C > B > A$ is obtained.

Thus, taking into account the time value of money and reducing cash flows to the observed moment, provided the defined observation period and the minimum profit rates, alternative C shows as the best choice.

8.2. The choice of alternative for investment project of construction firm

Construction firm in order to improve the business, decided to invest in an investment project which should bring certain profit. It was found that the project can be implemented over six alternatives. An assessment of investments and expected profit was conducted for individual alternatives. The service life of each alternative is ten years and MARR is 10% for the year. The observation period is ten years and the value of an alternative at the end of the observation period is zero. Alternatives are ranked by the amount of capital invested and given in Table 2.

	Alternatives					
	A	B	C	D	E	F
Investment	90 000 €	150 000 €	250 000 €	400 000 €	500 000 €	700 000 €
Profit	15 000 €	27 600 €	40 000 €	92 500 €	112 500 €	142 500 €

Table 2: Alternatives for the investment project

For each alternative, IRR on total cash flow can be obtained by determining the interest rate for which the present worth PW (Equation 8), the future worth FW (Equation 9), or the annual value equal to zero. The values of IRR are determined individually for all alternatives and given in Table 3.

	A	B	C	D	E	F
IRR of cash flow	10,6%	13,0%	9,6%	19,1%	18,3%	15,6%

Table 3: IRR values of certain alternative

Table 3 shows that alternative C is a priori unacceptable and can be eliminated from the comparison because its IRR is less than the MARR which is 10%. Also, it can be concluded that the alternative A is a basic alternative, from which starts the procedure of analyzing the additional invested capital because it is a possible alternative ($IRR > MARR$) with a minimum investment of capital. Preliminary analysis of the feasibility of each alternative using the IRR method, PW, AW, or FW is not necessary. However, it proves to be very useful when analyzing a larger number of possible alternatives. In this way, we can immediately eliminate unfeasible alternatives, but also can easily identify a basic alternative.

It is possible that it is wrong to choose an alternative that has a maximum value of IRR on total cash flow. This means that alternative D may not be the best solution, because the maximum value of IRR does not guarantee maximum profit to the organization. For this reason, in order to come up with the right choice, we must examine each additional investment to determine if it can pay itself. Table 4 shows the analysis for the other five alternatives. IRR for additional cash flow is obtained by equalizing the difference in cash flow to zero, at all alternatives.

	A	$\Delta(B-A)$	$\Delta(D-B)$	$\Delta(E-D)$	$\Delta(F-E)$
Δ Investment	-90 000 €	-60 000 €	-250 000 €	-100 000 €	-200 000 €
Δ Profit	15 000 €	12 600 €	64 900 €	20 000 €	30 000 €
IRR_{Δ}	10,6%	16,4%	22,6%	15,1%	8,1%
Justification?	YES	YES	YES	YES	NO

Table 4: Additional cash flows

From Table 4, it follows that the alternative E will be chosen because it requires the greatest investment for which the last additional investment of capital is justified. This is because we want to invest up to 70 000 € that are available for this project, or until all available additional investment can earn 10% per year or more.

It is assumed that the available capital for the project, which is not invested in any of the possible alternatives, may be invested in another project where the profit could be made, which is equal to the minimum acceptable rate of profit. Accordingly, in this case, 20.000,00 €, which is not invested into alternative F (alternative E was selected), maybe invested elsewhere with the profit of 10% per year or more, which is higher than it would be due to the investment in alternative F (8.1%).

Three mistakes can be made when selecting possible alternatives for this type of analysis: (1) the use of the highest IRR on total cash flow, (2) use the highest IRR on additional investment, or (3) by selecting the largest investment that has an IRR greater than or equal to MARR rate. For example, in this example, we might mistakenly chose an alternative D before the alternative E because the IRR is additionally invested capital from B to D equal to 22.6% and then from D to E, only 15.1% (error 2). Much more evident error is when a choice based on IRR on total cash flow is made and the alternative D is chosen (error 1). The third mistake would be to select alternative F because it has the largest total investment with an IRR that is greater than the MARR (15.6>10%).

9. CONCLUSION

For the evaluation of the economic viability of engineering design solutions the methods of equivalent value and method of return rate are used. To make the right choice among several alternatives it is necessary to consistently apply these methods because this fashion eliminates errors and possible wrong conclusions.

On specific examples, it is shown that the engineering economics is very important, both for the designer to consider the selection of parameters for the project that he works on and for of financial directors or top management of the firm, which is approving the investment of capital in new business.

References

- [1] Sullivan W.G., Wicks E.M., Koelling C.P., (2015). *Engineering Economy* - Sixteenth Edition, Pearson Higher Education, Inc., Upper Saddle River, NJ 07458, ISBN-13: 978-0-13-343927-4.
- [2] Newnan D.G., Eschenbach T.G., Lavelle J.P., (2004). *Engineering Economic Analysis* - Ninth Edition, Oxford University Press, ISBN 0-19-516807-0.
- [3] Newnan D.G., Wheller E., (2004). *Study Guide for Engineering Economic Analysis*, Oxford University Press, ISBN 0-19-517149-7.
- [4] Vukčević M.M., (2012). *Inženjerska ekonomija*, Mašinski fakultet Podgorica, Podgorica, ISBN 978-9940-527-29-7.
- [5] Vukcevic M., Vujadinovic V., (2008). Boost Quality of Engineering Project Solutions Through Economic Analysis and Comparing Alternatives, *International Journal for Quality Research*, Vol.2, No 4, ISSN 1800-6450.
- [6] Vukčević M., Zogović S., (2007). Economical Profitability Marking of Engineering Project Solutions, *Montenegrin Journal of Economics*, Volume III, No 6, ISSN 1800-5845.
- [7] Vukčević M., Radoman A., (2011). Izbor varijanti projektnih rješenja korišćenjem relacije novac-vrijeme, *Kvalitet*, godina XXI, NO 7-8, str. 24-28, ISSN 0354-2408.
- [8] Skupnjak D., Vukčević M., (2017). Analysis of Economic Justification of Constructing a Small Hydro Power Plant, *8th International Scientific Conference Research and Development of Mechanical Elements and Systems - IRMES*, p. 321-324, ISBN 978-9940-527-53-2, Trebinje.
- [9] Vukčević M., Janjić M., Ivanović I., (2017). Profitabilnost i izbor varijanti inženjerskih projekata, Uvodno predavanje, *Konferencija održavanje i proizvodni inženjering – KODIP*, str. 17-25, Budva, ISBN 978-9940-527-51-8.
- [10] Koprivica A., Vukčević M., Šibalić N., (2019). Economic Analysis of replacement of Conventional Welding Technology with Unconventional, *International journal for science, technics and innovations for the industry: Machines, Technologies, Materials*, Year XIII, Issue 6, ISSN 1313-0226, p. 268-272.

[11] Vukčević M., Šibalić N., Damjanović M., Vasković N., (2017). Evaluation of Engineering Solutions in Wine Production, *International journal for science, technics and innovations for the industry: Machines, Technologies, Materials*, Year XI, Issue 8, ISSN 1313-0226, p. 376-379.

[12] Kurbegović R., Janjić M., Vukčević M., (2019). Engineering Economics Analysis of Water, Electricity and Abrasives Costs and their Effect on the Price of Abrasive Water Jet Machining, *1st International Conference on New Research and Development in Technical and Natural Science - ICNRDTNS*, Radenci - Slovenia, pp- 32-36, ISBN 978-961-290-461-6.

Milan Vukčević. Ph.D., 1989. Full Professor at university of Montenegro, Faculty of Mechanical Engineering.

Mileta Janjić. Ph.D., 2005. Full Professor at university of Montenegro, Faculty of Mechanical Engineering. President of Engineering Academy of Montenegro.

Fractal dimension in microstructure of hardened materials

Matej Babič

Faculty of information studies, Novo mesto, Slovenia

Abstract

Porous structure in material is one of important mechanical property which impact on hardness of materials. Many objects observed in nature are typically complex, irregular in shape, thus they can incompletely be described by Euclidean geometry. The fractal geometry is becoming increasingly popular in material science to describe complex objects. Also fractal geometry is a new method to describe complex irregular object in material science. The key in fractal geometry is fractal dimension, who describe how complexity is fractal. The aim of the present study was to find parameters of robot laser cell, which improve result of porosity after hardening process. Also we present how speed and temperature impact on porous in two different process of robot laser hardening. Over more, we present how improve result after hardening with process overlap of hardening.

Introduction

Laser hardening is a metal surface treatment process complementary to conventional process and induction hardening processes. A high-power laser beam is used to heat a metal surface rapidly and selectively to produce hardened case depths of up to 1,5mm with the hardness of the martensitic micro-structure providing improved properties such as wear resistance and increased strength. Fractal patterns are observed in computational mechanics of elastic-plastic transitions. The Fractal dimension is a property of the fractal, which is maintained through all the extensions and is therefore well denoted. In addition, it shows how complex the fractal is. The Fractal dimension is generally not calculated by the above-mentioned procedure, as this is possible only on pure mathematical constructs, which do not exist in nature.



Fig. 1: Fractal structure in nature

Experimental work

Porous structure in material is one of important mechanical property which impact on hardness of materials. We study was limited on tool steel standard label DIN standard 1.7225. We can not apply Euclidian geometry to describe porous of hardened specimens, thus we use very good method, fractal geometry. The specimen test section had a cylindrical form dimension 25×10mm (diameter × high). Specimen with the porosity about 19% to 50%, were prepared by laser, followed by hardening at $T \in [800, 2000]$ °C and $v \in [2,5]$ mm/s. Also, we changed one parameter of robot laser cell, temperature $T \in [1000, 1400]$ °C to 50 °C steps. Microstructure of specimens was observed with an field emission scanning electron microscope JSM-7600F JEOL company.



Fig 2: Robot laser material 1.7225

To investigate the possibility of application of fractal analysis to heat-treated surface, we have examined the relation between surface porosity and fractal dimensions depending on various parameters of robot laser cell. In fractal geometry is the key parameter fractal dimension, D , which should be determined complexity microstructure of robot laser hardened specimens. The relation among fractal dimension D , volume V and length L can be indicated as follows with a concept similar to Eq. (1).

$$V \sim L^D \quad (1)$$

Fractal dimension were determined using the box counting method

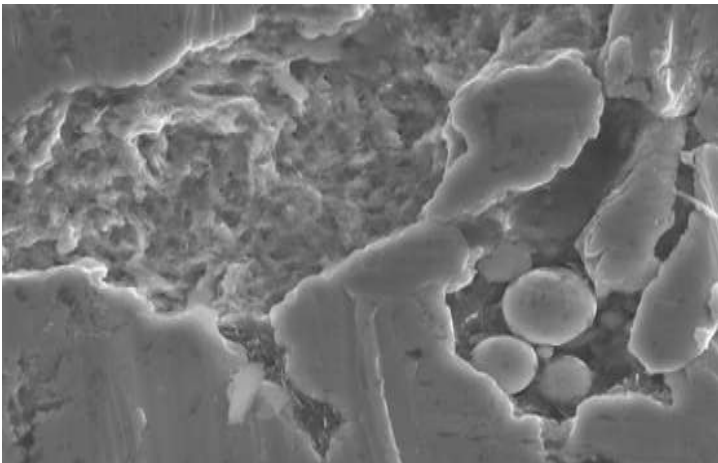


Fig 3: SEM picture of robot laser hardened specimen

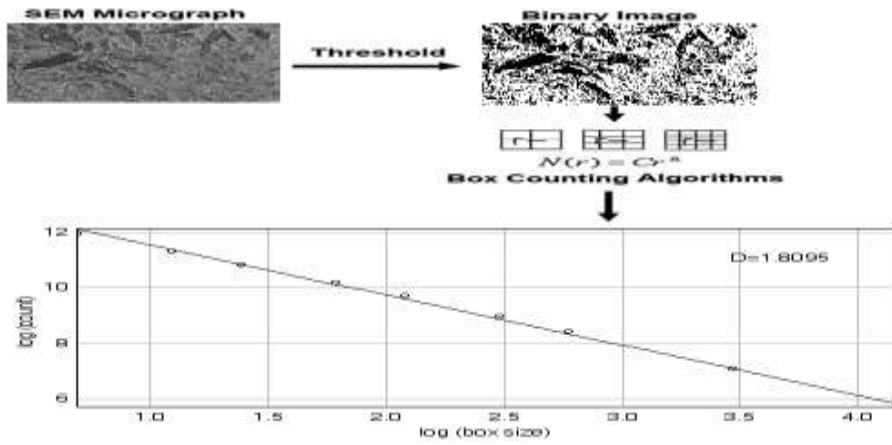
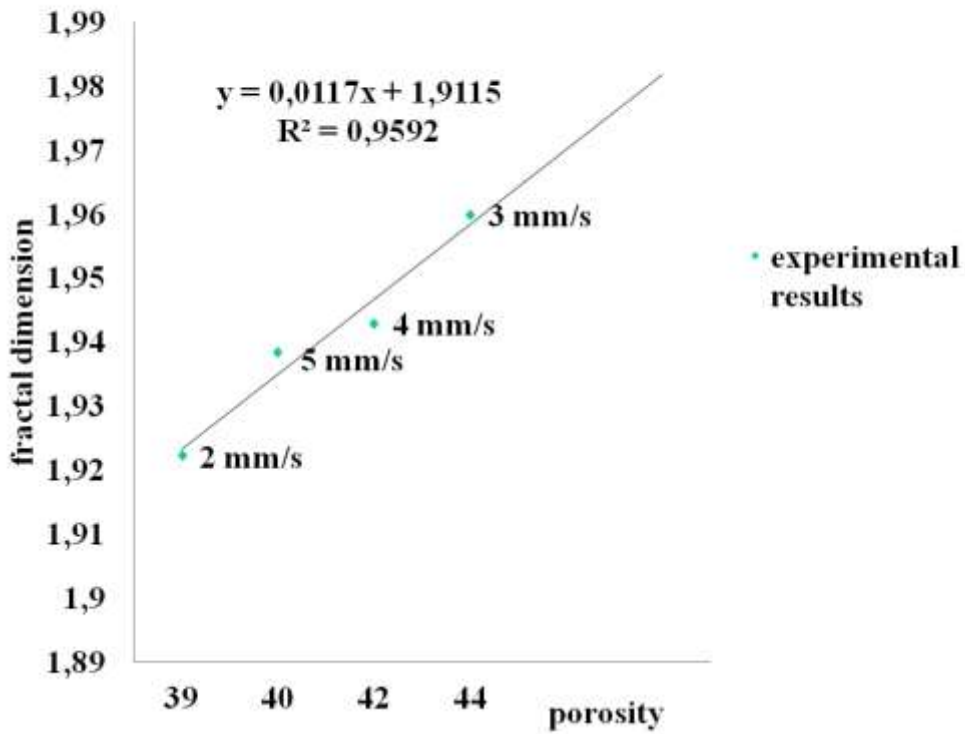
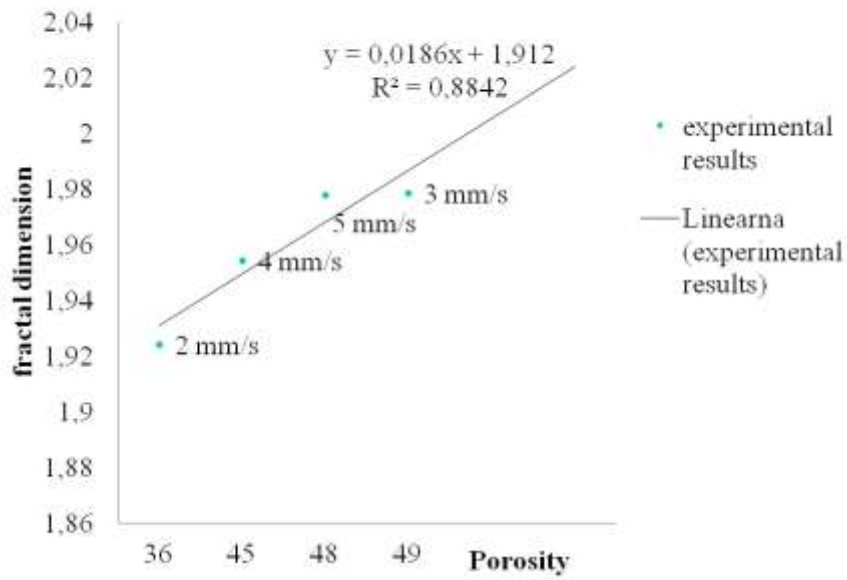


Fig 4: Calculation fractal dimension of Image

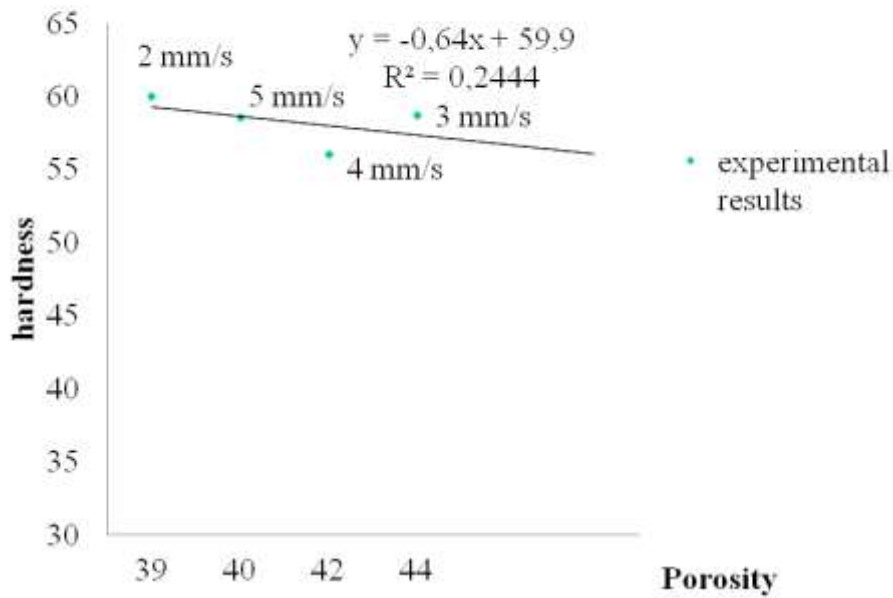
Results



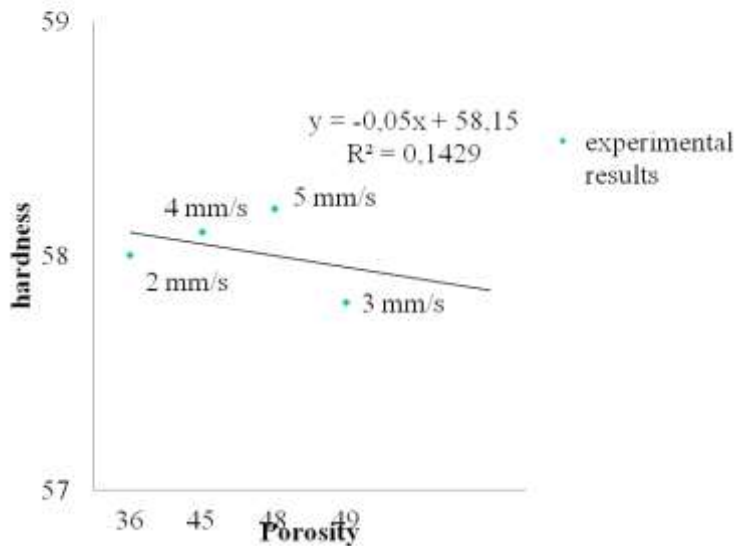
Graph 1: Relationship between fractal dimension and porosity for different speed at 1000 °C



Graph 2: Relationship between fractal dimension and porosity for different speed at 1400 °C



Graph 3: Relationship between hardness and porosity for different speed at 1000 °C



Graph 4: Relationship between hardness and porosity for different speed at 1400 °C

Conclusion

The paper present using fractal geometry to describe porous of robot laser hardened specimens with overlap. We use relative new method, fractal geometry to describe complexity of laser hardened specimens. The main findings can be summarized as follows:

1. There exist a fractal structure in the robot laser hardening specimens.
2. We describe complexity with fractal geometry of robot laser hardened specimens.
3. We have identified the optimal fractal dimension of different parameters robot laser hardened tool steel.
4. We use box-couting method to calculated fractal dimension for robot laser hardening specimens with different parameters.
5. Fractal dimension varies between 1 and 2. By increasing the temperature of the robot laser cell becomes a fractal dimension larger and grain size becomes smaller. But by increasing the temperature of the robot laser cell in hardening with overlap becomes a fractal dimension smaler. Then we can use the fractal dimension as an important factor to define the grain shape.

References

- [1] B. M. Yu, P. Cheng, A fractal permeability model for bi-dispersed porous media, International journal of Heat Mass Transfer 45 (2002) 2983–2993.
- [2] Barton, C. C., 1995, Fractal analysis of scaling and spatial clustering of fractures. In: Barton, C.C. and La Pointe, P.R. (eds.), Fractals in the earth sciences. Plenum Press. New York, p. 141–178.
- [3] Grumm J., Žerovnik, P., Šturm, R. 1996, Measurement and analysis of residual stresses after laser hardening and laser surface melt hardening on flat specimens; Proceedings of the Conference "Quenching '96", Ohio, Cleveland.

Flexural strengthening of composite pultruded bars by means of additional filament-wound composite overwrap

Szymon Duda¹, Grzegorz Lesiuk¹, Paweł Stabla¹, Paweł Zielonka¹

¹ Department of Mechanics, Materials Science and Biomedical Engineering, Wrocław University of Science and Technology
Wrocław, Lower Silesia, Poland

szymon.duda@pwr.edu.pl, grzegorz.lesiuk@pwr.edu.pl, pawel.stabla@pwr.edu.pl, pawel.zielonka@pwr.edu.pl

Abstract

This paper investigates the strengthening effect of pultruded bars under flexural loading. Pultrusion and filament winding methods were applied to manufacture and wrap the bars. The basic bar is a pultrusion-produced unidirectional carbon-reinforced polymer (CFRP). The hybrid version consists of the CFRP core overwrapped with glass fiber using the filament winding method. The four-point bending test was performed to assess the flexural behavior of these bars. The results show that the overwrapped bar can transmit a greater force, which is indicated by a higher maximum force as well as a strain energy density. The post-failure analysis provided relevant information about the failure mechanisms, that are delamination and cracking of matrix.

Keywords – Composite bars, Four-point bending test, Flexural behaviour, Pultrusion method, Filament winding method, GRFP, CFRP

10. Introduction

Pultrusion has its origins in 1951, when W.B. Gold - Sworthy applied for a patent for a device used to manufacture fishing equipment. Although the method was patented so early, it was used in large-scale production for the first time a decade later. Due to pultrusion, it has become possible to manufacture profiles from lightweight composite materials, which can successfully replace selected materials such as wood, PVC, or aluminium, in various engineering applications [1-5]. Profiles produced by the traditional pultrusion method have excellent mechanical properties in the longitudinal direction, i.e., the direction in which the roving strands are arranged. In the transverse direction, however, these properties are much worse. Therefore, a trend of the modification pultrusion system is observed in the literature using combinations of braiding [6-7] and filament winding [8]. One of the new ideas is the construction of hybrid profiles composed of different fibres and matrices to obtain an optimal structure for special applications. The potential risk of the lack of a yield region in the tensile diagrams of individual FRP members was recognised with all its indirect safety consequences in the building design. An alternative concept of ductility and buffer for tensile strength was therefore sought, in other words, to induce an actual load-bearing condition over the range of Hooke's law as a substitute for steel yield strength. In this context, such hybridization overcomes some disadvantages of the materials currently used in engineering as reinforcing bars. This paper attempts to evaluate the effect of braided reinforcement on the flexural strength of a hybrid bar. The created model will serve as a precast concrete reinforcement in further stages.

This paper shows the influence of overwrapped filaments on the composite bar. The four-point bending test is conducted to investigate the flexural behaviour of the overwrapped hybrid composite bar as well as of the unidirectional carbon fibre bar.

11. Materials & method

The specimens investigated in this paper were manufactured with a combination of two different technological processes. The unidirectional core made of carbon fibers in epoxy resin was produced by pultrusion (Fig. 1), while the overwrapped glass fibers (fibre orientation 45°) was provided using the filament winding method (Fig.2).

The pultrusion system is presented in Fig. 1. It is a continuous fiber laminating process that produces high fibre volume profiles with a constant cross section. This system consists of four subsystems (units) as follows. The fibre roving is pulled into the bath with resin provided thorough impregnation. The formed and impregnated reinforcement moves to the next stage with the heated pultrusion die, which delivers the established cross section of the profile. The appropriate pulling force is overcome by a twin reciprocating puller unit that provides the requested feed motion. Finally, the manufactured profile is cut to a certain length, set in the control panel.

Pultrusion allows the production of mainly unidirectional profiles. To enhance the mechanical strength of the manufactured bar, the filament winding method was applied. Considering the unidirectional reinforced composite bars, the greatest force can be carried in the axial direction (tension force), in the case of the other load cases such as perpendicular to the bar axis (bending moment), the load is carried mainly by the matrix. This issue can be overcome by a continuous reinforcement architecture such that the fibres are mechanically interlocked with each other. It can be given using the filament winding method (Fig.2). This process follows as a continuous fibre roving is fed through a resin bath and wound onto a rotating mandrel. The roving feed is fueled by a trolley that travels the length of the mandrel. Allows the use of various wrap patterns, increasing the mechanical strength of the bar. Furthermore, the design concept of the hybrid composite bar allows the core to be protected by using reinforced protective layers against aggressive environments.



Fig. 1: Pultrusion system. 1 - Resin impregnating unit, 2 - curing unit, 3 - pulling and control unit, 4 - cutting unit



Fig. 2: Machine for the filament winding method

In order to assess the influence of over-wrapping on the load-bearing capacity of the composite structure, it was decided to carry out comparative tests in a bending test. For the experimental campaign, two bar configurations were subjected to bending conditions. The four-point bending test was conducted on the MTS 793 servohydraulic test machine. The first set of specimens, called a hybrid,

consists of a core of carbon fibre reinforced polymer (CFRP) wound with glass fiber reinforced polymer (GFRP) indicated as follows: BG1 – BG3 (Fig. 3). The influence of the filament-wound overwrap is determined in comparison to the flexural behaviour of smooth unidirectional CFRP bar marked as CFRP1 – CFRP3. Dimension evaluation gives the diameter of the core 10 mm and thickness of the overwrap approximately 1.35 mm.



Fig. 3: Hybrid bars manufactured by the pultrusion and filament winding method. The structure consists of CFRP core and GFRP filament-wound overwrap

12. Results & discussion

This section contains the results from the four-point bending test for filament-wound overwrap and smooth pultruded bars (commonly used in industrial applications). The flexural behaviour of the bars is shown in Fig. 4, which corresponds to the reaction force with the normalized displacement. This allows one to correlating different bars in terms of diameter.

Two sets of specimens exhibit different behaviours. After reaching maximum force, CFRP samples (smooth CFRP bars) show a significant load drop (up to 50%), which is a typical effect for unidirectional composite structures. On the other hand, the hybrid bars demonstrate the pseudo-ductile behaviour provided by the GFRP overwrap (lack of the sudden force drop). This is a desirable effect that may protect against unexpected failures.

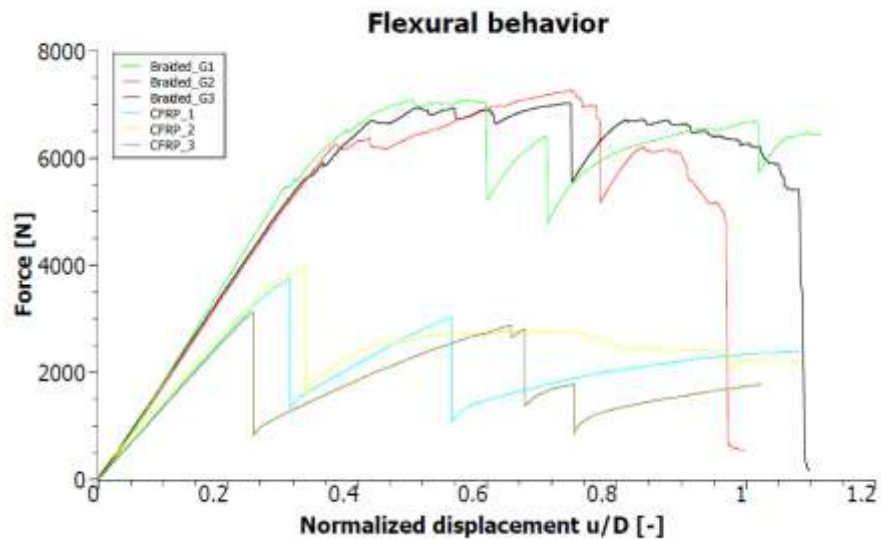


Fig. 4: Results of the Bending Test

The comparison of the results obtained is presented in Table 1. It is noticeable that the maximum force carried by the hybrid bars is approximately 3000 N higher. Furthermore, the curves vary in slope, suggesting that the stiffness of the bars may differ.

Furthermore, the strain energy density (required for static failure of the composite structure during loading) for each sample (area under load-displacement curves)—this term refers to the deformation gradient of the material per volume unit. Hybrid specimens

exhibit greater value in the wake of additional mechanically locked fibres that resist material deformation. Higher energy needs to be loaded to deform this profile's volume unit, which is crucial in the possible application to civil engineering structures.

N	Strain energy density [J/m]	Maximum force [N]
BG1	7641	7086
BG2	5054	7272
BG3	5900	7025
CFRP1	2815	3735
CFRP2	2894	3961
CFRP3	1788	3124

Table 1: Experimental and calculated data

The macroscopic failure of exemplary rods after the experiment is presented in Fig. 5 and Fig. 6 and Fig. 7, respectively. Hybrid specimens exhibited local damage in the contact area with the load support. Furthermore, changes in matrix transparency suggest that matrix cracking occurred – which was observed during the detailed SEM (Scanning Electron Microscope) study – Fig. 6. Visual inspection shows that the CFRP core was delaminated along the middle surface. Smooth CFRP samples were damaged on the surfaces perpendicular to the applied force mainly by delamination, which occurred suddenly, and the force decreased substantially.



Fig. 5: Hybrid bar after bending test. Visible local failures at the places of the applied force (load support). The white areas around suggest cracking of the matrix.

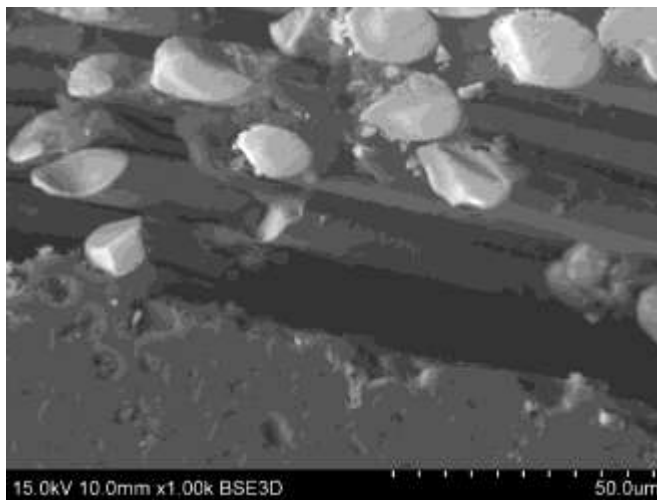


Fig. 6: Local damage of the interface and matrix at the load point of the hybrid bar, SEM BSE image



Fig. 7: Smooth CFRP bar after bending test. These samples show the brittle nature of such a structure with the type of delamination damage.

13. Conclusions

The following conclusions can be drawn.

- Two sets of specimen configurations were examined under flexural loading conditions. The four-point bending test determined the strengthening effect of the filament-wound overwrap. The smooth CFRP bars were able to transmit maximum force approximately 3600 N. Strengthened hybrid bars were able to transmit maximum force almost 7300 N. According to the obtained data, the strain energy density was calculated, provided that the filament-wound overwrap layer significantly increases the mechanical strength in the case of flexural loading conditions.
- The samples indicated various failure mechanisms. The major mechanism is delamination, which occurred in both sets of specimens. Additionally, cracking of the matrix and debonding along the interface between materials.

To summarizing, these results proves that additional reinforcement architecture (various orientation of the fibres toward the applied force) significantly increases mechanical strength and changes the behaviour of the structure after reaching the maximum force. This pseudo-ductile behaviour may positively increase applicability of these profiles in the industry.

Acknowledgment

The research was financed by the National Centre for Research and Development of Poland (NCBiR) grant number LIDER/40/0219/L-10/18/NCBR/2019.

References

1. Maji, A. K., Acree, R., Satpathi, D., & Donnelly, K. (1997). Evaluation of pultruded FRP composites for structural applications. *Journal of materials in civil engineering*, 9(3), 154-158.
2. Spagnuolo, S., Meda, A., Rinaldi, Z., & Nanni, A. (2018). Curvilinear GFRP bars for tunnel segments applications. *Composites Part B: Engineering*, 141, 137-147.
3. Volk, M., Arreguin, S., Ermanni, P., Wong, J., Bär, C., & Schmuck, F. (2020). Pultruded thermoplastic composites for high voltage insulator applications. *IEEE Transactions on Dielectrics and Electrical Insulation*, 27(4), 1280-1287.
4. Sousa, J. M., Correia, J. R., Cabral-Fonseca, S., & Diogo, A. C. (2014). Effects of thermal cycles on the mechanical response of pultruded GFRP profiles used in civil engineering applications. *Composite Structures*, 116, 720-731.
5. Stroński, P., Błażejowski, W., Socha, T., Denisiewicz, A., Kula, K., Lesiuk, G., & Correia, J. A. (2020). Influence of reinforcement type on the flexural behaviour of reinforced concrete beams. *Proceedings of the Institution of Civil Engineers- Forensic Engineering*, 172(4), 158-166.
6. Memon, A., & Nakai, A. (2013). Mechanical properties of jute spun yarn/PLA tubular braided composite by pultrusion molding. *Energy procedia*, 34, 818-829.
7. Schäfer, J., & Gries, T. (2016). Braiding pultrusion of thermoplastic composites. In *Advances in Braiding Technology* (pp. 405-428). Woodhead Publishing.
8. Rostamian, R., & Golzar, M. (2017). Effect of pull-winding process in thermoplastic composite rod on the impregnation of glass fiber. *Modares Mechanical Engineering*, 17(3), 405-413.

First Author. Szymon Duda is a Ph.D. candidate at Wroclaw University of Science and Technology. In 2019, he got a bachelor's degree in mechanical engineering. Since 2020, he holds a degree in Automotive Engineering (M.Sc.). Currently, a member of the Research Group of Strength and Fatigue Of Materials And Structures. In addition, he is a member of the conference organizing committee i.e., International Colloquium on Mechanical Fatigue of Metals XX. His professional interests are the behavior of composite materials, especially the fracture, fatigue, and failure process of fiber metal laminates, and computational mechanics employing the finite element method.

Second Author. Employed at Wroclaw University of Science and Technology (Faculty of Mechanical Engineering) since 2009. He obtained his Ph.D. in mechanical engineering in 2013. He obtained his habilitation in 2020 at the Faculty of Mechanical Engineering at Wroclaw University of Science and Technology. His scientific activity concerns mechanics, fracture mechanics, and fatigue of materials and structures, as well as new materials and modeling their durability under cyclic and static loads. In this field, he has published more than 90 scientific papers in reputable national and foreign scientific and technical journals, as well as more than 70 conference papers and 1 patent. He is a member of the Polish Society of Theoretical and Applied Mechanics and ESIS (European Structural Integrity Society). As part of his teaching activities, he conducts lectures and exercises at courses in mechanics, the strength of materials, fracture mechanics for students at Wroclaw University of Science Technology. He is a coauthor of an academic textbook on mechanics and a coauthor of a monograph (Springer) devoted to the problems of degradation of materials and structures. He is also the main supervisor of four Ph.D. students in Poland, an auxiliary supervisor in four doctoral dissertations in Poland, co-promoter of four foreign doctoral dissertations (Portugal, Brazil). For years, he has been intensively cooperating with foreign centers in Europe (mainly in Porto, Coimbra, Portugal, Oviedo, Spain, Milan, Cassino, Bologna-Italy, Brno, Prague-Czech Republic, Lviv, Kyiv-Ukraine, Chemnitz, Kaiserslautern, Germany, Trondheim, Norway, Nove Mesto, Slovenia) and beyond (Brazil - Sao Paulo, Minas Gerais, China - Chengdu, USA - Michigan, Canada - Waterloo, Zabol-Iran, Boumerdes-Algeria). He is a co-organizer of many international and national scientific events, i.e., XXICMFM (International Colloquium Mechanical Fatigue of Metals), XVIII KKMP (National Conference on Fracture Mechanics), 1st VCMF (Virtual Conference on Fatigue of Metals), IX Sympozjon - Layer Structures and the creator of a new initiative in the form of a Polish-Czech-German-Ukrainian winter school of fracture and fatigue mechanics. He has been awarded many times for his scientific activities: Acceptance as a member of the Academy of Young Scholars and Artists operating under the President of the City of Wroclaw - nomination received by the President of the City of Wroclaw (2018), Award of the Rector of Wroclaw University of Science and Technology (2018, 2020), International ESIS Award - TC12 (Merit Award) 2019 and 2 international awards TOP 1% Reviewers (Publons & Web of Science) - 2019, Lierati Award (2019) - Emerald Journals Group.

Roughness surface of materials after process of robot laser hardened

Matej Babič

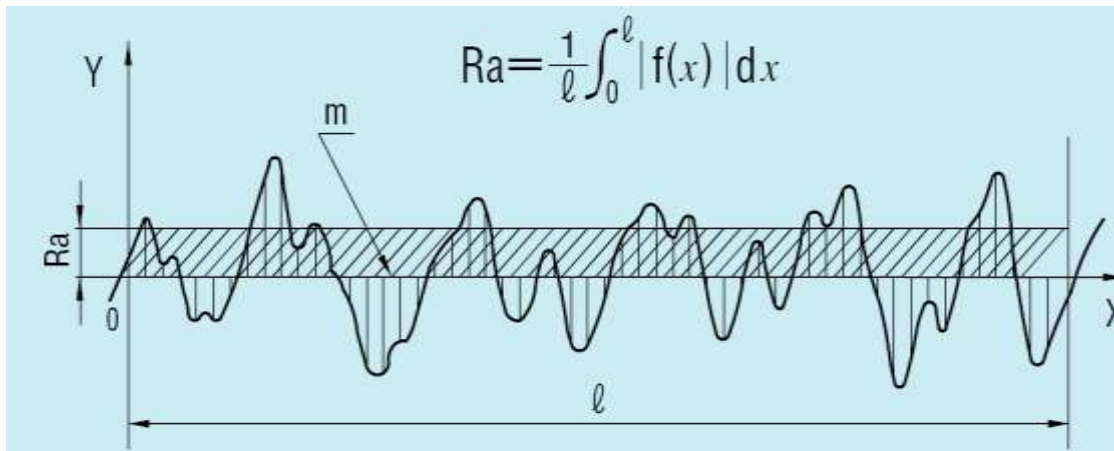
Faculty of information studies, Novo mesto, Slovenia

Abstract

This paper describes the roughness of surface of the robotically laser hardening microstructures with different parameters. We hardened patterns pattern of standard codes to the DIN standard 1.7225 with different speed and different temperature. At the end it is presented the geometry of surface of the robotic laser hardening. Characterization of surface topography is important in applications involving friction, lubrication, and wear (Thomas, 1999). In general, it has been found that friction increases with average roughness. Roughness parameters are, therefore, important in applications such as automobile brake linings, floor surfaces, and tires. The effect of roughness on lubrication has also been studied to determine its impact on issues regarding lubrication of sliding surfaces, compliant surfaces, and roller bearing fatigue. Finally, some researchers have found a correlation between initial roughness of sliding surfaces and their wear rate. Such correlations have been used to predict failure time of contact surfaces.

Introduction

Laser hardening is a metal surface treatment process complementary to conventional flame and induction hardening processes. A high-power laser beam is used to heat a metal surface rapidly and selectively to produce hardened case depths of up to 1,5mm with the hardness of the martensitic micro-structure providing improved properties such as wear resistance and increased strength. A section of standard length is sampled from the mean line on the roughness chart. The mean line is laid on a Cartesian coordinate system wherein the mean line runs in the direction of the x-axis and magnification is the y-axis. The value obtained with the formula on the right is expressed in micrometer (Om) when $y=f(x)$.



Graph 1: Arithmetical mean of roughness (Ra)

Experimental work

We made patterns to tool steel standard codes to DIN 1.7225. Chemical composition of the material contained 0.38 to 0.45 C%, max 0.4% Si, 0.6-0.9 Mn% P% max 0025, max 0035 S% and 0.15-0.3% Mo. Tool steel was forged with the laser at different speeds and different power. So we changed two parameters speed $v \in [2, 5]$ mm / s with step of 1 mm / s and temperature $T \in [1000, 1400]$ ° C with step 100 ° C.

In picture 3 we can see beautiful roughness surface of robot laser hardened specimen. With this geometry we can observe and describe deformation, which occurs in robot laser hardening. This deformation is so important for every materials. We will find parameters of robot laser hardened cell, because we will reduce deformations. And this can we do if we observe geometry of surface hardened material.

Each pattern was etching and polish, before we looked it with a microscope. First, we made recordings using an optical microscope and then with an electron microscope. Images were made by field emission scanning electron microscope JSM-7600F JEOL company. In Figures 4, 5, 6 and 7 are shown the microstructure of hardened tool steel at different magnifications.



Figure 1: Material 1.7225

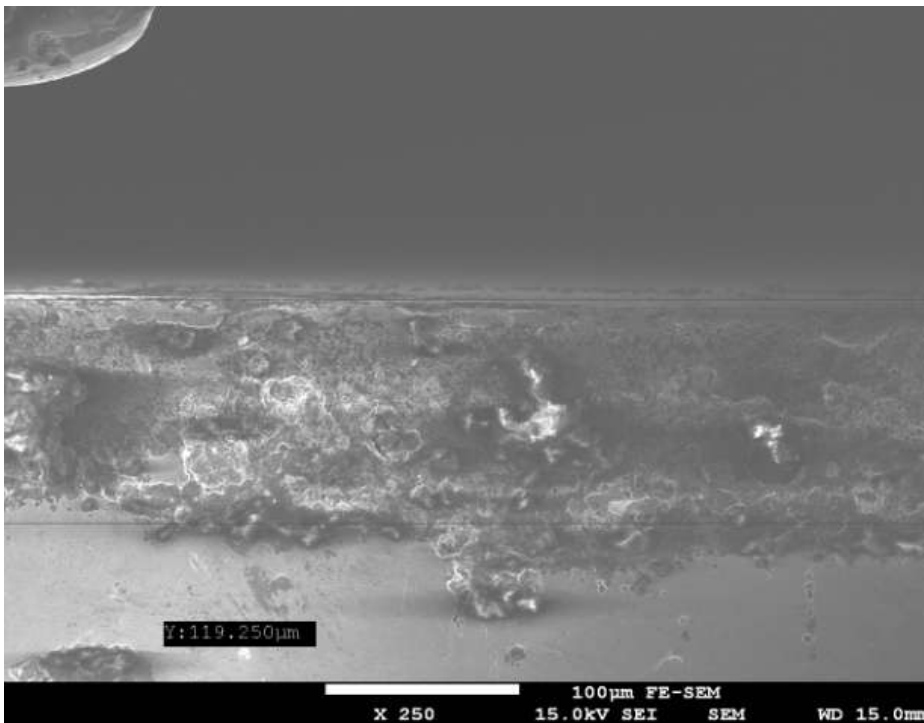


Figure 2: The boundary between work-hardened and non-hardened material

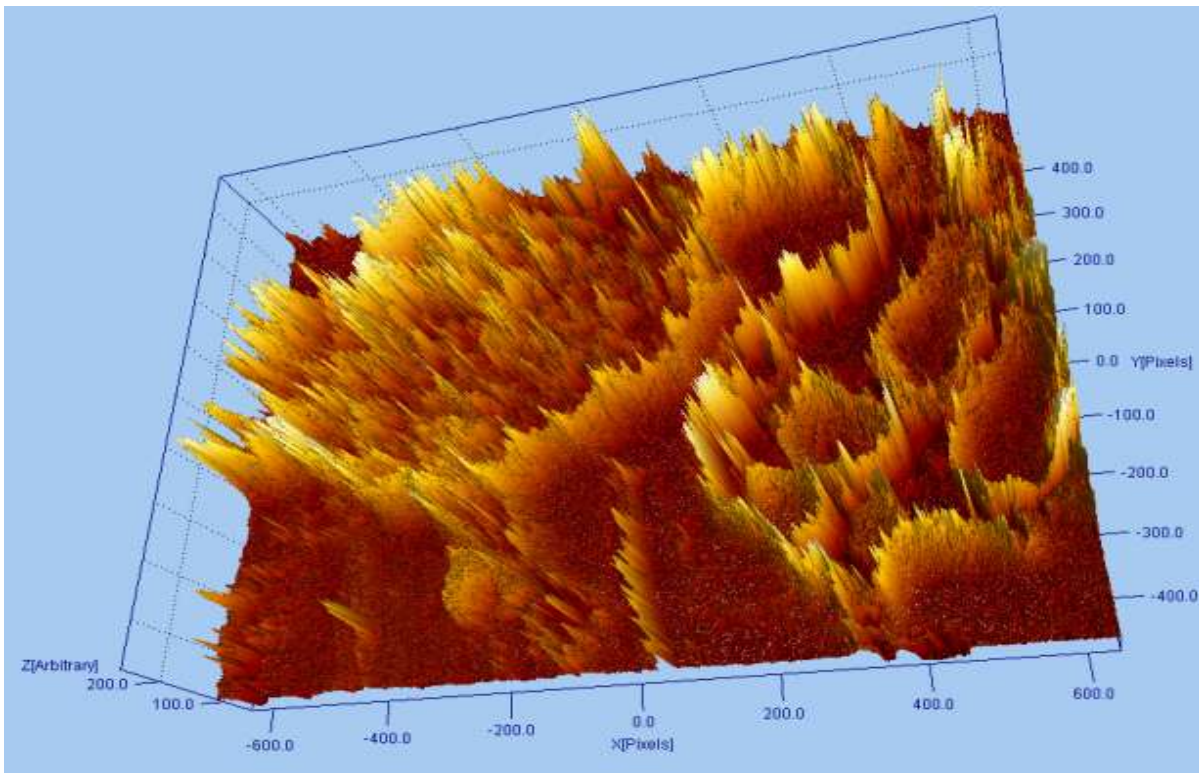


Figure 3: Geometry surface of robot laser hardened material

Results

A random process is statistically evaluated using Hurst parameter or by determining the distribution function. Hurst parameter H as self-similarity criteria can not be accurately calculated, but it can be only estimated. There are several different methods to produce estimates of the parameter H , which together more or less deviate. In doing so, we have no criteria to determine which method gives us the best result. Methods for evaluation Hurst parameter H can be 'rough' on divided into two categories, namely the assessment in the time domain and evaluation in the frequency or wavelet space.

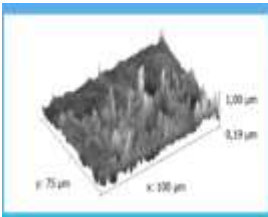


Figure 4: Roughness surface hardened with 1000 °C and 2 mm/s Ra=201nm

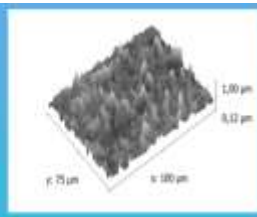


Figure 5: Roughness surface hardened with 1000 °C and 3 mm/s Ra=171nm

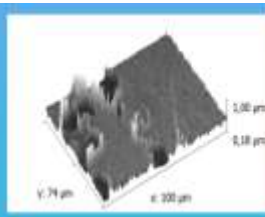


Figure 6: Roughness surface hardened with 1000 °C and 4 mm/s Ra=109 nm

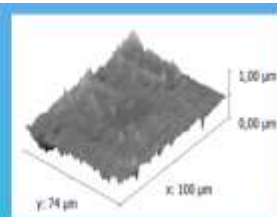


Figure 7: Roughness surface hardened with 1000 °C and 5 mm/s Ra=76,3 nm

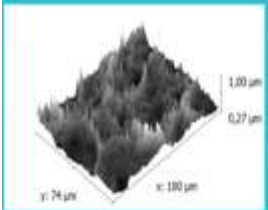


Figure 8: Roughness surface hardened with 1400 °C and 2 mm/s Ra=1,32 μm

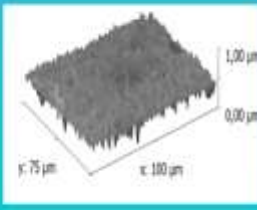


Figure 8: Roughness surface hardened with 1400 °C and 3 mm/s Ra=992 nm

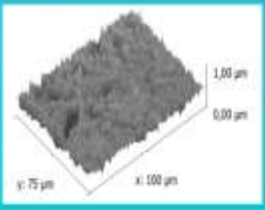


Figure 8: Roughness surface hardened with 1400 °C and 4 mm/s Ra=553 nm

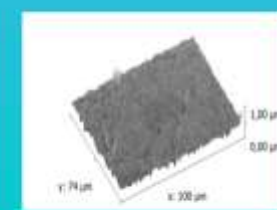


Figure 8: Roughness surface hardened with 1400 °C and 5 mm/s Ra=1,24 μm

Conclusion

We observed microstructures of robot laser hardened patterns, where we discovered roughness surface. We interested for investigate roughness surface of robot laser hardened patterns with different parameters. We will know how parameters of robot laser hardened cell impact to roughness of hardened surface. In the future we will discover how parameters of robot laser hardened cell impact to roughness of hardened surface in two-beams laser hardening.

References

- [1] J. Grum, P. Žerovnik, R. Šturm: Measurement and Analysis of Residual Stresses after Laser Hardening and Laser Surface Melt Hardening on Flat Specimens; *Proceedings of the Conference "Quenching '96"*, Ohio, Cleveland, 1996.
- [2] B. Ryu in S. Lowen, Fractal Trac Model for Internet Simulation, Proceedings of the Fifth IEEE Symposium on Computers and Communications (ISCC 2000).

Battens Design and Modelling of upwind sail battens

Michele Cali^{1*} [0000-0001-8753-8804] Ignazio Sapienza¹

¹ Department of Electric, Electronics and Computer Engineering, University of Catania
Catania 95123, Italy
[*mcali@dii.unict.it](mailto:mcali@dii.unict.it)

Abstract. Numerical codes can play an important function in the nautical design when advanced simulation tools are increasingly adopted for prediction purposes, in particular for the calculation of the interaction between boat parts and surrounding fluids. Fluid-structure interaction analysis (FSI) can help engineers to set the optimum design of a sail and also the influence of panels and battens sail arrangement. The paper describes a methodology that enhances the understanding of panel and battens arrangement, as well as their stiffness on sail performance. Specifically, through the battens position, shape and stiffness parametrization, the sail non-developable shape was optimized, in order to compensate the variation in the angle of attack that occurs following variations in the speed of the wind at different sail heights. For an efficient and robust implementation of integrated Reynolds Averaged Navier Stokes (RANS) equations with Shear Stress Transport (SST) turbulence model and Computational Structural Mechanics (CSM) analysis, the constitutive sailcloth and battens characterization was conducted experimentally. The case study of a mainsail in Dacron© TNF 240 of a Vaurien dinghy boat, offered tangible results to support the methodology by validating it with experimental data.

Keywords: CFD-CSM analysis, SST model, Sail battens arrangement, Flying shape, Twisting.

1 Introduction

In the last years sail manufacture has undergone significant development under the impulse of sailing races like America's Cup and the Volvo Around-The-World Race.

As expected also in industry 4.0, advanced technologies and new computational techniques are used to control the production process and optimize the final product.

Sail performance, especially in terms of speed, mainly depends on the boat the sails are designed for. Hull design is fundamentally important; however, sail geometry arrangement optimization plays the key role to improve sailboats' dynamic performance. The selection of suitably rigid and lightweight material with an effective sail panels and battens arrangement could improve the sailboat dynamic performance.

The methodology presented here improves the understanding of the influence shape, orientation and arrangement of panels and battens have on sail performance.

Present study was aimed at analyzing the influence of panels and battens arrangement on boat performance by applying fluid structure interaction (FSI) analysis. In particular the case study of the Dacron© TNF 240 main sail of a Vaurien was analyzed. Vaurien is a small (4 m) dinghy boat.

The workflow of the research activity, constitutive characteristics of Sailcloths and Battens were experimentally measured and battens arrangement and stiffness were optimized in air-sail interaction analysis using an aerodynamic approach.

2 Materials and Methods

2.1 Sail parametric modelling

Conforming to the ISO standard 13934-1 (2000) experimental cloth characterization was performed using a ZwickRoell Z100 twin column tensile testing machine and TestXpert® v11.02 software.

Tensile tests in the warp, weft and bias directions were performed and the stress-strain curves and the modulus of elasticity were evaluated.

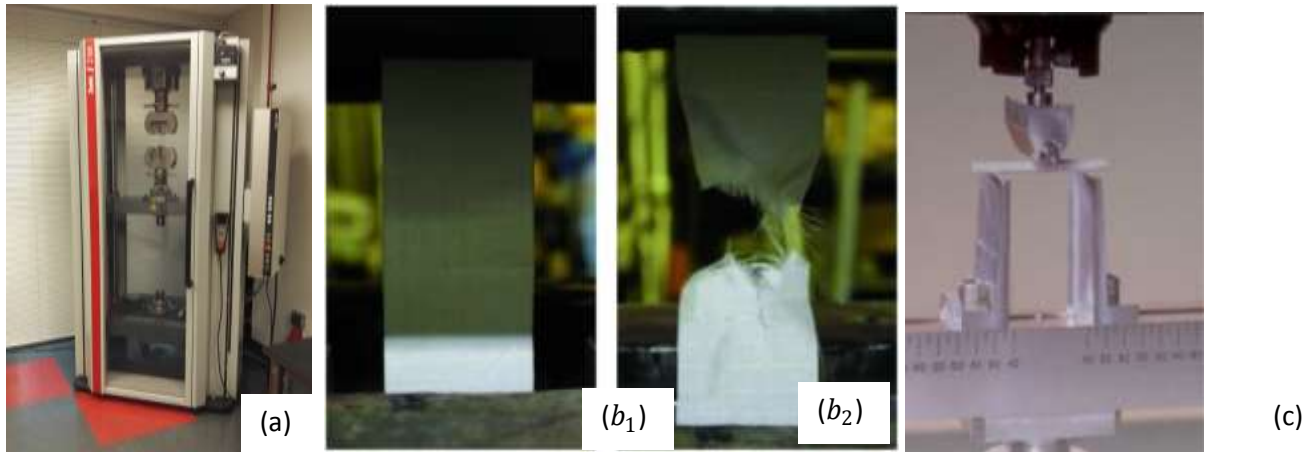


Fig. 1: a) Zwick & Roell Z100 tensile testing machine; (b) Tensile test on Dacron © TNF 240; (c) Three-point flexion on battens.

Curve which interpolates the tests carried out on five samples is obtained as a mean value of 2200 sampling points. Figures show the results from tensile tests performed in the weft (on the left) and in the warp (on the right) direction for the ten sail cloths.

Curves consisting of three different zones: an initial linear elastic region, followed by the second elastic/plastic region with a downward concavity and the third zone after which the cloth yielded. In this region of the curve the cloth continues to provide some resistance (even 40% stretching for some cloths) which decreases with the increasing tensile stress.

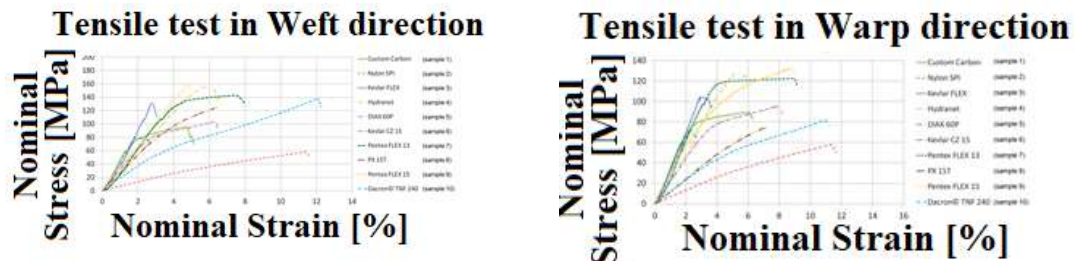


Fig. 2: tensile tests performed in the weft and in the warp direction.

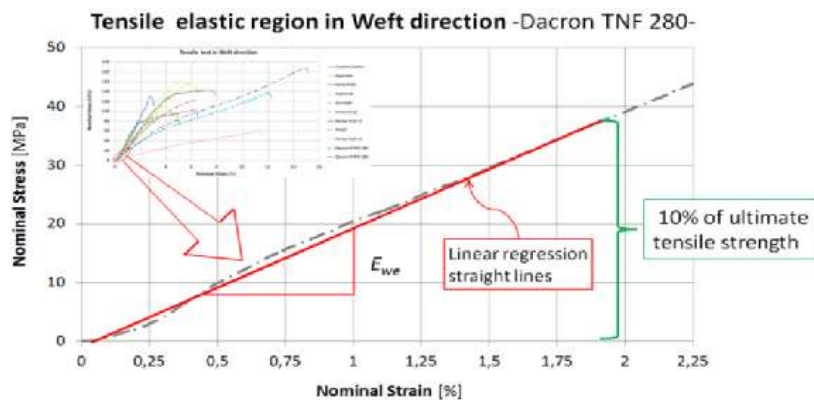


Fig. 3 elastic modulus.

The elastic modulus of sailcloth was evaluated as the slope of the initial linear region.

2.2 Sailcloth and battens characterization

The Poisson's ratios $\nu_{we,wa}$ was evaluated with the simplified formula:

where E_{med} is the average value of E_{we} and E_{wa} ; the shear modulus $G_{we,wa}$ was, instead, calculated using the following equation that Agarwal and Broutman proposed in 1990.

$$G_{we,wa} = \frac{1}{4} \left[\frac{1}{E_{bi}} - \frac{1}{4E_{wa}} - \frac{1}{4E_{we}} + \frac{2\nu_{we,wa}}{E_{we}} \right]^{-1} \quad (1)$$

The energy dissipated per unit of volume (E_d) was evaluated taking into account the loading-unloading cycles (i.e. hysteresis loops) at various frequencies in the linear elastic region of the tensile curves. The energy dissipated per unit of volume allowed assessing the equivalent viscous damping coefficients.

$$C_{eq} = \frac{E_d}{2\pi^2 \cdot f \cdot \Delta l_{max}^2} \quad (2)$$

The Young's modulus, the tangential modulus and flexional stiffness of battens in polyurethane resin were calculated with three-point flexion test. The mass-volume ratio was measured by an electro-optical single-pan precision balance (Gibertini mod. 704/N) with sensibility of 0.1 mg for mass measurement and a graduated cylinder with distilled water for volume measurement.

Table 1. Battens and sailcloth structural characteristics.

Battens	E [GPa]		□	G [GPa]	□ [$\frac{kg}{m^3}$]	K _r [GPa]
	6.96					
Dacron	E _{we} [GPa]	E _{wa} [GPa]	0.3	0.26	1300	
TNF 240	1.05	0.66				

Sail deflection was calculated from the flow forces. Flow simulation was repeated with deflected geometry, whereas the structural calculation was repeated in turn with modified flow forces until force convergence was reached (i.e. force residuals become less than 0.001). The maximum number of iterations was set to 1000.

2.3 Setup of aeroelastic-structural analysis

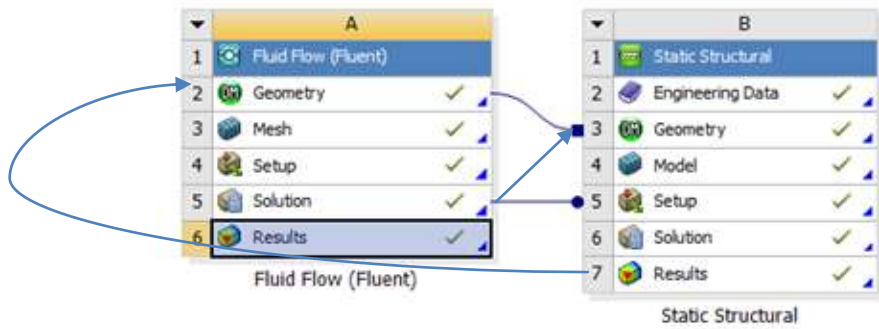


Fig. 4 Setup of aeroelastic-structural analysis.

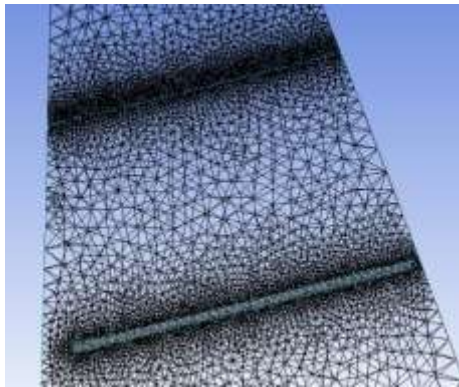


Fig.5 localized mesh.

The sail is discretized by triangular membrane elements; their structural deformation calculation is based on the method of Arcaro (Arcaro, 2004; Renzsch et al., 2008), which assumes homogeneous and orthotropic linear elastic material.

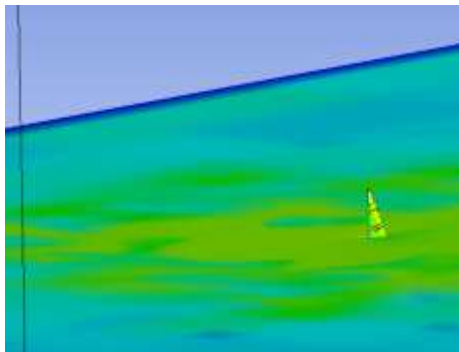


Fig.6 wind tunnel.

The sail was modelled with 1200 triangular membrane elements, varying in size from 35 mm to 100 mm; each batten was modelled with 480 tetrahedral elements, having dimensions of 5 mm; the air was modelled with 4 million of tetrahedral elements, varying in size from 10 mm to 1000 mm.

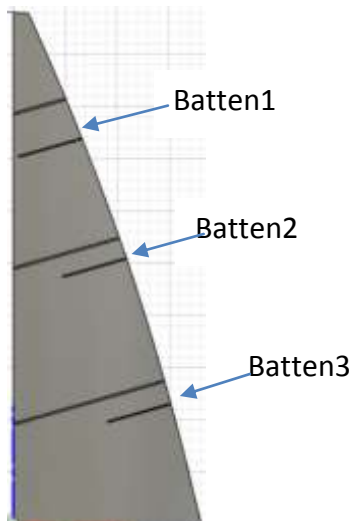


Fig. 7 panels and battens arrangement.

Table 1: Mainsail geometric characteristics.

Section	c [mm]	f [mm]	C [%]	Height [%]	Twisting β [°]	Incidence α [°]
Boma	1800	200	11	0	0	22
1/4	1494.2	133.5	8.9	25	5	17
1/2	1132.1	71.6	6.3	50	10	22
3/4	692.6	23.5	3.4	75	16	6

Employing commercial software CATIA V5 R19, the 3D model of the mainsail was created through the loft command, interpolating the R-Spline obtained in correspondence with 6 contours of the sections of the sail equally spaced along the vertical direction (z). The 6 sections were arranged in the space twisted together along the leech profile according to the design values.

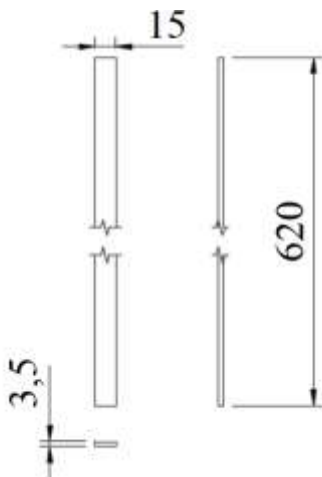


Fig.8 Batten in polyurethane resin.

Table 2: Sail battens parameters.

Parameters	Design value	Min value	Max value
Position	1141;2533;3684 mm	-20%	+20%
Lenght	620 mm	400	800
Width	15 mm	12	20
Height	3.5 mm	3	5
Stiffness	6.93 GPa	1/5	50x

The twisting angle values of the battens cross-section dimensions, of the chord c and of the battens position were parameterized together with the stiffness of the battens in order to find their optimal values.

3 Result and Discussion

You can see how the fluid fillets gradually move away from the sail as the angle increases, creating small eddies, consequently increasing the lift, up to stall, around 23°.

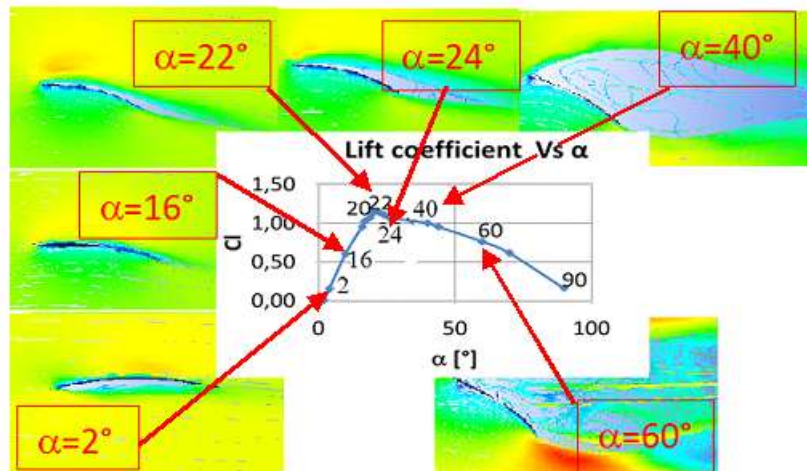


Fig. 9 Lift coefficient Vs incidence α at 2/5 of the sail height (wind = 20 knots).

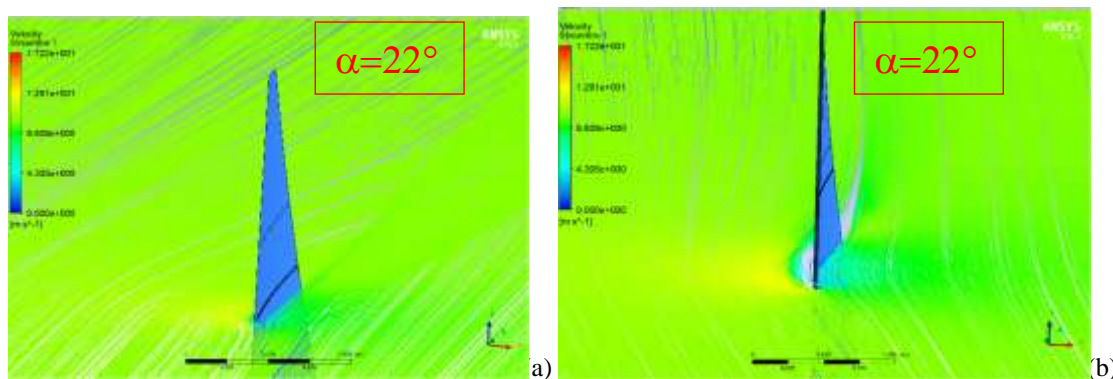


Fig.10 Streamlines and pressure on sail surface (wind 20 knots): (a) α at 3/4 of the sail height; (b) α at 1/2 of the sail height.

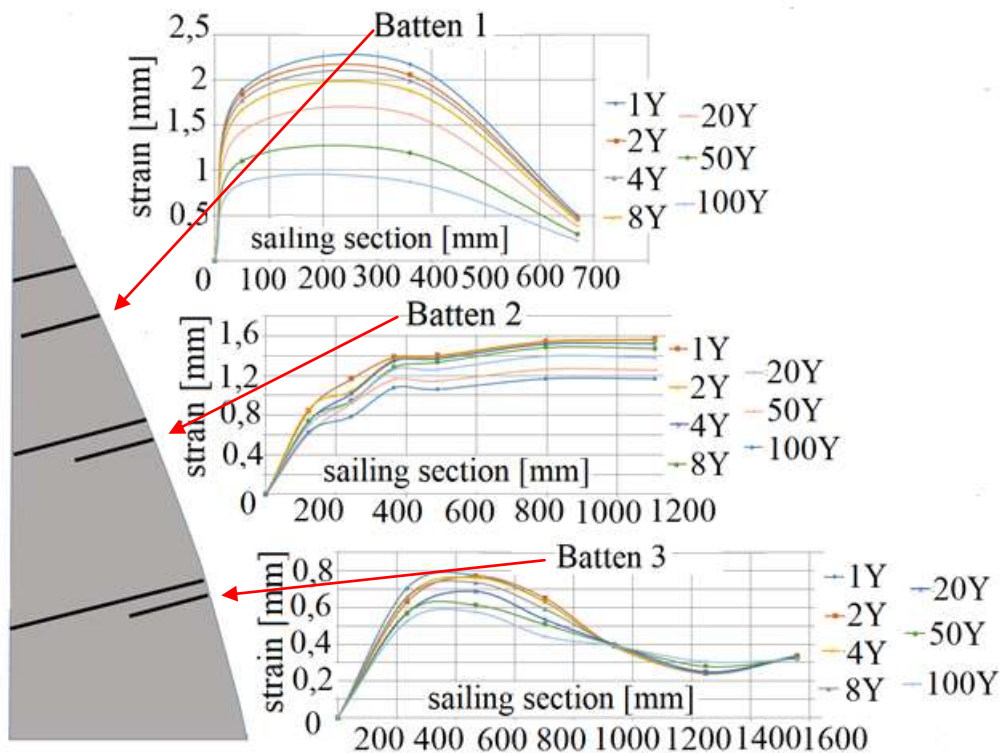


Fig.11 Sail strain for different battens stiffness

Thanks to the performed analyses, the phenomenon of the detachment of the threads and the consequent loss of lift were clearly evaluated. The behaviour of the fluid threads around the sail at an altitude of almost 2 m, corresponding to 2/5 of the sail height, when using the battens with the design values. Up to an angle of incidence of 22° an increase in the coefficient of lift was registered.

The deformations of the sail and battens were evaluated at various heights. It can be deduced that on batten 1, an increase of the stiffness beyond a certain value is not desirable, since keeping rigid the extremity of the sail is not convenient in very strong winds. In battens 2 and 3, on the other hand, the increase in stiffness is beneficial, limiting the rowing and detachment of the fluid threads in the trailing edge of the sail.

The use of battens with different stiffness, quadratically increasing towards the top of the sail, proved to be the best solution. In particular, by stiffening the battens in proportion to the speed profile and extending their length to the full width of the sail for the battens at higher altitudes, it was possible to give the sail a correct airfoil, controlling and maintaining its curvature even in its upper part where the wind is more intense.

4 Conclusions

The main advantages of the proposed method can be summarized as follows: less computational time to evaluate the optimal panel and batten arrangement due to the integration of CAD parametric model CFD and CSM simulation; correct simulation of the deformation of the sailcloth fabric due to its experimental characterization; The main results of the proposed method can be summarized as follows: a triangular membrane element formulation coupled with a solid mesh of the battens was found to be the most effective solution for studying the problem; use of battens with different stiffness, quadratically increasing towards the top of the sail. In particular, by stiffening the battens in proportion to the speed profile and extending their length to the full width of the sail for the battens at higher altitudes, it was possible to give the sail a correct airfoil.

Acknowledgments

Starting Grant 2020-22 Linea 3-Progetto NASCAR-University of Catania Pr. 308811.

References

- [1] Braun, J.B., Imas, L. High fidelity CFD simulations in racing yacht aerodynamic analysis. Proceedings 3rd High Performance Yacht Design Conference. Auckland, 168–175 (2008).
- [2] Bak, S., Yoo, J., & Song, C. Y. Fluid-structure interaction analysis of deformation of sail of 30-foot yacht. *International Journal of Naval Architecture and Ocean Engineering*, 5(2), 263-276 (2013).
- [3] Cali, M., Oliveri, S. M., Cella, U., Martorelli, M., Gloria, A., & Speranza, D. Mechanical characterization and modeling of downwind sailcloth in fluid-structure interaction analysis. *Ocean Engineering*, 165, 488-504 (2018).
- [4] Manikandan, A., & Rajkumar, R. Evaluation of Mechanical Properties of Synthetic Fiber Reinforced Polymer Composites by Mixture Design Analysis. *Polymers & Polymer Composites*, 24(7), 455-462 (2016).
- [5] Gazzo, S., Cuomo, M., Boutin, C., Contrafatto, L. Directional properties of fibre network materials evaluated by means of discrete homogenization. *European Journal of Mechanics, A/Solids*, 2020, 82, 104009.
- [6] Boutin, C., Contrafatto, L., Cuomo, M., Gazzo, S., Greco, L. Discrete homogenization procedure for estimating the mechanical properties of nets and pantographic structures. *Lecture Notes in Mechanical Engineering*, 2020, pp. 716–732.
- [7] Pearson, W. E. Textiles to composites: 3D moulding and automated fibre placement for flexible membranes. *Marine Applications of Advanced Fibre-reinforced Composites*, 305. 305-334 (2015).
- [8] Richter, H.J., Horrigan, K.C., Braun, J.B. Computational fluid dynamics for downwind sails. Proceedings 16th Chesapeake Sailing Yacht Symp. Annapolis, MD, 19–28 (2003).
- [9] Ranzenbach, R., Kleene, J. Utility of flying shapes in the development of offwind sail design database. In: *The High Performance Yacht Design Conference*. Auckland (2002).
- [10] Renzsch, H., Graf, K. An experimental validation case for fluid-structure interaction simulations of downwind sails. In: *Proceedings of the 21st Chesapeake Sailing Yacht Symposium*. Annapolis, p. 8 (2013).
- [11] Fossati, F., Bayati, I., Orlandini, F., Muggiasca, S., Vandone, A., Mainetti, G., Sala, R., Bertorello, C., Begovic, E. A novel full scale laboratory for yacht engineering research. *Ocean Eng.* 104, 219–237 (2015).
- [12] Hochkirch, K. Design and Construction of a Full-Scale Measurement System for the Analysis of Sailing Performance. Technical University of Berlin, PhD Thesis (2000).
- [13] Le Pelley, D.J., Modral, O. VSPARS: A combined sail and rig shape recognition system using imaging techniques. In: *Proceedings of 3rd High Performance Yacht Design Conference*. Auckland, pp. 57–66 (2008).
- [14] Graves, W., T. Barbera, J.B. Braun, Imas L. Measurement and Simulation of Pressure Distribution on Full Size Sails. *3rd High Performance Yacht Design Conference*,. Auckland, Vol. 2, p. 4 2008.
- [15] Augier, B., Bot, P., Hauville, F., Durand, M.. Experimental validation of unsteady models for fluid structure interaction: Application to yacht sails and rigs. *Journal of Wind Engineering and Industrial Aerodynamics* 101(0), 53–66 (2012).
- [16] Agarwal, B.D., Broutman, L.J., *Analysis and Performance of Fiber Composites*, vol. 2 Wiley, New York. (1990).